

ROLE OF HYDROPHOBIC INTERACTIONS ON THERMOSENSITIVITY,  
METAL COMPLEXATION AND RHEOLOGY OF  
ASSOCIATING POLYMERS

A THESIS  
SUBMITTED TO THE  
**UNIVERSITY OF PUNE**  
FOR THE DEGREE OF  
**DOCTOR OF PHILOSOPHY**  
(IN CHEMISTRY)

BY

**SHYNI VARGHESE**

CHEMICAL ENGINEERING DIVISION  
NATIONAL CHEMICAL LABORATORY  
PUNE-411 008, INDIA

FEBRUARY 2001

## **ACKNOWLEDGEMENTS**

The respect and gratitude for my guide Dr. R A Mashelkar cannot be expressed in words. He was a continuous source of inspiration throughout the course of my work. I am grateful to him for devoting time for thought provoking and stimulating discussions, in spite of his busy schedule. His logical and analytical thinking along with the deep involvement in my work has played a big role in shaping my approach towards the research. He has shown me the most unique efficiency and enthusiasm that have given me a new outlook. Indeed, I am fortunate to work under the guidance of a teacher with such a versatile personality.

I would like to thank my supervisor and friend Dr. Ashish Lele for his moral support and patient guidance through out my stay in NCL. I thank him for teaching me the skills of a researcher such as generating ideas with logical thoughts and setting up the experiments, keeping the records, analyzing the data, presenting and writing the technical material. I am grateful to him for being a good critic and a good teacher. I thank him for the faith he has shown and the freedom he has given to explore my capabilities. Finally I would like to thank him and his wife Mrs. Ashwini Lele for the friendship and the secure feeling that they had given to a student like me who is away from the hometown.

It is my honour to acknowledge Dr. P. Ratnaswamy, Director NCL for permitting me to present this work in the form of thesis. I also thank Dr. B. D. Kulkarni, head Chemical Engineering Division and Dr. M. G. Kulkarni, head Polymer Science and Engineering Division for their encouragement.

I am grateful to Dr. Badiger, Dr. Murali Sastry Dr. Srinivas Dr. Premnath, Dr. Ramesh, Dr. (Mrs). Jyothi Jog and Dr. Sainkar for their helpful suggestions and comments.

I appreciate the financial support from Council of Scientific and Industrial Research in the form of Senior Research Fellow.

I would also like to express my debt and gratitude to the many of my colleagues and friends. Their contributions are varied but they have always been stimulating over a period of years they include in particular the following:

Nivedita, Vaishali, Bakul, Rohini, Leena, Padmaja, Vivek, Vinayak, Yogesh, Sunil, Girish, Prashant, Ajit, Rajendra, Sameer, Abhijit, Umesh, Alankar, Jayant, Mahesh, Raghu. It gives me an immense pleasure to thank all my friends for their constant support and the discussions, which made my days lively in NCL. I would like to thank my friend Dr. Ashish Kawl for his inspiring friendship, whose influence goes beyond words. My thanks to K R Nair, Ravindranath, Venugopal, Satwant Kaur, Madhu, Jitu, Nandakumar, Vinita Kiran, Vrinda and Jisha for their warm friendship and care. I would like to thank Mrs. Mariamma John and Rathanlal Sharma for their warm and cheerful consideration. My sincere thanks to Dr. Harrinder Dhaliwal for his unconditional friendship and moral support. I thank all NCL staff for their cooperation and help. I would like to thank Dhupe, Shukla, Radhakrishnan, Banerjee, Bhalerao, Sujatha and Lalitha

My deepest thanks to my parents, grand parents, Prasanna Aunty, Shybi and Biji, whose unconditional support, encouragement and love has made it possible for me to achieve this. They are always been a source of inspiration for me. Finally I would like to thank my grand father, Eapen Varghese, who has taught me the strength of an Indian woman. He has guided me to take independent decisions and inspired me to achieve the goals. I am glad to dedicate this thesis to him even though he is no more to share the happiness.

(Shyni Varghese)

## TABLE OF CONTENTS

	Page No.
ABSTRACT	vi
LIST OF FIGURES	x
LIST OF TABLES	xiv
NOMENCLATURE	xv
1 INTRODUCTION	1
2 LITERATURE SURVEY ON INTELLIGENT GELS	9
2.1 Introduction	9
2.2 Gels	10
2.2.1 Superabsorbent gels	13
2.2.2 Equilibrium swelling of hydrogels	14
2.2.3 Mechanical Properties of hydrogels	17
2.3 Stimuli responsive hydrogels	19
2.3.1 pH sensitive hydrogels	24
2.3.2 Electric field sensitive hydrogels	25
2.3.3 Light sensitive gels	26
2.3.4 Magnetic field sensitive gels	26
2.3.5 Temperature sensitive gels	27
2.4 Temperature induced volume phase transition in polymer gels	29
2.4.1 Phase separation in polymer solutions	29
2.4.2 Thermoreversible hydrogels	33
2.5 Hydrogel hybrids	49
2.5.1 Polymer metal complexation	50
2.5.2 Swelling behaviour of gels in metal salt solutions	51
2.5.3 Effect of hydrophobicity on metal complexation	52



4.4.3.2 Swelling behaviour of AMPS-co-NtBAm copolymer gels	96
4.4.3.3 Swelling behaviour of AMPS-co-NIPAm copolymer gels	96
4.5 Conclusions	99
5 METAL COMPLEXATION IN SMART GELS	100
5.1 Introduction	100
5.2 Experimental section	101
5.2.1 Materials	102
5.2.2 Synthesis of Acryloyl Chloride	102
5.2.3 Synthesis of monomers	102
5.2.4 Synthesis of gels	105
5.2.5. Complexation of the gels with transition metal ions	107
5.2.6 Characterization of the complexed gels	108
5.3 Results and Discussion	109
5.3.1 Effect of metal complexation on VPT	109
5.3.2 Effect of hydrophobicity on metal complexation	117
5.4 Conclusion	130
6. SELF-ORGANIZATION IN HYDROGELS	132
6.1 Introduction	132
6.2 Experimental section	134
6.2.1 Materials	134
6.2.2 Synthesis of gels	134

6.2.3	Complexation of the gels with metal ions	135
6.2.4	Swelling measurements of the gels in metal salt solutions	135
6.2.5	EPR measurements	135
6.2.6	Entrapment and release of hemoglobin	135
6.3	Experimental observations	136
6.3.1	Metal induced shaper transition	136
6.3.2	Shape memory	142
6.3.3	Swelling behaviour of the gel in metal salt solutions	144
6.3.4	EPR structure	149
6.4	Results and Discussion	149
6.5	Conclusion	158
7.	SELF-HEALING IN GELS	159
7.1	Introduction	159
7.2	Experimental section	160
7.2.1	Materials	160
7.2.2	Synthesis of gels	161
7.2.3	Tensile measurements	161
7.2.4	Dynamic mechanical analysis	161
7.2.5	Moisture absorption	162
7.3	Results and Discussion	162
7.3.1	Mechanism	176
7.3.2	Reversible healing	181
7.4	Conclusion	182

8. SUMMARY OF THE PRESENT WORK AND RECCOMENDATIONS FOR FUTURE WORK	183
Bibliography	191
List of publications/patents	200
Synopsis	201



## ABSTRACT

Macromolecules containing hydrophilic and hydrophobic groups with strong inter and intra molecular associations are known as associating polymers. Smart polymers such as polymeric gels, which mimic biological systems by using the same types of fundamental molecular interactions, have been creatively used in a number of novel applications. In this work we have investigated the effect of hydrophobic and hydrophilic interactions on some novel and interesting phenomena in gels, which include volume transition, metal complexation, self-organization and self-healing.

The first order volume phase transition phenomenon observed in thermoreversible gels is well predicted by the Lattice Fluid Hydrogen Bond (LFHB) model. According to the LFHB model predictions, a fine balance of hydrophilic and hydrophobic interactions is a pre-requisite for volume phase transition. In this work we present an experimental validation of this hypothesis by showing that the thermoreversible gels can be designed from two monomers, whose homopolymers do not show any LCST in the observable temperature range. We developed a new thermoreversible gel (Bu-AMPS 10/1) from copolymerisation of a hydrophilic 2-acrylamido-2-methyl-1-propane sulfonic acid (AMPS) monomer and a hydrophobic N-tertiary butylacrylamide (N-t-BAM) monomer. The copolymer gel exhibited a distinct first order volume transition at a critical composition of the two monomers. A small change in the composition of the monomers resulted in a loss of the discontinuous transition. Also, a subtle change in the hydrophobicity of one of the monomers also resulted in a loss of the discontinuous volume transition. Such a

demonstration clearly indicates the importance of hydrophilic and hydrophobic interactions as being a pre-requisite for LCST polymers.

Surfactants are widely used to alter the volume phase transition (VPT) temperature of thermoreversible gels. Metal salt solutions also have the same effect although the cause might be different, especially for transition metal salts. This has not been investigated in detail so far. The shift in the transition temperature in the case of metal ions has been mainly attributed to an extra attraction between the metal ions and the polymers. We show in this work that the shift in VPT in the presence of metal ions occurs due to the modulation of the hydrophobic-hydrophilic balance by metal complexation. We investigate the effect of trace amounts of metal-complexation on the VPT of the N-t-BAm-co-AMPS gel. A substantial shift in the transition temperature of the copolymer gel, (AMPS-co-NtBAm), was observed after complexation with trace amount of  $\text{Cr}^{6+}$  and  $\text{Cu}^{2+}$  ions. Electron Paramagnetic Resonance spectroscopy (EPR) was used to detect the complexed structure. We propose that the complexation of hydrophilic  $-\text{SO}_3\text{H}$  groups of the gel with trace amounts of the metal ions renders the gel effectively more hydrophobic, which in turn causes the shift in volume transition temperature to lower temperatures.

As a complimentary problem we also investigate the influence of hydrophobicity on metal complexation. We have investigated the metal uptake of a series of hydrogels of acrylic acid and acryloyl amino acids of different alkyl chain lengths ( $n = 0$  to  $7$ ) simultaneously with an investigation of the structure of the coordination complex using electron spin resonance spectroscopy (EPR). We observed that both the metal uptake as well as the structure of the polymer-metal complex is greatly influenced by the

hydrophilic-hydrophobic balance of the gel. Gels with increased hydrophobicity showed two distinct types of structures namely, monomeric complex and dimeric complex. Such an investigation gives valuable insights into designing catalysts or understanding complexation in biopolymers.

During the course of our work on metal complexed polymer gels, we observed for the first time a novel self-organization phenomenon wherein a solid cylindrical piece of a gel transformed spontaneously into a hollow spherical/ellipsoidal object in the presence of specific transition metal ions. We found that the self-organization is reversible and occurs only for those polymer gels, which show a critical balance of hydrophilic and hydrophobic interactions. This phenomenon was investigated by studying the complexation of polymer chains with metal ions together with the swelling behaviour of the gels in metal salt solutions. The process of self-organization demonstrated here is a kind of shape-memory effect, however it is more complicated than mere bending of gel strips that has been shown earlier in the literature. We have also demonstrated some interesting potential applications of this phenomenon.

This work also reports another novel phenomenon namely, “self-healing” of gels. We demonstrate here that two cylindrical gel pieces unite in the presence of Cu(II) ions into a single object while retaining a thick weld line at the interface. The novelty of the observation is the fact that crosslinked gels cannot self-weld in a manner similar to linear thermoplastic polymers due to the complete lack of reptation ability of the covalently bonded chains of the network. The metal induced healing shown here for the first time is reversible and observed only in certain gels that are viscoelastic in nature. The phenomenon is explained on the basis of formation of physical crosslinking via

polymer-metal complexation and the swelling of the gel accompanied by its ability to deform and thereby increase the welding area.

## LIST OF FIGURES

2.1	Schematic of gel	11
2.2	Polymer segment distributed along with the solvent in the liquid lattice.	15
2.3	Number of papers published in Nature and Science for the last twenty years on intelligent gels	20
2.4	First order volume phase transition accompanied by hysteresis as a function of temperature	22
2.5	Fundamental forces those are responsible for the volume transition phenomenon in hydrogels	23
2.6	Co-existence of swollen as well as collapsed phase at the transition temperature	28
2.7	Schematic picture exhibiting the co-existence curve for polymer - solvent binary system	29
2.8	Schematic picture showing the LCST as well as VPT for polymer-solvent systems	32
2.9	Volume phase transition of PNIPAm gel in water	43
2.10a	Rearrangements of hydrogen bonds in PNIPAM-water systems	43
2.10b	Hydrophobicity increases as a function of temperature	44
2.11	Swelling behavior of Poly (NIPAm-co-AAc) gels in $\text{CuCl}_2$ solution	52
2.12	Shape memory gels	57
4.1	Reaction scheme for the synthesis of copolymer gels.	75
4.2	Schematic of the compression rig used to measure the compression modulus of the gel samples.	77
4.3	Stress-strain curve for Bu-AMPS (10/1)	79
4.4	Qualitative predictions of the LFHB model for the swelling behaviour of copolymer gels	80

4.5	FT-IR spectra of the of the N-t-BAm- AMPS copolymer gels	82
4.6	FT-IR spectra of the of the NIPAm- AMPS copolymer gels	83
4.7	Swelling behaviour of AMPS-co-N-t-BAm copolymer gels	85
4.8	Co-existence of swollen and collapsed phases at the transition temperature	86
4.9	Swelling behaviour of AMPS-co-NIPAm copolymer gels	88
4.10	Correlation between AMPS content, modulus and swelling behaviour of the copolymer gels	90
4.11	Quantitative comparison of the experimental data with model calculations for AMPS-co-N-t-BAm copolymer gels	97
4.12	Quantitative comparison of experimental data with model calculations for AMPS-co-NIPAm gels	98
5.1	Structure of the monomers used to prepare the gels	103
5.2	Stand curve of aqueous Cu(II) solution at 810nm	110
5.3	EPR spectra for the Cu(II)-complexed (N-t-BAm-co-BisAm-co-AMPS) gel in the dried state	112
5.4	EPR spectra for the Cu(II)-complexed (N-t-BAm-co-BisAm-co-AMPS) gel in the swollen state	113
5.5	Probable structure of the Cu(II) complexed gel	114
5.6	Effect of metal complexation on the swelling behaviour of the thermoreversible gels	115
5.7	EPR spectra of Cu(II)-AAc gels as a function of degree of ionization	121
5.8	EPR spectra of the monomeric Cu(II) species in A6ACA gels as a Function of degree of ionization at 298 K	123
5.9	EPR spectra at 298 K showing the effect of hydrophobic alkyl chain length on the Cu(II) species in the completely ionized	

	Cu(II) complexed AAc, A4ABA, A6ACA and A8ACA gels	125
5.10	EPR spectra at Q-band frequency of (a) A6ACA gel and (b) dimeric copper acetate monomhydrate at 298 K	127
5.11	EPR spectra of Cu(II) complexed A6ACA (Na) gels at (a) 298 K (b) 80K and (c) dotted portion of (b) in expanded scale	128
5.12	Structure of monomeric and dimeric Cu(II) species in metal ion complexed gels	129
6.1	Standard curve for hemoglobin at 460nm	137
6.2	Morphological change of the A6ACA gel in CuCl <sub>2</sub> solution	138
6.3	Development of hollow interior of the A6ACA copper complexed gel over a period of time	139
6.4	Morphological change of the A6ACA gel in PbCl <sub>2</sub> solution	140
6.5	Optical micrograph of the Pb(II) complexed A6ACA gel	141
6.6	Shape memory: The self-organized A6ACA gel reverted back to the original solid cylindrical structure	143
6.7	Swelling behaviour of the A6ACA gel in CuCl <sub>2</sub> solution	145
6.8	Swelling behaviour of the A6ACA gel in PbCl <sub>2</sub> solution	146
6.9	Swelling behaviour of the A6ACA gel in CdSO <sub>4</sub> solution	147
6.10	Swelling behaviour of the A6ACA gel in FeCl <sub>3</sub> solution	148
6.11	EPR spectra of the Cu(II) complexed A6ACA gel (a) Hard shell (b) Soft core	150
6.12	Release of hemoglobin as a function of time	156
6.13	CdS nanoparticle in gel matrix	157
7.1	Moisture absorbance of the gel as a function of time	163
7.2	Healed A6ACA gel	164
7.3	Initial stages of healing, formation of thick weld line	165
7.4	Completely healed cylindrical A6ACA gel	166

7.5	Cross section of the completely healed A6ACA gel	167
7.6a	SEM photograph of the fused A6ACA particles	169
7.6b	SEM photograph of the fused A6ACA particles	170
7.6c	SEM photograph of the fused A6ACA particles	171
7.7	SEM photograph of the dried A6ACA particles	172
7.8	Stress-strain curve of pure A6ACA gel containing 1.16g/g moisture	174
7.9	Stress-strain curve of the healed A6ACA gel containing 1.16g/g moisture	175
7.10	Elastic and viscous moduli of A6ACA gel at different moisture level	177
7.11	Elastic and viscous moduli of A4ABA gel at different moisture level	178
7.12	Dynamic $T_g$ of gels as a function of alkyl side chain length	179



## LIST OF TABLES

4.1	Feed composition of the AMPS-co-N-t-BAm gels	73
4.2	Feed composition of AMPS-co-NIPAm gels	74
4.3	Hydrogen bonding parameters	94
4.4	Molecular parameters	95
4.5	Binary interaction parameters and crosslink density	95
5.1	Swelling behaviour of polyacid gels in water and $\text{CuCl}_2$ solution	118
5.2	EPR spin Hamiltonian parameters of Cu(II) complexed polymer gels	124
6.1	Swelling behaviour of gels in $\text{CuCl}_2$ solution	154

## NOMENCLATURE

$E_{ij}^0$	hydrogen bond energy
$\Delta G_{mix}$	free energy of mixing
$\Delta G_{el}$	elastic contribution to free energy
$\Delta G_{HB}$	hydrogen bonding contribution to free energy change
$\Delta G_{LF}$	lattice fluid contribution to free energy change
$\Delta H_N$	enthalpy of dissociation
$\Delta H$	enthalpy of mixing
$\Delta S$	entropy of mixing
$\Delta F$	free energy difference between the polymer segment-segment and polymer-solvent interactions
$G_{ij}^0$	standard-state of free energy of hydrogen –bond formation between $i - j$ pair
$k$	Boltzmann constant
$N$	number of molecules
$N_i^d$	number of donors of type $i$
$N_a^j$	number of acceptors of type $j$
$N_{ij}$	number of hydrogen bonds formed between an $i - j$ pair
$P$	pressure
$Q$	partition function
$r$	segment length

$R$	gas constant
$S_{ij}^{\circ}$	standard-state entropy change of hydrogen bonding
$T$	absolute temperature
$v$	volume
$V_{ij}^0$	standard-state hydrogen bonding volume change
$V$	volume of gel
$V_0$	Volume of gel synthesized
$C_0$	Concentration of the metal solution outside the gel
$V_1$	Amount of water picked up by the gel
$M_c$	molecular weight of the polymer chains between the crosslinks
$M_N$	number average molecular weight
$f$	number of ionizable groups per chain
$G$	modulus of the gel

Greek letters

<b><math>d</math></b>	flexibility parameter of an $r$ -mer
<b><math>e</math></b>	mean field interaction energy per mer
<b><math>z</math></b>	binary interaction parameter
<b><math>m</math></b>	chemical potential
<b><math>m</math></b>	chemical potential of the solvent within the gel
<b><math>m^0</math></b>	chemical potential of the solvent outside the gel
<b><math>n</math></b>	fraction of hydrogen bonds

$n_e$	number of elastically active chains
$\mathbf{r}$	density
$\mathbf{s}$	symmetry parameter of an $r$ -mer
$\mathbf{f}$	close packed volume fraction
$\mathbf{f}_2$	volume fraction of the network
$\mathbf{f}_0$	polymer volume fraction in the as synthesized gel
$\mathbf{w}$	$=\mathbf{dr}/\mathbf{se}^{r-1}$
$\mathbf{c}$	interaction parameter between the polymer and the solvent
$\bar{\mathbf{n}}$	specific volume of the polymer
$\mathbf{a}$	strain
$\mathbf{s}$	stress
$\mathbf{t}$	reduced temperature
$\mathbf{j}_p$	Concentration
$\mathbf{p}$	Osmotic pressure

#### Subscripts

1	polymer
2	solvent

#### Superscripts

~	reduced
*	close packed

#### Acronyms

DEAA	Diethylacrylamide
MMA	Methyl methacrylate
NVP	N-vinyl-2-pyrrolidone
HEMA	2-hydroxy ethyl methacrylate
DMEMA	N, N <sub>1</sub> -dimethylamino ethyl methacrylate
PMA	poly (metacrylic acid)
PEG	poly (ethylene glycol)
AAc	Acrylic acid
Am	Acrylamide
NIPAm	N-isopropylacrylamide
LCST	Lower critical solution temperature
UCST	Upper Critical Solution Temperature
VPT	Volume phase transition
LF	Lattice-Fluid
LFHB	Lattice-Fluid-Hydrogen-Bond
NnPAm	N-n-propylacrylamide
NCPAm	N-cyclopropylacrylamide
DEAMA	Diethylamino ethyl methacrylate
DMAEMA	N.N-dimethylamino ethyl methacrylate
CCA	Crystalline colloid arrays
AMPS	2-acrylamido-2-methyl-1-propane sulfonic acid
AAA	2-acetamido acrylic acid
EMAc	Ethylene-co-methacrylic acid
Nafion	Flourinated polymer
SSA	Styrene sulfonic acid

MIP	Molecularly imprinted polymer
SA	Stearyl acrylate
HA	Hexadecyl acrylate
DA	Dodecyl acrylate
N-t-Bam	N-tertiary-butylacrylamide
NIPAm	N-isopropyl acrylamide
Bis-Am	N, N'-methylene bis-acrylamide
DMSO	Dimethyl sulfoxide
AIBN	Azo isobutyronitrile
FT-IR	Fourier Transform Infrared spectroscopy
Bu-AMPS	Copolymer of N-tertiary-butylacrylamide and 2-acrylamido-2-methyl propane sulfonic acid
ip-AMPS	Copolymer of N-isopropyl acrylamide and 2-acrylamido-2-methyl propane sulfonic acid
A4ABA	Acryloyl-4-amino butyric acid
A6ACA	Acryloyl-6-amino caproic acid
CrO <sub>3</sub>	Chromium trioxide
CoCl <sub>2</sub>	Cobalt chloride
CuCl <sub>2</sub>	Copper chloride
TEMED	N, N, N', N'-tetramethylethylenediamine
APS	Ammonium persulphate
EPR	Electron paramagnetic resonance

# Chapter 1

## INTRODUCTION

*“All human knowledge begins with intuition proceeds then to concepts and ends up with ideas”*

*-I Kant*

Development in the field of gel science and technology has gained considerable momentum in the past decade mainly due to the discovery of stimuli responsive properties of polymeric gels. Although conventional superabsorbing properties of polymer gels continue to dominate the commercial applications of these materials, some of the gels are increasingly being looked at as “intelligent” or “smart” materials because of their ability to undergo volume and/or shape transitions in response to external stimuli.

Numerous stimuli such as temperature, pH, electric field, magnetic field and chemical triggers have been shown to induce volume phase transition (VPT) in hydrogels (Tanaka, 1978; Katchalsky *et al.*, 1950; Tanaka *et al.*, 1982; Katayama *et al.*, 1985; Suzuki *et al.*, 1990; Osada *et al.*, 1992; Zrinyi *et al.*, 1996; Kataoka *et al.*, 1998; Miyata *et al.*, 1999). The stimuli responsive behaviour continues to drive innovation of a high degree in the chemistry and technology of gels and has opened a new field of inter-disciplinary research. For example, gels have been designed for use as smart windows that can modulate the intensity of sunlight coming into a room (Dagani, 1997). Gels

have been designed to produce smart shoe soles that can accurately conform to the contours of human foot thus providing comfort during movement (Dagani 1997). Gels have been tailored to produce smart sensors that can detect small levels of blood-glucose (Holtz *et al.*, 1997) and as in situ insulin pumps to control glucose levels (Kataoka *et al.*, 1998). Gels have been used as soft actuators for applications in robotics and bio-medical devices, for instance, as soft fingers of robots (Hu *et al.*, 1995) and as smart valves in hearts (Osada *et al.*, 1993). Gels are also used to pick up or release molecules through recognition (Oya *et al.*, 1999; Alvarez-Lorenzo *et al.*, 2000) and as smart catalysts to modulate chemical reactions (Bergbreiter *et al.*, 1998).

In recent years, there has been an interesting focus on combining hydrogels with other materials such as nano-particles to form “hydrogel hybrids” or “gel + materials” that have novel properties and applications (Weisman *et al.*, 1996; Tsuji *et al.*, 1997). Several of these applications are commercialized (Dagani, 1997) and new ones are being enthusiastically investigated worldwide.

Smart gels are also considered to be excellent model systems for developing biomimicking devices. The motivation for such research is due to the fact that nature has evolved smart gel-like living objects, for instance a jelly-fish, that can carry out complex functions such as sensitive responsiveness, shape memory, selectivity, self-mobility, self-organization, self-healing and reproduction. Of these, the first four features have already been demonstrated in synthetic gels. We will demonstrate in this work that



synthetic gels can also self-organize and self-heal. The last feature remains perhaps the greatest challenge to development of bio-mimicking synthetics.

Polymer gels belong to a general class of materials called associating polymers, which contain in their chemical structure both hydrophilic and hydrophobic groups that form intra and inter molecular associations. These associations have significant implications in the functioning of biopolymers, polyelectrolytes, stimuli responsive polymer gels and rheological modifiers. In the case of stimuli sensitive polymer gels the volume and/or shape transitions are driven by the formation and breakage of associations between the hydrophilic and hydrophobic groups on the network. Among the various types of stimuli responsive gels, those sensitive to small temperature changes, i.e., thermoreversible gels, have attracted much attention. The most widely studied thermoreversible gel namely, a lightly cross-linked poly (N-isopropylacrylamide) (PNIPAm) gel shows discontinuous swelling-collapse volume phase transition at 34°C, which is close to the lower critical solution temperature (LCST) of the linear polymer (Hirokawa *et al.*, 1984).

The mechanism of temperature induced volume phase transition of hydrogels has been extensively investigated experimentally and theoretically (Dusek and Patterson, 1968; Heskin *et al.*, 1968; Otake *et al.*, 1989; Prange *et al.*, 1989; Marchetti *et al.*, 1990; Schild *et al.*, 1990, 1992; Shibayama *et al.*, 1994, 1996; Lele *et al.*, 1995; Badiger *et al.*, 1998; Grinberg *et al.*, 1999). The macroscopic VPT of thermoreversible gels has been shown to occur by a rearrangement of hydrogen bonds in the polymer-water mixture (Walker *et al.*,

1987; Prange *et al.*, 1989) or by the hydrophobic interactions (Otake *et al.*, 1989) or a combination of these two (Lele *et al.*, 1995).

Understanding the effect of hydrophilic–hydrophobic balance on LCST phenomenon has been an active research area and some correlations have been identified so far. For example, it has been shown that the chemical structure and the concentration of hydrophilic and hydrophobic groups in thermoreversible gels can be used to fine-tune the volume phase transition temperature (e.g., Inomata *et al.*, 1995 and Katakai *et al.*, 1996). Similarly, it has been shown that hydrophilic comonomers increase the volume transition temperature, while hydrophobic comonomers decrease the volume transition temperature of thermoreversible gels (see for example, Feil *et al.*, 1993; Badiger *et al.*, 1998). Thus it is known that in general, the hydrophilic and hydrophobic groups can modulate volume phase transition phenomenon in gels. However, the question of why only certain polymer gels show a distinct thermoreversible volume phase transition has remained unanswered to a large extent. This is because the quantification of the combination of hydrophilic and hydrophobic interactions on VPT is still not complete. The understanding of the fundamental reasons underlying VPT is crucial to the development of new, tailor-made gels that can be used for novel applications. In this work we will demonstrate that a critical balance of hydrophilic and hydrophobic interactions is essential for a gel to exhibit a temperature driven discontinuous volume phase transition.

Another dimension that has been added in recent years in the development of new gels and their novel applications is that of “hydrogel hybrids”, which are composite materials formed by combining a hydrogel matrix with other materials to yield unique set of properties. For example, hydrogels have been combined with regularly arranged array of nanoparticles to produce optical devices that can act as smart molecular sensors (Weisman *et al.*, 1996; Holtz *et al.*, 1997). Another example of a hydrogel hybrid is that of metal-complexed stimuli-responsive gels, which have recently been used as catalysts, wherein the complexed metal acted as the catalytic site and the VPT of the gel was independently used to control the reaction rate (Bergbreiter *et al.*, 1998a). Such catalysts potentially enjoy the advantages of homogeneous and heterogeneous catalysis. Metal-complexed gel catalysts can also be used in biotechnology. For instance, copper protein complexes having various nuclearity are known to catalyze many biological functions such as oxygen transport and ion metabolism (Solomon, 1994). Another application of metal complexed polymers is in the area of wastewater treatment, wherein gels can be tailored to remove toxic metal ions from effluents (Tanaka *et al.*, 1996).

The capacity of a polyelectrolyte gel to pick-up metal ions depends on the chemical structure of the gel, i.e., on the hydrophilic and hydrophobic interactions of the gel. Although a series of studies have been carried out in literature to investigate the swelling behavior of polyelectrolyte gels in monovalent, divalent and polyvalent ions, no attempts other than those of Sasaki *et al.* (1998) have been made for understanding the effect of

hydrophobicity of the polymer on its binding efficiency with the cations. Similarly, although it is known that linear polyelectrolytes, when complexed with divalent ions adopt a compact conformation, and many of them precipitate out from the system, no attempts have been made to examine the possible changes in the effective hydrophobicity of a polyelectrolyte gel on complexation with metal ions. In this work we will show that metal-complexation induces an effectively higher hydrophobicity in a thermoreversible gel, thereby directly affecting its volume transition temperature. Thus, metal-complexation offers a subtle way to tailor the hydrophilic-hydrophobic balance in gels. We will also show that the hydrophobicity of the gel, in turn affects the coordination structure of the polymer-metal complex and the metal uptake. This has implications in designing gels for effluent treatment and for potential gel-catalysts.

Another novel and exciting set of results reported in this thesis are those related to metal-complexation driven macroscopic self-organization and self-healing in amphiphilic hydrogels. Self-organization (or self-assembly) is a new area in gel science and technology and not much work has been reported yet. Osada and coworkers (Matsuda *et al.*, 1994, 2000; Osada *et al.*, 1995; Uchida *et al.*, 1995) have molecularly tailored new amphiphilic hydrogels exhibiting supra molecular self-assembly by using hydrophilic-hydrophobic interactions. Such gels have been shown to exhibit shape memory and it has been proposed that they could find applications as fingers for robotics.

Nature uses the phenomenon of self-organization at microscopic and macroscopic levels to create a variety of intricate structures, which carry out complex functions. At a microscopic level, biomolecules self assemble into micelles, vesicles, sheets and tubules (Israelechivili, 1992). The structure of biological macromolecules such as proteins, DNA, lipids, is determined by the way in which they organize themselves. The claim of gels to be called true biomimetic systems would certainly improve if the gels can self-organize into ordered structures. An insight into self-assembly technique may help to design, engineer and fabricate synthetic structures for the development of advanced materials, which can function like living organisms.

In summary, the work reported in this dissertation pertains to several novel aspects of stimuli-responsive hydrogels. These are:

1. Understanding the role of the balance of hydrophilic-hydrophobic interactions on volume phase transitions in thermoreversible hydrogels.
2. Understanding the inter-relations between metal complexation and the effective hydrophobicity of hydrogels
3. A demonstration of metal-complexation driven self-organization and self-healing phenomenon in lightly cross-linked hydrogels that have a critical balance of hydrophobic and hydrophilic interactions.

It is evident that the crucial role played by the hydrophobic and hydrophilic interactions in these associating polymer gels is common to all of the above seemingly diverse phenomena. We believe that this work, for the first time, has been able to provide answers to some important fundamental

questions on the cause of volume phase transitions in gels as well as to demonstrate several new phenomena in hydrogels that bring such materials closer to be called true bio-mimetics.

# Chapter 2

## LITERATURE SURVEY ON INTELLIGENT GELS

### 2.1 Introduction

Associating polymers display unusual physico-chemical properties, which arise due to the strong inter/intra molecular associations between the hydrophilic and/or hydrophobic groups present in these polymers. Such associations have significant ramifications in the properties of biopolymers, polyelectrolytes, thickeners and coatings. Biopolymers show strong associations because of which they self assemble into complex structures such as a DNA double helix. Similarly, proteins and lipids fold in such a way as to expose their hydrophilic parts to the surrounding aqueous solution and hide the hydrophobic parts into a core. The self-assembled structures driven by molecular associations perform highly specific and complex functions in living organisms.

Synthetic associating polymers have found applications in rheology modification, coatings and soft solids (gels). In 1948 B. A. Tom first observed drag reduction, i.e., a decrease in pressure drop for turbulent flow in a pipe, when a small amount of polymeric additives were present in the fluid. Hence this phenomenon is also known as Tom's phenomenon. Many theories have been proposed to explain the effect of polymeric additives on drag reduction. Among them the most popular concept is that the polymer molecules avoid the growth of the vortices in a turbulent flow due to their ability to stretch elastically. However, stretching also induces chain scission, which in turn decreases the ability to cause drag reduction.

Hydrophobically modified polymers provide a facile method of drag reduction by associating to form long macromolecules and by dissociating without chain scission to retain the drag-reduction efficiency (McCormick *et al.*, 1989a, 1989b; Mumick *et al.*, 1994). Hydrophobically modified associating polymers are also widely used as thickening agents because of their ability to show an increase in viscosity due to intermolecular association (Gelmen *et al.*, 1986; Winnik, 1987; Glass, 1989). Such polymers find applications in the paint industry.

Hydrophobically modified polymers have also found applications in enhanced oil recovery. Water flooding is the conventional method used to recover the petroleum oil trapped within the small pores of rock matrix in reservoirs. Hydrophobically modified polymers are added to the water in order to increase the viscosity of the solution, which significantly reduces the fingering of water through high permeability stacks. Similarly, the retention of polymer results in the diversion of the solution into the oil rich zones thereby sweeping the additional oil.

## **2.2 Gels**

In a dilute solution polymer chains are independent of each other, however, in the case of concentrated solutions they entangle to form viscoelastic solutions and soft gels. In the case of strongly associating polymers the macromolecular chains in the solution do not merely entangle but form intermolecular associations to create a stronger network (soft gel). Rubber comes under the category of hard gels, whereas jellies and soft contact lens belongs to the class of soft gels. In particular, soft gels possess the cohesive properties of solids and the transport properties of liquids.

This chapter presents an overview of gels and their swelling



behaviour. It covers both super absorbents and stimuli-responsive gels. Among the various types of stimuli responsive gels, those of the thermoreversible type have been discussed in detail because of their direct relevance to the present work. We discuss the various theoretical models used to predict the swelling -collapse transition in gels and their molecular implications. The role of hydrophilic-hydrophobic interaction on the Volume Phase Transition (VPT) observed in gels has been discussed in detail. The current trends in gels such as "gel + materials" or "gel hybrids" have been discussed with special effort. Finally, the current state of art in gels such as biomimicking gels and supramolecular self-assembled gels has also been discussed in detail.

As the eminent chemist Dorothy Jordan Lloyd noted nearly 75 years ago, gels are "easier to recognize than define". In general, a gel represents a state of matter, which is in between a solid state and a liquid state. Gels consist of a three-dimensional network of macromolecular chains filled with a compatible solvent, as shown in Figure 2.1, in which the network provides elasticity to the system.

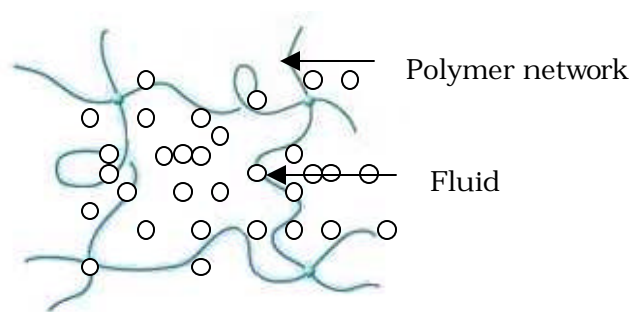


**Figure 2.1:** Schematic of a gel

The elastic network holds the solvent inside the matrix by osmotic forces, while the liquid prevents the polymer network from collapsing into a compact mass. The combination of these two parameters, namely, the osmotic forces and the elastic reactivity, defines the properties of the gels. Depending upon the chemical composition and other factors, gels can vary in consistency from viscous fluids to fairly rigid solids. But basically they are wet, soft and capable of undergoing large deformation.

There are many natural and artificial gels. One of the familiar natural gels is the dessert jello, wherein the network is comprised of macromolecular chains derived from gelatin, an animal protein. Of the total volume, the network constitutes only 3% while the remainder is colored, flavored, sweetened water. Living organisms are largely made of gels. Mammalian tissues are aqueous gels, made up of proteins and polysaccharide networks. This helps the organisms to transport oxygen, nutrients and other molecules easily and effectively while retaining their solid nature. Indeed, biological systems consist mainly of soft substance. For instance, the sea cucumber is essentially a water-swollen gel containing primitive organs, nevertheless, it can function like other living organisms as well as protect itself from enemies (Osada *et al.*, 1993). Examples of artificial gels are abundant in cosmetics and food industry (Dagani, 1997). Another important example of an artificial gel is that of superabsorbent polymers, which will be described shortly.

In principle, gels can be divided into two categories: physically crosslinked gels and chemically crosslinked gels. Materials in which polymer chains form a transient network through chain entanglements and/or intermolecular associations are typically known as physical gels. In such gels the network structure is formed by secondary forces such as

hydrogen bonding, dispersion forces, van der Waal's forces, hydrophobic and ionic interactions. Soaps, phospholipids, natural polymers such as jello, etc., fall under this category. Physical crosslinks are semipermanent in nature and can be broken or formed by subjecting the gel to changes in temperature, pressure and stress. Chemically crosslinked gels are those in which the network structure is formed by covalent linkages. These gels are irreversible in the sense that the network structure cannot be destroyed until the covalent bonds are destroyed and the polymer is degraded. Covalently crosslinked networks of water-soluble polyelectrolytes are generally referred as hydrogels.

### **2.2.1 Superabsorbent gels**

Superabsorbents constitute the single largest type of industrially manufactured polymeric gels. They find applications in personal care products and agricultural aids (Buchholz, 1994, 1999; Wang *et al.*, 1997). Global capacity for super absorbent polymers is being increased in an anticipation of a strong demand in the coming years. For instance, Dow Chemicals has started two plants of 30,000 tonnes/year in Asia (Chemical Market Reporter. 24, May, 1999). It has also established a new acrylic acid unit in Germany with a capacity of 10,000 tones/year. Chemdal, the leader of superabsorbents in US market has commissioned a new 80,000 tonnes/year plant in Thailand and also expanded the production of other units (Chemical Market Reporter. 24, May, 1999). US demand for acrylic superabsorbents is 2,84,000 tonnes/year and is rising at 5-10% per year.

Super absorbent gels are ionic in nature. One of the striking properties of ionic gels is their ability to swell to nearly thousand times of their own weight with water. This swelling property forms the basis of

application of superabsorbent gels in personal care products. The extent of swelling under conditions of low pH and/or salt concentrations that are typically found in body fluids is the principal specification for superabsorbent polymers. Superabsorbent polymeric networks can be anionic, cationic or zwitterionic in nature. The ionic groups on the networks are mainly carboxyl ions, sulfonic ions or quaternary ammonium ions. The repulsion between the ionic groups on the network is responsible for keeping the network chains away from each other, thereby greatly enhancing the swelling capacity of the gels.

### **2.2.2. Equilibrium swelling of hydrogels**

Swelling of gels arises from the osmotic affinity between macromolecules and solvent molecules. The capacity of hydrogels to absorb and retain water is restricted by the crosslink density of the network, which determines its elasticity. The "equilibrium" swelling capacity of a gel is the balance of two opposing forces, namely the osmotic pressure, which swells the gel, and the elastic retraction, which restricts swelling. Flory (1953) proposed an analogy between the swelling equilibrium and the osmotic equilibrium. The original Flory-Huggin's regular solution theory, also known as Liquid Lattice Theory, calculates the entropy and enthalpy change required for randomly distributing the polymer molecules on a lattice along with the solvent molecules as shown in the following schematic, Figure 2.2.

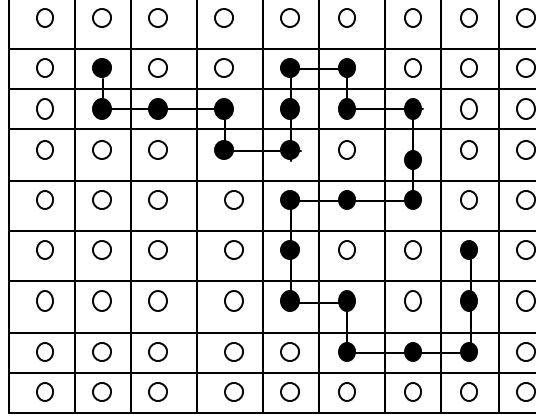


**Figure 2.2:** Polymer segment distributed along with the solvent in the liquid lattice.

According to his theory the net osmotic pressure ( $\mathbf{p}$ ) acting on the gel is the total force arising from polymer-polymer affinity and rubber elasticity. Thus,

$$\mathbf{p} = \mathbf{m}_1 - \mathbf{m}_1^0 = RT \left\{ \ln(1 - \mathbf{f}_2) + \mathbf{f}_2 + \mathbf{c} \mathbf{f}_2^2 + V_1 \left( \frac{\mathbf{n}_e}{V_0} \right) \left( \mathbf{f}_2^{1/3} - \frac{\mathbf{f}_2}{2} \right) \right\} \quad (2.1)$$

Here  $\mathbf{m}_1$  and  $\mathbf{m}_1^0$  are chemical potentials of the solvent within the gel and outside the gel, respectively.  $\mathbf{f}_2$  is the volume fraction of the network,  $\mathbf{c}$  is the interaction parameter between the polymer and the solvent,  $R$  is the gas constant,  $T$  is the absolute temperature,  $V_1$  is the molar volume of the solvent  $\mathbf{n}_e$  represents the moles of crosslinks in the network and the term

$\frac{\mathbf{n}_e}{V_0}$  is the crosslink density of the as-synthesized gel. The first three terms

on the right hand side of equation (2.1) arise from the free energy change during mixing of the polymer and the solvent molecules, while the last term arises from the entropic free energy change of classical rubber elasticity

assuming Gaussian chains. At equilibrium swelling, the net osmotic pressure should be zero. Hence equation (2.1) becomes

$$-\{\ln(1-f_2)+f_2+cf_2^2\}=\left(\frac{V_1}{\bar{n}M_c}\right)\left[1-\frac{2M_c}{M_n}\right]\left(f_2^{1/3}-\frac{f_2}{2}\right) \quad (2.2)$$

Here,  $\bar{n}$  is the specific volume of the polymer,  $M_c$  is the molecular weight between the crosslinks and  $M_n$  the number average molecular weight. The term  $\left(1-\frac{2M_c}{M_n}\right)$  is the correction factor of network imperfection resulting from dangling chain end segments. Equation (2.2) can be simplified to

$$q^{5/3}=\left(\frac{\bar{n}M_c}{V_1}\right)\left[1-\frac{2M_c}{M_n}\right]\left(\frac{1}{2}-c\right) \quad (2.3)$$

where  $q$ , the swelling ratio, is given by

$$q=\frac{\text{volume of swollen gel}}{\text{volume of dry gel}}=\frac{1}{f_2} \quad (2.4)$$

Equations (2.2 - 2.4) show the relationship between the swelling ratio, the crosslink density and the thermodynamic quality of the solvent. The swelling capacity of nonionic gels is limited compared to that of ionic gels. The super swelling of ionic gels is attributed to the long-range electrostatic repulsion between ionic groups that are fixed on the network. The dissociation of the ionic groups influences the Donnan equilibrium of mobile counterions between those inside the gel and outside of it. The observed rise in osmotic pressure is dependent on the mobile ion concentration. Tanaka *et al.* (1980) modified the Flory-Huggin's formula by including the contribution of H<sup>+</sup> ions dissociated from the ionizable groups. For ionic gels the osmotic pressure ( $p$ ) can be written as,

$$\begin{aligned}
\mathbf{p} = & -\frac{NkT}{V_1}[\mathbf{f}_2 + \ln(1-\mathbf{f}_2) + c\mathbf{f}_2^2] + \mathbf{n}_e kT \left[ \frac{\mathbf{f}_2}{2\mathbf{f}_0} - \left( \frac{\mathbf{f}_2}{\mathbf{f}_0} \right)^{1/3} \right] \\
& + \mathbf{n}_e f kT \left( \frac{\mathbf{f}_2}{\mathbf{f}_0} \right)
\end{aligned} \tag{2.5}$$

Here  $\mathbf{f}_0$  is the polymer volume fraction in the as-synthesized gel,  $f$  denotes the number of ionizable groups per chain incorporated into the network. As the value of  $f$  increases the swelling ratio increases.

### 2.2.3 Mechanical properties of hydrogels

The mechanical properties of a hydrogel depend upon various parameters such as the chemical nature of the macromolecules from which it is synthesized, synthesis procedure, the extent of swelling, the initial monomer concentration, the temperature of measurements and the crosslink density of the network (Hirotzu *et al.*, 1990; Shibayama *et al.*, 1994; Chen *et al.*, 1997; Patil *et al.*, 1996; Perera *et al.*, 1996). Ulbrich and Kopeck (1979) have pointed out the importance of hydrophobic interactions on the mechanical properties. They observed better mechanical properties for copolymer gels of N, N-diethylacrylamide (DEAA) and N-tert-butylacrylamide (N-t-BAm) than that of the DEAA homopolymer gel. According to the authors the observed improvement in the mechanical properties is mainly due to the influence of hydrophobic interactions between the individual segments of the polymer network along with the lower equilibrium degree of swelling.

Perera *et al.* (1996) have drawn an analogy between the overall crosslinking density and modulus by showing that as the crosslinking density ( $\mathbf{n}_e$ ) increases the modulus increases. They have also

demonstrated the role of chemical nature of the polymers on modulus. For example, the modulus of poly (methyl methacrylate-co-N-vinyl-2-pyrrolidone) gel (MMA/NVP) is higher than that of poly (2-hydroxy ethyl methacrylate-co-N-vinyl-2-pyrrolidone) gel (HEMA/NVP). According to them the higher modulus observed in the case of MMA/NVP is attributed to the additionally incorporated physical interactions due to the hydrophobic comonomer, which limit the swelling of the gel. Similarly, Davis *et al.* (1988) have elucidate the contribution of hydrophobic interactions in the gel to the effective crosslink density and hence to the elastic modulus.

Patil *et al.* (1996) have shown the effect of initial monomer concentration on the modulus of the polymer gel in poly (sucrose acrylate) gels. According to them by increasing the initial monomer concentration from 15% to 50%, the swelling ratio is decreased from 18 to 5, which in turn leads to an enhancement in modulus. The decrease in swelling ratio with higher initial monomer concentration is due to the increase in polymer chain entanglements that would effectively increases the cross-link density. According to Chen *et al.* (1997) the mechanical properties of the gels strongly depend on the preparation procedure. For example, N, N<sup>1</sup>-dimethylamino ethyl methacrylate (DMEMA) gels prepared by bulk polymerization show good mechanical properties which are attributed to the small swelling ratio of the gels due to the additional physical cross-linking. On the contrary, hydrogels prepared by solution polymerization using aqueous medium show poor mechanical properties with large swelling ratios.

The characteristic features of a polymer gel that define it as a solid are its non-flowing nature and a finite modulus. A lightly crosslinked



polymer gel has a finite modulus, which is directly proportional to its crosslink density by the simple relation,

$$G = \frac{n_e}{V} RT = \left( \frac{n_e}{V_0} \right) \frac{f}{f_0} RT \quad (2.6)$$

where,  $G$  is the modulus,  $R$  is the gas constant and  $T$  is the absolute temperature. The modulus of the gel is measured by a compression test in which the gel is compressed by controlling the strain ( $\mathbf{a}$ ), while the stress ( $\mathbf{s}$ ) required for compression is recorded. For small strain the relation between stress and strain for a swollen polymer gel is given by (Tobolsky, 1961)

$$\mathbf{s} = \frac{n_e}{V_0} RT \left( \frac{f}{f_0} \right)^{1/3} \left( \mathbf{a} - \frac{1}{\mathbf{a}^2} \right) \quad (2.7)$$

Thus a plot of  $\mathbf{s}$  versus  $\left( \mathbf{a} - \frac{1}{\mathbf{a}^2} \right)$  gives the modulus as the slope of the best-fit line to the data. Equation (2.7) also describes the fact that higher the swelling capacity, lower is the modulus of the gel. However, the scaling  $G \sim f^{1/3}$  predicted by the linear rubber elasticity theory is not found to be valid at large swelling (Patil *et al.*, 1996).

### 2.3 Stimuli-responsive hydrogels

Although superabsorbent gels continue to dominate the industrial market among all known applications of synthetic polymer gels, the recent spurt of R & D activity in hydrogels has been stimulated by a different class of gels known as "stimuli-responsive" gels. In fact the Japanese have recognized this class of gels as one of the materials of the 21<sup>st</sup> Century

mainly because of the "smartness" or "intelligence" displayed by such gels. The Figure 2.3 shows the number of research publications in *Nature* and *Science* in the area of stimuli responsive gels in the last twenty years.

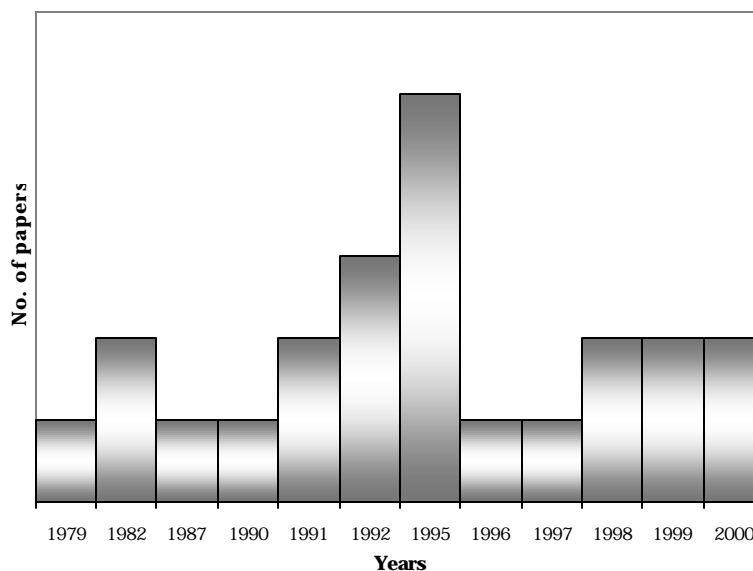


**Figure 2.3:** Number of papers published in *Nature* and *Science* for the last twenty years on intelligent gels

Stimuli-responsive gels undergo a discontinuous and large volume phase transition (VPT) between a swollen and a collapsed state when subjected to a small change in one or more environmental stimuli such as temperature (Tanaka, 1978), pH (Katchalsky *et al.*, 1950; Siegel *et al.*, 1988), solvent composition (Tanaka, 1978, 1981; Ilavsky *et al.*, 1982, 1984), salt concentration (Ohmine *et al.*, 1982; Annaka *et al.*, 2000), electrolyte concentration (Badiger *et al.*, 1992), electric field (Tanaka *et al.*, 1982; Osada *et al.*, 1992), magnetic field (Barsi *et al.*, 1996; Zrinyi *et al.*, 1996, 1997a, 1997b, 1997c; Szabo *et al.*, 1998; Xulu *et al.*, 2000), light (Irie., 1986,1993; Suzuki *et al.*, 1990; Willner *et al.*, 1991) and chemical triggers (Kokufuta, *et al.*, 1991; Kataoka *et al.*, 1994, 1998; Miyata *et al.*, 1999).

Gels can also be engineered to respond to an internal stimulus (Yoshida *et al.*, 1997).

In general, the volume transition between the swollen and the collapsed phases can be either continuous (e.g. PEO gels) or discontinuous (e.g. PNIPAm gel) in nature and is strongly dependent on the degree of ionization, the stiffness of the polymer chains (Tanaka *et al.*, 1980; Nicoli *et al.*, 1983) and the chemical structure of the monomer comprising the gel (Inomata *et al.*, 1990). The swelling-collapse VPT exhibited by PNIPAm gel is discontinuous and reversible in nature. It is also accompanied by hysteresis i.e., the threshold temperature at which the swollen phase transforms into a collapsed phase is different from the threshold temperature at which the reverse transition occurs as shown in the Figure 2.4 and is a characteristic property of volume transition in gel systems (Hoirokawa *et al.*, 1984; Matsuo *et al.*, 1988; Sekimoto, 1993; Tomari *et al.*, 1995; Seker *et al.*, 1998). The hysteresis arises due to the difference in the dynamics of the swelling and deswelling phenomena. The threshold temperature difference is only 0.2°C for nonionic gels where as for ionic gels it can be large as 10°C. Thus, a discontinuous VPT has all the characteristics of a first order transition.

In addition to the synthetic polymeric materials, natural polymers like gelatin, agrose polypeptides and DNA also exhibit phase transition (Amiya *et al.*, 1987). Verdugo (1986) found a fascinating example of phase transition in biological systems: Slug mucin is stored in the body in an extremely compact form. When secreted out of the body, it absorbs water and swells more than 1000 times. The slugs are thus able to retain water and maintain the moist environment necessary for their survival. When the calcium concentration around the mucins increases, they deswell.

Similarly, Takushi *et al.* (1990) reported that a boiled egg turns from whitish to translucent (close to transparency) at subzero temperatures.

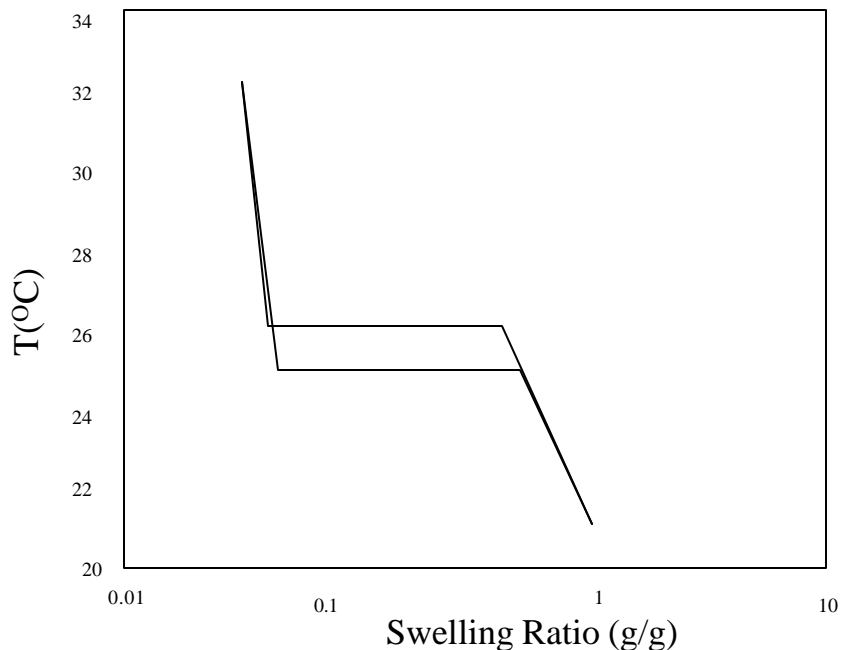


**Figure 2.4:** First order volume phase transition accompanied by hysteresis as a function of temperature

Intelligent gels have been creatively utilized in a number of novel applications such as for example, in molecular sensors (Kokufuta *et al.*, 1991; Holtz *et al.*, 1997), chemical and bio-separations (Cussler *et al.*, 1984; Gehrke *et al.*, 1986; Freitas *et al.*, 1987; Feil *et al.*, 1991; Badiger *et al.*, 1992; Wang *et al.*, 1993), separation method for immunoassay (Monji *et al.*, 1987), actuators (Kwon *et al.*, 1991; Liu *et al.*, 2000), controlled drug-delivery systems (Hoffman, *et al.*, 1986, 1987; Bae *et al.*, 1987; Okano *et al.*, 1990; Karmalkar *et al.*, 2000) artificial muscles (Osada *et al.*, 1992, 1993; Yoshida *et al.*, 1997; Szabo *et al.*, 1998; Liu *et al.*, 2000) and biocatalysts (Park *et al.*, 1988, 1990)

The stimuli responsiveness of hydrogels is attributed to the various types of polymer-polymer and polymer-solvent interactions. The fundamental interactions, which control the swelling-deswelling behavior of thermoreversible gels are ionic interactions, hydrophobic interactions, hydrogen bonding and van der Waals forces (Ilmain *et al.*, 1991) as shown schematically in Figure 2.5.

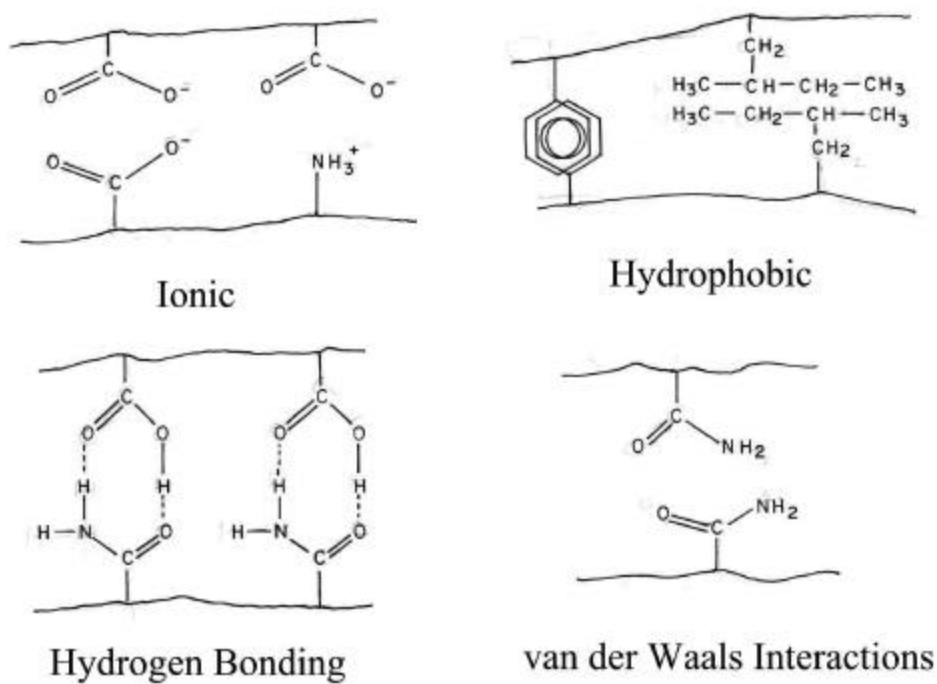


**Figure 2.5:** Fundamental forces those are responsible for the volume transition phenomenon in hydrogels

It is believed that these interactions may be independently or jointly responsible for discontinuous volume transitions in polymeric gels.

Interestingly, the reversible interactions in molecular biology also originate from the same forces that control the stimuli responsive properties in intelligent gels. These four fundamental forces are responsible for the unique configuration and biological functions (such as catalytic reactions and molecular recognition) in biopolymers. Hydrogen bonding associations between a poly (methacrylic acid) (PMA) gel and poly (ethylene glycol) (PEG) linear polymer has been used to demonstrate a chemo-mechanical device (Osada *et al.*, 1983)

### **2.3.1 pH-sensitive hydrogels**

pH sensitive gels usually contain ionic groups, which are known to change ionization with pH and thereby modify the properties of the gel. The first ionic gel investigated was based on acrylic acid and methacrylic acid (Katchalsky *et al.*, 1955; Michaeli *et al.*, 1957). Anionic pH sensitive gels show an increase in swelling ratio as the pH increases. This is attributed to the increase in the concentration of ions inside the macromolecular network due to the dissociation of ionic groups and the diffusion of counter ions into the network matrix from the surrounding medium. The higher concentration of ions inside the network increases the water flow into the gel due to the osmosis. Another important factor, which increases swelling, is the long-range repulsion of charges on the polymer chain. Chen *et al.* (1995) have studied graft copolymers that exhibit temperature induced phase transition over a wide range of pH.

### 2.3.2 Electric field-sensitive gel:

Hydrogels, which respond to an electric field potential, are targeted for development of chemo-mechanical systems. They can potentially convert chemical, electrical and thermal energies into mechanical energy (Osada *et al.*, 1993). For example, Osada *et al.* (1991) have developed a chemomechanical valve from poly (ethylene glycol-co-methacrylic acid) gel that is capable of controlling solute penetration using pulses in an electric current. An electric field-induced deformation in hydrogels was first observed by Tanaka *et al.* (1982), who showed that a copolymer gel of acrylic acid (AAc) and acrylamide (Am) shrinks under a small applied electric field potential between 0 to 5V. The electric field imposes a force on the cation causing a stationary current in the gel from anode to cathode. Similarly the field imposes a force on the negatively charged acrylic acid groups of the polymer network, thus pulling the gel towards the positive electrode. This creates a stress gradient across the width of the gel such that the part of the gel towards anode preferentially collapses while that near the cathode preferentially swells. This differential stress bends the gel.

Osada *et al.* (1992) have observed similar phenomena in the case of weakly crosslinked AMPS gels. When the anionic gel was dipped in positively charged aqueous surfactant solution and placed between two electrodes, the positively charged surfactant molecules got preferentially bound to one of the surfaces inducing a local shrinkage. When the field was reversed, the contraction was observed on the opposite side. The repeated action of this caused the gel to move in a worm-like fashion. Kwon *et al.* (1991) synthesized an electrically erodible gel based on poly (ethyloxazoline) and poly (methacrylic acid) or poly (acrylic acid). These polymers form complexes due to hydrogen bonding between carboxyl and oxazoline

groups. Under a small electrical current, the gel disintegrated into two water-soluble polymers.

### **2.3.3 Light sensitive gels**

Light sensitive gels are prepared by incorporating photosensitive molecules into the hydrogel network. Ishihara *et al.* (1982,1984) have reported a photosensitive hydrogel containing azo linkages. In 1990 Mamada *et al.* have reported a UV light sensitive gel, based on N-isopropylacrylamide and a photosensitive molecule like bis {4-(dimethylamino) phenyl (4-vinyl phenyl) methyl leucocyanide. Here the UV light initiates an ionic reaction within the gel creating an osmotic pressure, which induces swelling. In the absence of this light, the equilibrium moves towards the neutral polymer system and the gel collapses. Later Suzuki *et al.* (1990) have reported a visible light sensitive gel that is synthesized from N-isopropylacrylamide (PNIPAm) and a light sensitive chromophore, trisodium salt of copper chlorophyllin. Here the phase transition is induced by the direct heating of the polymer network by light. Willner *et al.* (1991) have demonstrated the photoregulation of the enzyme by using light sensitive gels. Recently Juodkazis *et al.* (2000) have reported reversible swelling collapse transition in PNIPAm gel due to the radiation force generated by laser beams.

### **2.3.4 Magnetic field sensitive gels:**

Magnetic field sensitive gels, called ferrogels, have been prepared by introducing magnetite particles of colloidal size into chemically crosslinked hydrogels (Zrinyi *et al.*, 1996, 1997a; Xulu *et al.*, 2000; Mayer *et al.*, 2000). Introduction of magnetite particles can be done by swelling the hydrogel in



ferrofluids. In ferrogels, the magnetic and elastic properties are coupled so that a significant shape distortion occurs instantaneously and disappears abruptly when an external magnetic field is applied or removed. The ability of magnetic field sensitive gels to undergo an abrupt change in shape can be used to create artificial muscles, soft actuator for robots, etc. (Szabo *et al.*, 1998; Liu *et al.*, 2000).

### **2.3.5 Temperature sensitive gels**

Crosslinked polymeric networks that undergo discontinuous swelling - collapse volume transition with respect to a slight change in temperature are known as thermoreversible gels. The swelling-collapse transition is discontinuous and reversible. For example, poly (N-isopropylacrylamide) (PNIPAm) gel shows a discontinuous swelling - collapse volume transition at a temperature near about 34°C, which is close to the lower critical solution temperature (LCST) of the linear polymer (Hirokawa *et al.*, 1984). Thermoreversible gels also exhibit a biphasic state in which swollen and collapsed phases coexists (Hirotsu, 1988; Suzuki *et al.*, 1990) at the transition temperature as shown in Figure 2. 6. Hu *et al.* (1995b) studied the phase transition in PNIPAm using IR beam as a trigger. The transparent gel turned opaque when the temperature rose above the transition temperature by the localized heating effect of the IR beam. This is attributed to the decomposition of gel network into dilute and dense regions. When the size of the micro-domains became comparable to the wavelength of the visible light, the light was scattered and the gel becomes opaque. A similar concept has been used to develop “smart window screens” that allow a controlled amount of light into the room (Dagani,

1997). Several such novel applications on thermoreversible gels have been developed (Snowden *et al.*, 1996).

Thermosensitive hydrogels can be divided generally into two categories: those, which exhibit an increase in swelling with temperature and those, which show a decrease in swelling capacity with temperature. Amongst all stimuli responsive gels, the thermoreversible gels have attracted most attention in published literature. They are also most pertinent to our studies in this work and are therefore described separately and in a more detailed way is what follows.

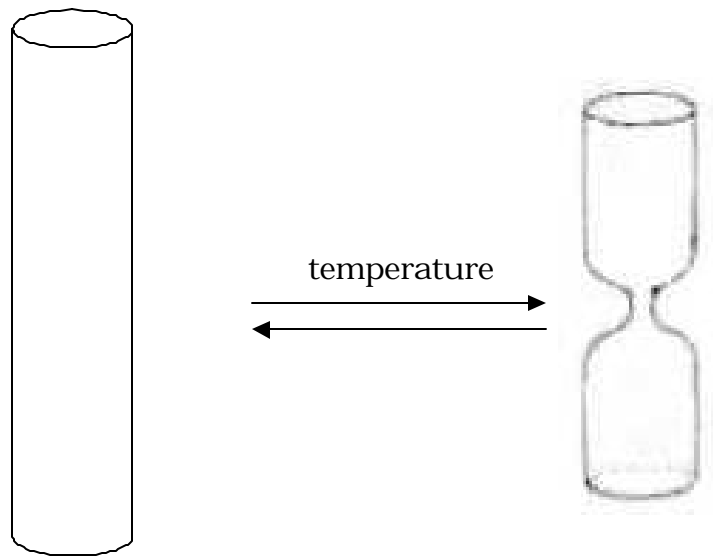


**Figure 2.6:** Co-existence of swollen as well as collapsed phase at the transition temperature

## 2.4 Temperature induced volume phase transition in polymer gels

### 2.4.1 Phase separation in polymer solutions

Phase separation in a miscible polymer-solvent binary system can be brought about by variations in temperature, pressure and/or composition. The two major classes of phase separations are (i) liquid-solid phase separation and (ii) liquid-liquid phase separation. The former is due to the nucleation and growth of solid crystals from a metastable solution, whereas in the latter two liquid phases separate out by either nucleation and growth or by spinoidal decomposition mechanisms.

Consider a homogeneous solution of a polymer in which the solvent chosen for the polymer becomes poorer in quality as the temperature lowers until finally a stage reaches where the polymer separates completely out of the solution. A temperature-composition phase diagram in Figure 2.7 shows the single-phase and two-phase regions of the mixture.

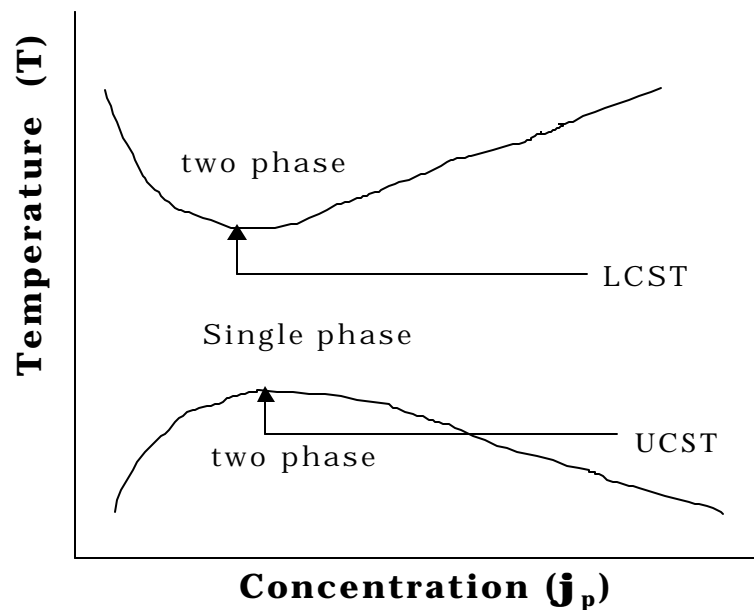


**Figure 2. 7:** Schematic picture exhibiting the co-existence curve for polymer - solvent binary system

A central feature of the phase diagram is the binodal (or the coexistence) curve. The extremism on the binodal curve is called the critical points at which the compositions of the coexisting phases merge. Since polymer-solvent binary systems exhibit a liquid-liquid type phase separation, the two phases namely, the polymer rich phase and the solvent rich phase, contain both components. The two-phase region is further divided into metastable and unstable regions. These regions exhibit different phase separation mechanisms and kinetics.

There are mainly two types of phase diagrams: UCST type and LCST type as shown in Figure 2.7. If the binodal curve shows a maximum then the temperature at this critical point is called the Upper Critical Solution Temperature (UCST). Similarly, if the binodal curve shows a minimum then the temperature at this critical point is called the Lower Critical Solution Temperature (LCST). The UCST type of phase behaviour is the 'normal' solubility behavior indicating that the polymer dissolves in the solvent on heating. It is commonly seen in non-polar polymers dissolved in non-polar solvents. For example, dissolution of polystyrene in dioctyl phthalate and polyisobutylene in benzene are facilitated by heating the mixtures. The UCST phase behaviour can be easily explained from the enthalpy and entropy changes during mixing. The free energy of mixing is given by,

$$\Delta G = \Delta H - T\Delta S \quad (2.9)$$

where  $\Delta G$  is the free energy of mixing,  $\Delta H$  is the enthalpy of mixing,  $T$  is the absolute temperature and  $\Delta S$  is the entropy of mixing. The polymer will remain in solution if the free energy of mixing is negative. For non-polar polymers dissolved in non-polar solvents, the enthalpy of mixing and the entropy of mixing are positive, which implies that the solution will become single phase on increasing the temperature.

The LCST type of phase behaviour is unusual and counter intuitive, where polymer precipitates on heating. The LCST type phase diagram is seen in two types of binary polymer solutions: (a) non-polar polymers in non-polar solvents at high temperature and pressure near the critical point of the solvent, and (b) polar polymers in polar solvents at much lower temperatures and ambient pressures. The former is attributed to the compressibility of the solvent, while the latter is attributed to the presence of specific interactions between the polymer and solvent molecules. In both cases, the entropy change and the enthalpy change during mixing are negative because of formation of specific configurations and interactions between the components of the mixture. Hence, the free energy of mixing is negative at lower temperatures and becomes positive on increasing the temperature. Thus, phase separation occurs on heating.

In an aqueous solution of a polar polymer such as PNIPAm, the phase behaviour is dictated by polar interactions such as hydrogen bonding associations between the polymer and the solvent molecules. Hydrogen bond formation between the polar groups on the polymer chain and the solvent molecule gives rise to a negative enthalpy of mixing and thereby lowers the free energy of the solution. However, now the molecules are forced to orient in particular configurations in order to form the hydrogen bonds thereby decreasing the entropy of the solution. It is also believed that the solvent molecules structure around the hydrophobic parts of the polymer (the so-called hydrophobic cage effect) resulting in a decreased entropy of mixing (negative  $\Delta S$ ) and hence a positive contribution to the free energy ( $\Delta G$ ). As the temperature of the solution increases the positive ( $T\Delta S$ ) term of the equation (2.9) dominates the negative ( $\Delta H$ ) terms and thus the polymer phase separates from the aqueous phase.

In the case of crosslinked polymers, the LCST phenomenon results in a volume phase transition (VPT). Below the volume transition temperature the gel swells in water and above the temperature it collapses. Quite naturally, the volume transition temperature is close the LCST of the corresponding linear polymers as shown in Figure 2.8.

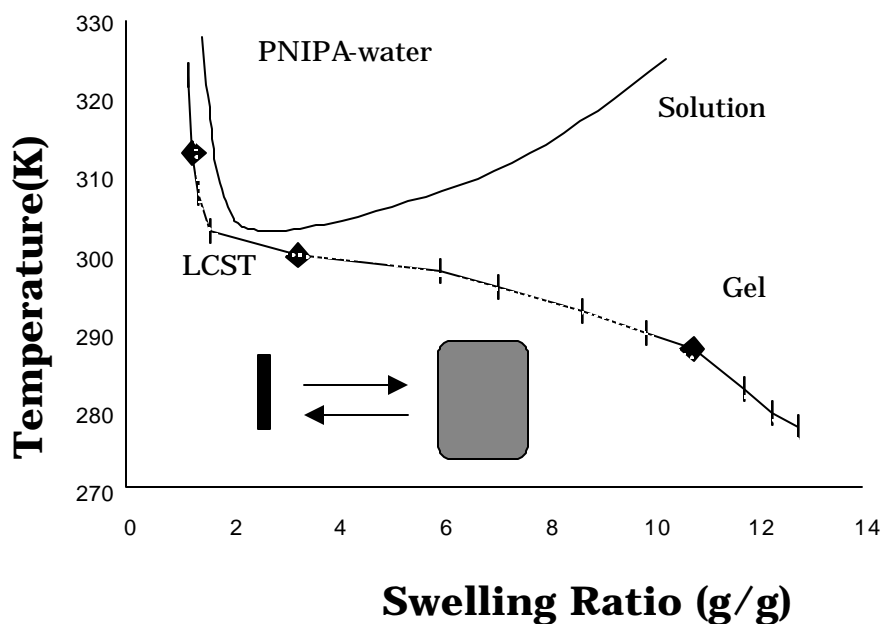


**Figure 2.8:** Schematic picture showing the LCST as well as VPT for polymer-solvent systems.

Interestingly, Dusek and Patterson (1968) had theoretically predicted the existence of a volume phase transition for cross-linked networks almost a decade before the swelling-collapse transition was experimentally demonstrated in hydrogels (Tanaka, 1978). They suggested that the VPT is

analogous to a coil-to-globule transition of a single chain in a dilute solution above the LCST.

#### **2.4.2 Thermoreversible hydrogels**

Thermoreversible hydrogels exhibiting an LCST-type discontinuous first order volume transition phenomenon have received increasing attention in the technological as well as in the scientific fields. As mentioned earlier, the smart behavior of gels have been creatively utilized in a number of applications such as molecular sensors (Kokufuta *et al.*, 1991; Holtz *et al.*, 1997), actuators (Kwon *et al.*, 1991), controlled drug delivery systems (Bae *et al.*, 1987; Hoffman *et al.*, 1987; Kulkarni *et al.*, 1992; Kim *et al.*, 1990; Kim, 1994), separations (Cussler *et al.*, 1984; Gehrke *et al.*, 1991), cosmetics (Dagani, 1997), artificial muscles (Hu *et al.*, 1995a; Osada *et al.*, 1995; Shahinopoor, 1996; Shiga, 1997; Szabo *et al.*, 1998), valves (Osada *et al.*, 1993) etc. Discoveries of new applications of these materials have stimulated scientific research for understanding the molecular level interactions that govern the temperature induced phase transition in thermoreversible gels.

Among the LCST polymers PNIPAm has attracted much attention due to its easily observable LCST at a temperature of about 34°C. The mechanism of temperature induced macroscopic volume transition in hydrogels has been extensively investigated experimentally (Hirotsu *et al.*, 1987; Fujishige *et al.*, 1989; Otake *et al.*, 1990; Inomata *et al.*, 1990; Schild 1990, 1992; Shibayama *et al.*, 1994, 1996), and theoretically (Heskin, 1968; Tanaka, 1978; Otake *et al.*, 1989; Prange *et al.*, 1989; Marchetti *et al.*, 1990; Lele *et al.*, 1995).

The LCST-type volume phase transition observed in thermoreversible hydrogels cannot be predicted by the Flory-Huggin's regular solution theory (F-H) of polymeric networks (equations 2.1 to 2.5) because this theory does not consider the specific interaction forces such as hydrogen bonding. The F-H theory holds for an incompressible mixture and mainly predicts a UCST-type phase behaviour.

Tanaka (1978) made the first attempt to explain the volume transition phenomenon observed in hydrogels using Flory-Huggin's lattice model. They modified the F-H theory by basically considering an arbitrary entropic contribution to the Flory-Huggins interaction parameter. According to their model,

$$\mathbf{p} = \mathbf{p}_{mixing} + \mathbf{p}_{elastic} + \mathbf{p}_{ion} \quad (2.10)$$

$$= -\frac{NkT}{V_1} \left[ \mathbf{f} + \ln(1-\mathbf{f}) + \frac{\Delta F}{2kT} \mathbf{f}^2 \right] + \mathbf{n}_e kT \left[ \frac{\mathbf{f}}{2\mathbf{f}_0} - \left( \frac{\mathbf{f}}{\mathbf{f}_0} \right)^{1/3} \right] \quad (2.11)$$

$$+ \mathbf{n}_e f kT \left( \frac{\mathbf{f}}{\mathbf{f}_0} \right)$$

where,  $\mathbf{f}_0$  is the volume fraction of the uncrosslinked single polymer chain without any interactions,  $\mathbf{n}_e$  is the crosslink density at  $\mathbf{f} = \mathbf{f}_0$ , and  $\Delta F$  represents the difference between the free energies of a polymer segment-segment and polymer-solvent interactions. Comparing equations (2.1) and (2.11) it is clear that  $\Delta F$  is essentially the interaction parameter. Tanaka *et al.* argued that  $\Delta F$  can be written as,

$$\Delta F = \Delta H - T\Delta S \quad (2.12)$$

so that



$$\begin{aligned}
\mathbf{t} = 1 - \frac{\Delta F}{kT} = & -\frac{\mathbf{n}_e V}{N \mathbf{f}^2} \left[ (2f+1) \left( \frac{\mathbf{f}_2}{\mathbf{f}_0} \right) - 2 \left( \frac{\mathbf{f}_2}{\mathbf{f}_0} \right)^{3/2} \right] \\
& + 1 + \frac{2}{\mathbf{f}^2} + \frac{2 \ln(1-\mathbf{f})}{\mathbf{f}^2}
\end{aligned} \tag{2.13}$$

where  $\mathbf{t}$  is the reduced temperature that depends both on temperature and solvent composition. The parameter  $f$  denotes the number of ionizable groups per effective chain incorporated into the network. As the  $f$  value increases, the magnitude of the volume change increases, and the reduced temperature of the volume transition becomes lower. For certain values of the reduced temperature, the equation (2.13) is satisfied by three values of  $\mathbf{f}_2$ , corresponding to two minima and one maximum of the free energy. The value of  $\mathbf{f}_2$  corresponding to the lower minimum represents the equilibrium value. A discrete volume transition occurs when the two free-energy minima have the same value. This can be understood by expanding the term  $\ln(1-\mathbf{f})$  of the equation (2.13). This gives,

$$t = S \left( \mathbf{r}^{-5/3} - \frac{1}{2} \mathbf{r}^{-1} \right) - \frac{\mathbf{r}}{3} \tag{2.14}$$

where

$$t = \left( 1 - \frac{\Delta F}{kT} \right) (2f+1)^{3/2} / 2\mathbf{f}_2 \tag{2.15}$$

$$S = S_0 (2f+1)^4 \tag{2.16}$$

and

$$\mathbf{r} = \left( \frac{\mathbf{f}}{\mathbf{f}_0} \right) (2f+1)^{3/2} \tag{2.17}$$

The value of the parameter  $S$  governs the magnitude of collapse. Eqn. (2.16) shows that the value of  $S$  increases rapidly with degree of ionization.

For a reduced temperature greater than  $-0.338$ ,  $\frac{f_2}{f_0}$ , increases continuously with  $f$ , while below this value the swelling ratio changes discretely. It is thus clear that whether the polymer would undergo a continuous or discrete volume phase transition would depend upon the relative contribution of rubber elasticity and the free energy of mixing to the osmotic pressure. Higher degree of ionization and stiffer chains will increase the possibility of discontinuous volume phase transition. Hence, Tanaka's modified version of F-H theory shows that the volume phase transition could be affected by various parameters such as temperature (1978), solvent composition (1978) and degree of ionization (1980). However, Tanaka's interpretation of volume transition based on the value of  $S$  was not substantiated by experimental evidences.

The lattice model has been extended in several ways (Koningsveld *et al.*, 1968; Sanchez *et al.*, 1976, 1977, 1978, 1980; Lacombe *et al.*, 1976; Panayiotou *et al.*, 1981, 1982; Niles, *et al.*, 1983; Blas *et al.*, 1998a, 1998b; Suresh *et al.*, 1996, 1998) to include the effects of compressibility and specific interactions in the solution. These models have been successful to a great extent in predicting the LCST-type phase behaviour of linear polymer solutions. In this work we will focus our attention on the Lattice-Fluid model (LF) proposed by Sanchez and Lacombe (1976), which can successfully predict several types of liquid-liquid as well as vapor-liquid phase transitions. In the LF theory, a long chain polymer is hypothetically broken into mers (repeat unit), which are distributed, while retaining their connectivity, on a lattice along with the solvent molecules and holes. The holes are introduced in order to account for the finite compressibility of the mixture, which can become significant at high pressures and temperatures

near the critical point of the solvent. The free energy of the system is calculated by accounting for the different number of ways in which the mers, the solvent molecules and the holes can be placed on the lattice and by calculating the mean-field energies of interactions. An important aspect of the LF model is that the various parameters in the model have molecular significance and many of them can be estimated from pure component P-V-T data. Indeed, the LF model can successfully predict LCST-type of phase behaviour arising from the compressibility of the solvent near its critical point. However, it cannot predict the LCST behaviour observed at much lower temperatures and pressures in polar polymer-solvent binary mixtures.

Panayoutou and Sanchez (1991) extended the LF model to account specifically for hydrogen bonding interactions in mixtures. This model, called as the Lattice-Fluid-Hydrogen-Bond (LFHB) model assumes a decoupling of the mean-field dispersion interactions and the hydrogen bonding interactions. This leads to a partition function that is separable into physical and chemical contributions. The physical contribution considers the dispersion forces while the chemical contribution considers the hydrogen bonding forces between the molecules.

The LFHB model also takes into consideration the compressibility of the solution and the equation-of-state properties of individual components like in the LF model. The hydrogen bonding contribution to the free energy is calculated by counting the different types of hydrogen bonds formed between the different types of donors and acceptors that are randomly distributed on a lattice. The hydrogen bonding energy is also calculated in a mean-field sense. The highlight of the model is that it provides an analytical equation for the free energy of the mixture as a result of the decoupling

assumption. This model successfully predicts hydrogen bonding in water (Gupta *et al.*, 1992) and in polymer solutions of supercritical solvents (Haschets *et al.*, 1993).

Marchetti *et al.* (1990) have proposed the first adaptation of the Sanchez-Lacombe LF model for a cross-linked gel. Although their model does not directly account for any specific interactions such as hydrogen bonding in the mixture, it indirectly accounts for such interactions by defining the interaction parameter as being based on large differences in cohesive energy densities of the components. Their model indeed predicted LCST-type phase behaviour for large cohesive energy differences between polymer and solvent.

As mentioned earlier, the main reason for the occurrence of LCST type phase behaviour in polar polymer-solvent mixtures at near-ambient temperatures and pressure is the presence of specific interactions such as hydrogen bonding (walker *et al.*, 1987; Tager, 1972; Plate *et al.*, 1999). Indeed hydrogels are highly polar systems, with a polar solvent (water) imbibed in a polar polymeric network. The influence of hydrogen bonding associations on VPT has been experimentally verified. For example, Ilmain *et al.* (1991) have shown that hydrogen bonding in an interpenetrating network of acrylic acid – acrylamide gel influences the phase transition of the gel. The non-ionized gel undergoes a continuous transition at 20°C whereas that of the ionized gel undergoes a discontinuous transition. To confirm the role of the hydrogen bonding on the phase transition, the authors have added urea, which is known to break the hydrogen bonds, to the system. In the presence of 1M urea, no phase separation is observed. This observation indicates that in the present system, the phase transition behaviour is due to the hydrogen bonding interactions.

The thermoreversible nature of the LCST polymers is also thought to be due to the breakage of hydrogen-bonded associations in the gel water system (Walker and Vause, 1987; Hirotsu, *et al.*, 1987; Mukae *et al.*, 1993; Urry, 1995; Liu *et al.*, 1999). For example, Hirotsu (1987) suggested that the volume phase transition observed in hydrogels is due to the thermal destruction of hydrogen bonds between water molecules and hydrophilic groups such as C=O and -NH in the PNIPAm gels. Therefore the lattice theory must take into account the specific interactions in the system for explaining the LCST behaviour at ambient conditions.

A model, which accounts for such interactions, was first put forward by Prange *et al.* (1989). Their theory was focused on oriented hydrogen bonding interactions between mers on a lattice. They proposed that every segment of a molecule on the lattice exhibits three types of contact sites: proton donating, proton accepting, and those, which interact through dispersion forces. Their model also accounted for non-random distribution of molecules in a mixture due to hydrogen bonding interactions. The model could quantitatively predict the LCST of linear as well as cross-linked PNIPAm-water system. From a computational point of view the model is highly complicated due to the need of solving 22 simultaneous non-linear equations for a binary mixture.

Water molecules are known to structure around non-polar hydrophobic solutes through the formation of a hydrophobic hydration layer (Bein-Neim, 1980). The swelling behaviour of a hydrophobic polymer gel in water has been explained on the basis of the formation of an ice-like structure of water molecule around the hydrophobic groups, a concept that is similar to the phenomenon reported in the case of proteins. The formation of ice like structure around the hydrophobic group makes it

thermodynamically favourable for the hydrophobic groups to take an extended conformation and thereby the gels to attain a swollen state. However, with increasing hydrophobicity of the polymer chains, the polymer-polymer interaction dominates over the polymer-solvent interaction, which destabilizes the ice-like structure. The hydrogel then changes to a collapsed state by the aggregation of the polymer chains through the destruction of the structured water molecules around the hydrophobic moiety. Such a destruction of structured water molecules leads to an endothermic phase separation.

It has been suggested that the endothermic peak detected by DSC during the VPT is related to the breakage of the hydration layers (Otake *et al.*, 1989,1990; Winnik *et al.*, 1990; Bae *et al.*, 1990; Feil *et al.*, 1993; Shibayama *et al.*, 1994, 1996; Zeng *et al.*, 1998). Shibayama *et al.* (1994) have reported that about 750 cal per mol of NIPAm monomer is required for the dissociation of the hydrophobic layer and about 13 water molecules are released from a NIPAm monomer unit with an enthalpy of dissociation equal to 3.1kJ/mol. In a different study the same authors (Shibayama *et al.*, 1996) have investigated the effect of comonomer on the enthalpy of dissociation ( $\Delta H_N$ ) of the hydrophobic interaction per molar unit of NIPAm monomer using copolymer gels such as p(NIPAm-co-AAc) and p(NIPAm-co-DMAA). They showed that the structure of the comonomer have a pronounced effect on  $\Delta H_N$ . A large decrease in  $\Delta H_N$  was observed for p(NIPAm-co-AAc) than for p(NIPAm-co-DMAA), which is attributed to the strong hydrophilic effect of charged AAc comonomer. Zeng *et al.* (1998) have reported the network formation in PNIPAm during phase separation. This is attributed to the intermolecular aggregation via hydrophobic interactions, which results physical crosslinks and the network formation. The authors

have further confirmed the formation of hydrophobic interaction using NMR measurements.

Otake *et al.* (1989) proposed a model that ascribed the volume phase transition to the breakage of hydrophobic hydration layers. In their model, the free energy of a hydrogel is divided into four parts: the elastic free energy of network, the free energy arising from osmotic pressure of dissociated counter ions, the free energy of dispersion interactions and the free energy of the hydrophobic interactions. For lack of a more fundamental understanding of the so-called hydrophobic interactions, theory by Otake *et al.*, uses an empirical approach to model hydrophobic interactions in the system. Further, they do not consider the hydrogen bonding interactions between the donor-acceptor pairs in the hydrogel.

From the foregoing discussion, it is obvious that the observed thermoreversible transition in hydrogels cannot be ascribed to only hydrogen bonding or hydrophobic interactions. This is evident from the fact that very hydrophilic polymers such as polyacrylamide (PAm) or a very hydrophobic polymer such as poly (N-t-butylacrylamide) (PN-t-BAm) do not show any observable LCST in water. However, polymers such as poly (N-isopropylacrylamide) (PNIPAm) and poly (n-propylacrylamide) (P-n-NPAm) exhibit a distinct VPT. So, what is so special about PNIPAm or P-n-NPAm? Obviously, the molecular structure of NIPAm has a certain balance of hydrophobic groups (isopropyl) and hydrophilic groups (NH, C=O), which gives rise to a distinctly observable LCST behaviour.

On this background, Lele *et al.* (1995) adapted the Lattice Fluid Hydrogen Bond (LFHB) model for the case of gels by incorporating the stored elastic energy of affine polymeric networks into the total free energy of the gel and successfully predicted the discontinuous VPT observed in

thermoreversible gels (see Figure 2.9). The LFHB model predicts that the discontinuous volume transition occurring in thermoreversible gels is a result of the combination of two molecular events: (a) a rearrangement of hydrogen bonds in the gel-water system (as shown in Figure 2.10a for PNIPAm-water), and (b) a temperature dependent 'effective' hydrophobicity of the polymer (as shown in Figure 2.10b for the same hydrogel). The model predicts that at the LCST, the inter-polymer hydrogen bonds increase while those between polymer and water decrease, which is supported by experimental observations (for example, Walker and Vause, 1987) and also by simulations (Mandhare, 1998). The prediction of an increase in hydrophobicity with temperature has been experimentally demonstrated by Takei *et al.* (1994) for PNIPAm by measuring the contact angle between water and a gel bead that is surface grafted with PNIPAm chains. PNIPAm grafted polymer surfaces showed hydrophilic property till 24°C. As temperature increased, the contact angle also increased, demonstrating hydrophobic surface properties above 24°C. In the LFHB model, the effective hydrophobicity of the polymer is considered only in a mean-field sense through the dispersion interactions. The model does not account for local caging of hydrophobic groups by structuring of the water molecules around them. Clearly, there is a trade-off between the complexity involved in accounting for local non-random distribution of water molecules and retaining the simplicity of the LFHB model.

The success of the simple LFHB model lies in its ability to predict several experimentally observed phenomena. For example, the model correctly predicts the heat release associated with the VPT (Badiger *et al.*, 1998) although it does not specifically account for the so-called hydrophobic caging effect



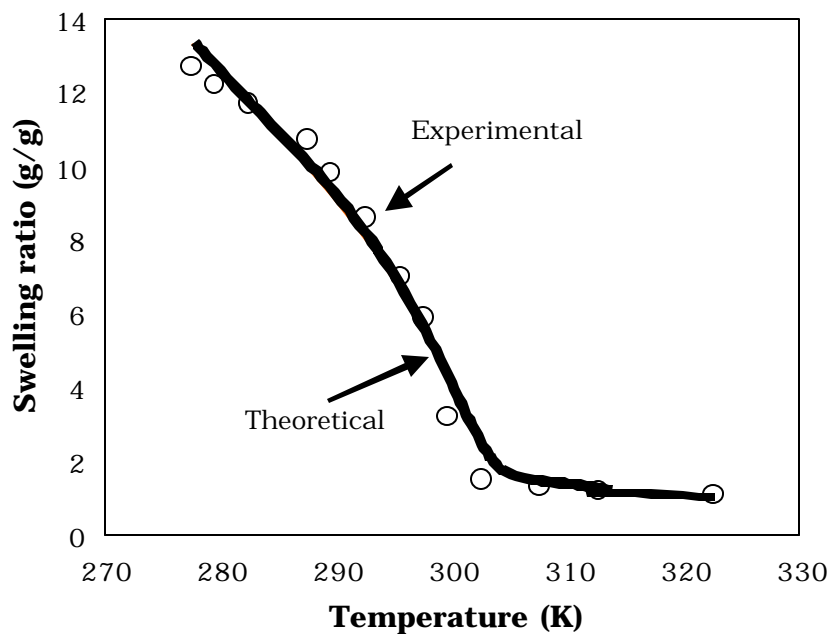


**Figure 2.9:** Volume phase transition of PNIPAm gel in water

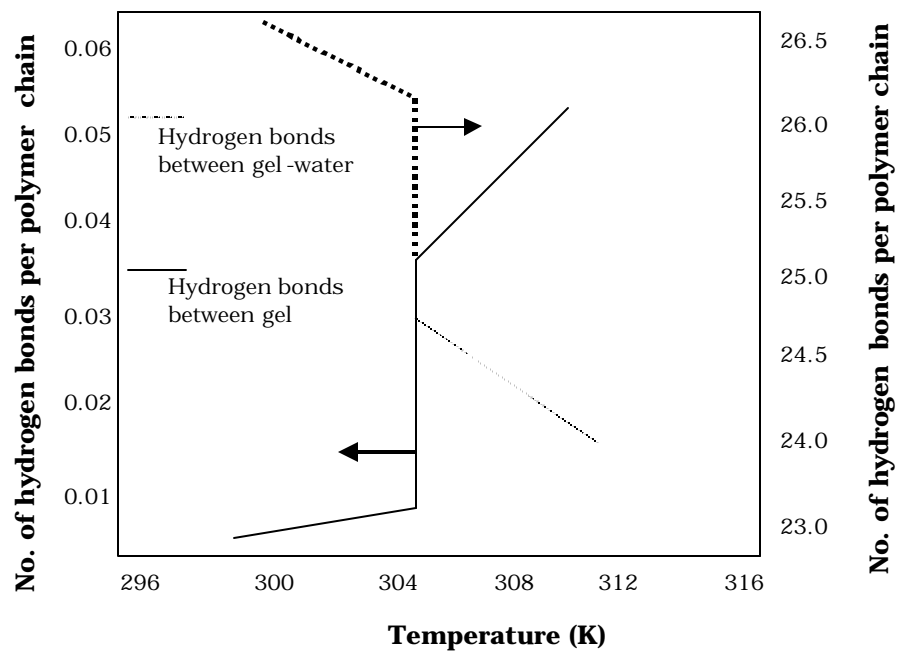


**Figure 2.10a:** Rearrangements of hydrogen bonds in PNIPAm-water systems

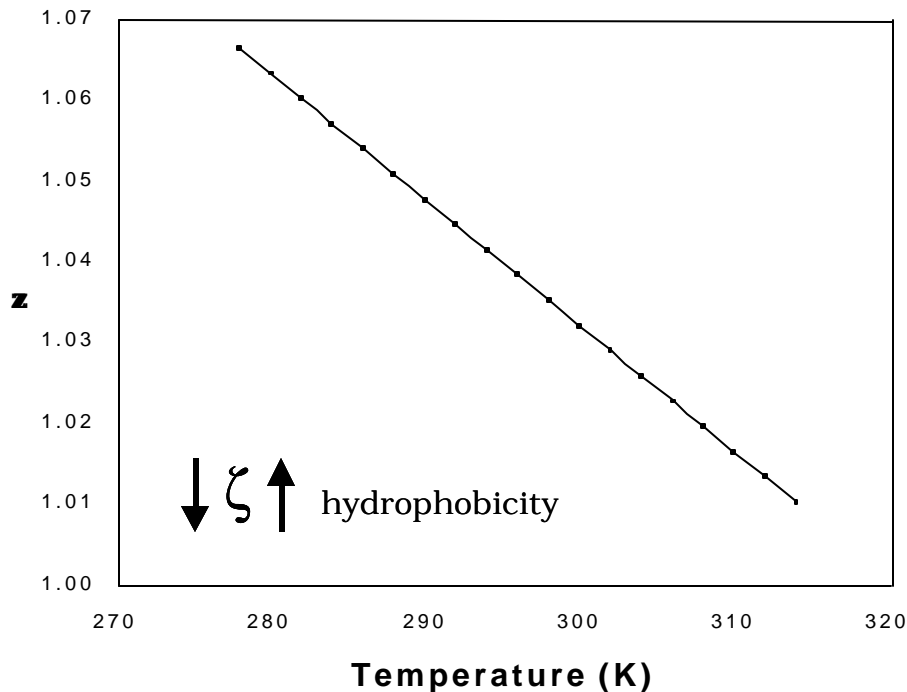


**Figure 2.10b:** Hydrophobicity increases as a function of temperature

Another important prediction of the LFHB model concerns the influence of hydrophobic and hydrophilic groups on the VPT temperature of thermoreversible gels (Lele *et al.*, 1997). The model predicts that a small change in the effective hydrophobicity can dramatically influence the VPT temperature and magnitude. Also, it was found that the VPT is significantly affected by altering the hydrogen bonding contributions. Further, the model also predicts that an increase in hydrophobicity decreases the VPT temperature and similarly, an increase in hydrophilicity increases the VPT temperature.

Many of these theoretical predictions of the LFHB model have been validated by experimental observations. For example, the ratio of hydrophobic to hydrophilic parts of the polymer chain is known to have a pronounced effect on VPT in thermoreversible gels (Inomata *et al.*, 1995;

Brazel, *et al.*, 1995; Katakai *et al.*, 1996; Shibayama *et al.*, 1996; Young *et al.*, 1997).

Inomata *et al.* (1990) studied the swelling behaviour of N-n-propylacrylamide (nNPAm), N-isopropylacrylamide (NIPAm) and N-cyclopropylacrylamide (NCPAm) to investigate the effect of the hydrophobicity of alkyl groups on VPT. The P-n-NPAm gel showed a first order VPT at 24°C, 10°C lower than that of PNIPAm gel (34°C). The PNCPm gel showed a continuous swelling deswelling behavior without any first order VPT. The authors have interpreted the observation based on hydrophobic interaction. The strength of the hydrophobic interaction is proportional to the number of water molecules that form the hydrophobic hydration and increases with temperature. Hence the gel whose hydrophobic group has a larger surface area undergoes a discontinuous volume phase transition at lower temperature due to the strength of the hydrophobic interaction. Among the earlier mentioned alkyl substitutes of the alkylacrylamides, the hydrophobic group of PNCPA has the minimum surface area and that of P-n-NPAm has the maximum. The maximum surface area of the P-n-NPAm enhances the hydrophobic hydration and hence a discontinuous volume transition at 24°C, 10°C less than PNIPAm. In the case of PNCPA, the strain of the bond angles of the cyclopropyl group and its surface area weakens the hydrophobic interaction between the cyclopropyl groups at higher temperature, because the strain reduces the overlap of electron clouds and makes the cyclopropyl group more hydrophilic.

Similarly Seker *et al.* (1998) have drawn an analogy between the chemical structure of N-alkylacrylamides and its effect on swelling behavior of the gels. They studied the swelling behaviour of a series of N-

alkylacrylamide gels such as methyl, ethyl, isopropyl and n-propylacrylamide gels. It was observed that the swelling behaviour of the gels changed from a continuous to discontinuous type when the alkyl group was changed from ethyl to propyl derivatives.

Katakai *et al.* (1996) have shown that a large change in the transition temperature of the thermoreversible gels can be induced by a pinpoint variation in the chemical structure of the hydrophobic side group of the polymer chain. They found large differences in the VPT temperatures of gels containing methacryloyl-L-alanine ethyl ester and methacryloyl-L-alanine methyl ester, which differ slightly in the hydrophobicity of the terminal alkyl groups. Shibayama *et al.* (1996) showed that the chemical structure of the comonomer also has an effect on the swelling behavior of the thermoreversible polymers. They investigated the swelling behaviour of PNIPAm copolymer gels having two different comonomers such as poly(NIPAm-co-dimethylacrylamide) [p(NIPAm-co-DMAA)] and poly(NIPAm-co-acrylic acid) [p(NIPAm-co-AAc)]. Among the two copolymer gels, p(NIPAm-co-DMAA) exhibited a continuous volume phase transition, whereas p(NIPAm-co-AAc) gels showed a discontinuous volume phase transition.

An important and highly useful feature of thermoreversible polymers is the possibility of controlling their LCST by either changing the composition of the comonomers by a small amount or by slightly changing the hydrophobicity in the gel (Taylor, *et al.*, 1975; Dong *et al.*, 1986; Priest *et al.*, 1987; Feil *et al.*, 1993; Katakai, *et al.*, 1996; Badiger *et al.*, 1998). Several studies have shown that the incorporation of hydrophobic comonomer decreases the LCST (Feil *et al.*, 1993; Yu *et al.*, 1994; Badiger *et al.*, 1998) and that of hydrophilic comonomer increases the LCST (Taylor *et al.*, 1975; Hirotsu *et al.*, 1987; Urry *et al.*, 1992; Feil *et al.*, 1992, 1993;

Mumick *et al.*, 1994; Takai *et al.*, 1994; Shibayama *et al.*, 1996; Liu *et al.*, 1999). For example, Feil *et al.* (1993) investigated the effect of hydrophilicity/ hydrophobicity and ionic charge on the LCST phenomenon. The polymers studied were poly (NIPAM-co-butyl methacrylate-co-X), where X = butyl methacrylate (BMA, hydrophobic comonomer), acrylamide (Am, hydrophilic), acrylic acid (AAc, hydrophilic) and diethylamino ethyl methacrylate (DEAMA, hydrophobic). According to the authors, the incorporation of hydrophilic or charged comonomers increases the hydrophilicity and favors strong interaction between the charged or hydrophilic groups on the polymer and water. This leads to an increased LCST and a reduced heat of phase separation ( $\Delta H_N$ ) due to the smaller amount of structured water.

A same observation has been made in the case of natural LCST polymers such as polypeptides. In the case of polypeptides it was found that increasing the ionization of the carboxylic side groups decreased the heat of phase separation where as the temperature of phase separation increased (Urry, 1992). It is also reported that the copolymerization of hydrophilic acrylamide with hydrophobic N,N-dimethylamino ethyl methacrylate (DMAEMA) results in lower LCST than pure DMAEMA gels (Cho *et al.*, 1997), which is in apparent contradiction to the earlier reports. The authors have interpreted the observation on the basis of formation of hydrogen bonds between the amide (from acylamide) and N, N dimethylamino groups (from DMAEMA). The hydrogen bonding apparently protects the N,N-dimethylamino groups from exposure to water and results in a hydrophobic contribution to the LCST. In general, the LFHB model predictions for VPT temperature and heat of VPT are in qualitative agreement with most of the experimental observations and in quantitative

agreement with the experimental observations from our own group (Badiger *et al.*, 1998).

From the above discussion it is clear that a significant amount of research has been carried out to understand the VPT of thermoreversible gels. It is now well known that the hydrophilic and hydrophobic groups can modulate volume transition phenomenon in gels. However, the question of why only certain polymer gels show a distinct thermoreversible volume transition has remained unanswered to a large extent. As a result, the thermoreversible gels that are known today are mainly restricted to a few poly (alkyl acrylamides) and their copolymers. The understanding of the fundamental reasons underlying volume transitions is crucial to the development of new, tailor-made gels that can be used for novel applications. A definitive way of moving ahead on this front would be to use the tools of molecular dynamics simulations. However, mean field models such as the LFHB model can still provide important clues and directions since it has the ability to link the macroscopic VPT to molecular events such as hydrogen bond rearrangement and temperature sensitive hydrophobicity of the polymer as discussed earlier.

By far, the most important prediction of the LFHB model is that the hydrogel requires a fine balance of hydrophilic and hydrophobic interactions in order to exhibit a discontinuous volume transition in water. Thus, it is theoretically possible to synthesize a thermoreversible gel from two monomers whose individual homopolymers do not show a discontinuous VPT. Such a demonstration would clearly indicate that the role of hydrophilic-hydrophobic balance as prerequisite for LCST polymers.

## 2.5 Hydrogel hybrids

Another dimension that has been added in recent years in the development of gels and their novel applications is that of “hydrogel hybrids,” which are composite materials formed by combining a hydrogel matrix with other novel materials to yield unique set of properties. For example, hybrid hydrogels have been prepared by dispersing nanoparticles and magnetic particles into the gel matrix. Several unique properties and applications of these materials have been demonstrated in literature. Weissman *et al.* (1996) used gels as a matrix to prepare crystalline colloid arrays (CCA) of polystyrene nanoparticles. Such CCA hydrogel films have found applications as intelligent chemical sensing materials (optical sensors) in which the ability of the hydrogels to undergo visual colour change has cleverly been used for molecular recognition (Holtz *et al.*, 1997). Similarly, Fe<sub>2</sub>O<sub>3</sub> reinforced hydrogels are widely used as magnetic responsive materials (Zrinyi *et al.*, 1997a, 1997b).

Tsuji *et al.* (1997) have developed a hybrid gel out of polymer gels and bilayer membranes where in the bilayer membranes of polymeric surfactants are stacked periodically in the network of the polymer gel. Their studies indicate that the hybrid gel exhibits coupling effects in its properties of the bilayer membranes and the polymer gels. Another example for hydrogel hybrids is organo-metallic hybrids, which are obtained by a process called metal complexation in which inorganic metal ions coordinates with organic functional groups through ionic bonds, coordination bonds and ion dipole interactions. Metal-complexed hydrogels is one of the topics of investigations in the present work and we will therefore summarize pertinent literature in the following.

### 2.5.1 Polymer metal complexation

Metal complexation is a process by which inorganic functions can be introduced into an organic molecule. Polymer metal complexes are mainly composed of polymeric ligands and metal ions in which the metal ions are attached to the polymer ligand by a coordinate bond. Polymer metal complexation may be of intra polymer chelate type or inter polymer chelate type. Polymer metal complexes without any inter or intra chelate is formed when the polymer backbone has multidentate ligands. A pendant type polymer metal complex is formed when the polymer ligand reacts with a metal complex having one coordinate site free. Polymer metal complex can also be obtained by polymerizing a monomeric metal complex (Tsuchida *et al.*, 1977). Presence of ionic groups on polymer is known to enhance the metal complexation (Lehto *et al.*, 1998). The two major areas where metal complexed polymers have found applications are catalysis (Case *et al.*, 1998a, 1998b; Bergbreiter *et al.*, 1998a, 1998b; Yakura *et al.*, 1998, Toshima *et al.*, 1998) and wastewater treatment (Thompson *et al.*, 1999).

Catalytically active organic polymers can be obtained by reacting transition metal ions with polymers having functional groups. Metal complexed stimuli responsive polymer gels have recently been used as catalysts, wherein the volume transition phenomenon of gels was independently used to control the reaction rate (Case *et al.*, 1998a; Bergbreiter *et al.*, 1998a). The main advantages of using metal complexed polymers as the catalysis is that they combine the advantages of homogeneous catalysis (high activity and selectivity, well defined catalytic sites, good reproducibility) in their swollen state with those of heterogeneous catalysis (long life time and ease of separation) in the



collapsed state. The catalytic activity of the polymer-metal complex depends on the structure of the complex (Solomon, 1994; Chavan *et al.*, 2000)

### **2.5.2 Swelling behavior of the gels in metal salt solutions**

Swelling behavior of polymer gels in monovalent, divalent and polyvalent metal ions has been investigated earlier (Ricka *et al.*, 1984; Budtova *et al.*, 1993, 1998; Starodoubtsev *et al.*, 1995; Liu *et al.*, 1995; Lee *et al.*, 1998). In general it has been observed that the swelling ratio of a gel decreases when immersed in solutions of metal ions. There can be several reasons for such a decrease. The observed decrease in swelling capacity of an ionic gel in the presence of monovalent and divalent alkaline earth metals is mainly due to a decrease in the Donnan potential arising from the screening of negative charges on the gel network by the metal ions. However in the case of multivalent transition metal ions, the reduction is mainly because of complexation (Budtova *et al.*, 1998), which provides additional cross-links in the gel. The swelling behavior of the gels depends on the type and the concentration of the metal ions (Budtova *et al.*, 1993, 1998). Metal salt solution as well as surfactants is reported to shift the LCST of the polymer systems (Inomata *et al.*, 1992). Transition metal ions are reported to shift the volume transition temperature of thermoreversible gels (Tanaka *et al.*, 1996). The transition temperature of the copolymer gel (NIPAm-co-AAC) shifted to the lower side as the concentration of the metal ion increased as shown in the Figure.2.11. Similarly, the acrylic acid-acrylamide copolymer gel immersed in aqueous Cu(II) salt solutions exhibited a discontinuous volume collapse upon increasing the Cu(II) concentration (Ricka *et al.*, 1985). This is attributed to the formation of Cu(II) complexes with the ligands (COOH) presented in the network.

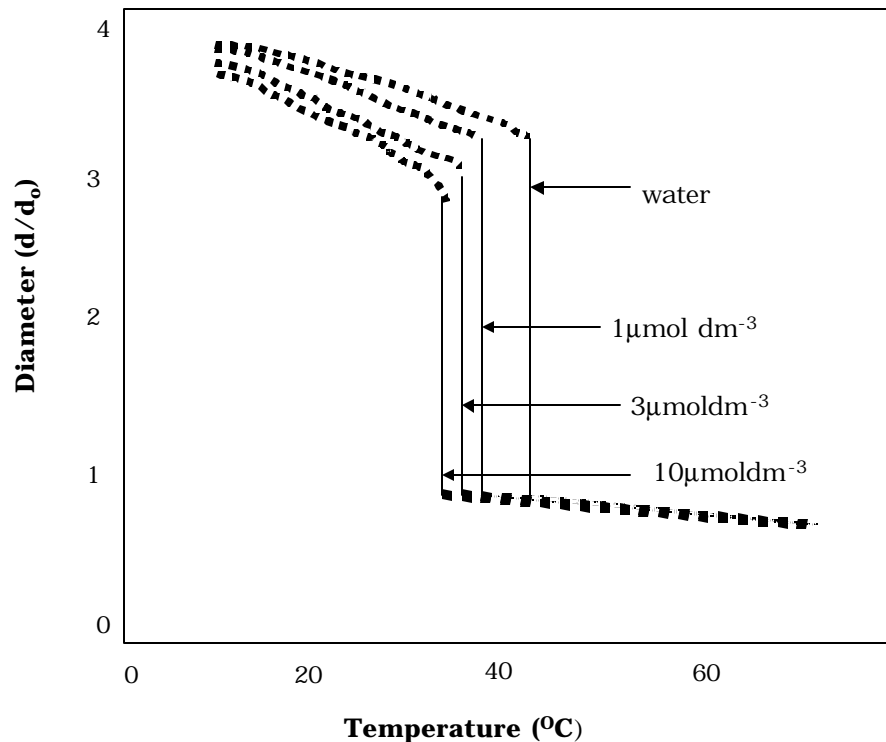


**Figure 2.11:** Swelling behavior of Poly(NIPAm-co-AAC) gels in  $\text{CuCl}_2$  solution

### 2.5.3 Effect of hydrophobicity on metal complexation

Polyelectrolytes complexed with the divalent ions are known to adopt a compact conformation (Huber, 1993) and in some other cases precipitate out from the solution (Wall *et al.*, 1951). This is mainly attributed to the complexation-induced hydrophobicity, which leads to the poor affinity of the chain segments to water. Sasaki *et al.* (1998) studied  $\text{Ca}^{2+}$  binding to polyelectrolyte gels containing different hydrophobic alkyl groups. They observed the highest binding constant and the largest shrinkage in the volume for the copolymer gel of n-butyl acrylate and acrylate, which has the maximum hydrophobicity among the gels used. Lehto *et al.* (1997) have studied a series of copolymer gels such as NIPAm-co-AMPS, NIPAm-co-AAC

and NIPAm-co-AAA to investigate the effect of chemical structure on metal complexation. Better metal uptake efficiency was observed in NIPAM-AAA gel. According to the authors, the observed efficiency was due to the close proximity of acid group with the lone pair of electrons on the nitrogen of amide group. This allows the transition metal ions to bind the gel by ion exchange (through carboxylic group) as well as by coordination (through lone pairs of electrons present in the nitrogen).

Kruczala *et al.* (1999) studied the interaction of polyelectrolytes with divalent metal ions. The systems studied were poly (ethylene-co-methacrylic acid) p(EMAc), fluorinated polymer (nafion), poly(acrylic acid) p(AAc) and poly(styrene sulfonic acid) p(SSA). They observed two types of Cu(II) complexes with p(AAc) depending on whether the Cu(II) ion was ligated to one or two carboxylic acid groups on the polymer chain.

Although a series of studies have been carried out in the literature to investigate the swelling behavior of polyelectrolyte gels in monovalent, divalent and polyvalent ions, there are no attempts to understand the role of hydrophobicity on metal complexation phenomenon and their structural changes.

## **2.6 Biomimicking gels**

Smart gels are also considered to be excellent model systems for developing biomimicking devices. The motivation for such research is driven by the fact that Nature has evolved smart gel-like living objects, for instance a jelly-fish, that can carry out complex functions such as sensitive responsiveness, shape memory, selectivity, self-mobility, self-organization, self-healing and reproduction. Of these, the first four features have already been demonstrated in synthetic gels as described below. Studies on

synthetic stimuli-responsive hydrogels could provide clues to the functioning of body parts containing biological gels. Thus the design and synthesis of synthetic biomimicking materials is a rapidly growing interdisciplinary research area, in which the molecules found in nature are mimicked to produce materials with unusual properties.

### **2.6.1 Molecular recognition induced selectivity**

Molecular recognition is an important characteristic feature observed in biological systems. For example, purine and pyrimidine bases present in nucleic acids show selectivity for their counter parts. Purine base adanine always combines with thaimine where as guanine always combines with cytosine (Stryer, 1981). The high selectivity is interpreted in terms of hydrogen bonding between these bases and it leads to the perfect replication of DNA and RNA that encode all the vital genetic information about an organism. Mismatch of the pairs can be in fact be fatal. Indeed, the selectivity of base pairing in DNA/RNA replication is so accurate that a mismatch occurs only once in billion base pairs. Similarly, antibodies have high selectivity for antigens. Another example of bioploymers showing selectivity is in the case of enzymes. For instance, the selectivity in enzymatic catalysis is achieved as a result of recognition of a substrate molecule by the enzyme followed by the selective binding.

Many synthetic materials such as molecularly imprinted polymers (MIPs) have been developed for selectively "recognizing" the target molecules. (see for example, Leonardt, 1987; Wulff, 1989). Molecularly imprinted hydrogels exhibiting enzyme-like activity were developed by Karmalkar *et al.*, (1996). Functionalized hydrogels can potentially enjoy an advantage over MIPs since the removal of the template from the polymer

network is not required. Several such gels have been recently developed. For example, the thermosensitivity of PNIPAm is effectively used for ligand recognition of biomolecules (Stayton *et al.*, 1995). Similarly, Miyata *et al.* (1999) have developed a hydrogel, which can swell reversibly in response to a specific antigen (rabbit IgG) and change the structure. The hydrogel was prepared by grafting the antigen (rabbit IgG) and the corresponding antibody (GAR IgG) to the polymer network such that the binding between the antibody and antigen resulted in a crosslinked network. The hydrogel swelled in the presence of free antigen because the physical crosslinks created by the antigen-antibody binding was dissociated by the exchange of grafted antigen with the free antigen.

Kataoka *et al.* (1998) developed a hydrogel, which recognizes glucose molecules and responds to it depending upon its concentration in the surrounding aqueous medium. The glyco sensitive gel was made out of PNIPAm modified with a glucose-sensing moiety (phenylboronic acid) where in the transition temperature of the modified PNIPAm gel was regulated by the glucose concentration due to the presence of phenylboronic acid. An increase in glucose concentration from 0 to 5g/L led to shift the LCST temperature of the gel from 22 to 36°C. Such gels can find potential application in self-regulating insulin delivery systems by on-off regulation of the entrapped insulin release from the gel with the external glucose concentration. Similarly, cationically modified boronic acid copolymers are designed for molecular recognition, wherein the gel responds to specific nucleotides (Kanekiyo *et al.*, 2000). Tanaka and his coworkers (Tanaka *et al.*, 1996; Oya *et al.*, 1999; Alvarez-Lorenzo *et al.*, 2000) have developed hydrogels, which can selectively absorb and release toxic targets such as lead ions.

### 2.6.2 Shape memory in hydrogels

A shape memory hydrogel is considered to be an example of synthetic bio-mimicking materials that can self-organize into specific shapes in response to an external stimulus (Hu *et al.*, 1995; Osada *et al.*, 1995). Shape memory in hydrogels has been demonstrated by bending of cylindrical pieces or flat strips of gels in response to thermal (Hu *et al.*, 1995; Osada, *et al.*, 1995), electrical (Tanaka *et al.*, 1982; Osada *et al.*, 1992) or magnetic stimuli (Zrinyi *et al.*, 1996) as shown in Figure 2.12. Magnetic field sensitive gels or ferrogels are a typical example for shape memory gels in which magnetic and elastic properties are coupled. Under an external magnetic field, ferrogels undergo an instantaneous and significant shape distortion, which disappears abruptly when the external magnetic field is removed.

The shape memory gels developed so far maintain their cylindrical or flat strip nature while bending along the length to form different shapes. Another example of a shape memory gel is that demonstrated by Osada *et al.* (1995). A swollen cylindrical copolymer gel of acrylic acid with n-stearyl acrylate was coiled at 50°C. The coiled gel retained its shape at room temperature. But on re-heating, the rigid coiled gel became soft and recovered its original straight cylindrical shape. The shape memory of this gel is attributed to a reversible order-disorder transition of the long alkyl hydrophobic n-stearyl acrylate group on the gel.

The shape memory demonstrated in the literature so far is restricted to changes in the shape of cylindrical or flat gel pieces. For example, Hu *et al.* (1995) developed a bi-gel strip, which can bend into a circle with response to external stimuli such as temperature and acetone concentration as shown in the following Figure 2.12. They used two

polymers with different sensitivities such as PAm and PNIPAm to develop the bi-gel strips. The two polymers respond differently such as PNIPAm shrinks drastically when warmed above 37°C, whereas the PAm gel does not. However, the PAm gels shrinks much more than PNIPAm when the acetone concentration of the aqueous solution increases beyond 34%. Thus by choosing the appropriate stimuli the bi-gel strips can be made into bend. The following figure shows gel hand that is used to grasp and release the object by temperature adjustment. Moreover, such modulated gels could find applications in toys, switches, sensors, valves and display devices.

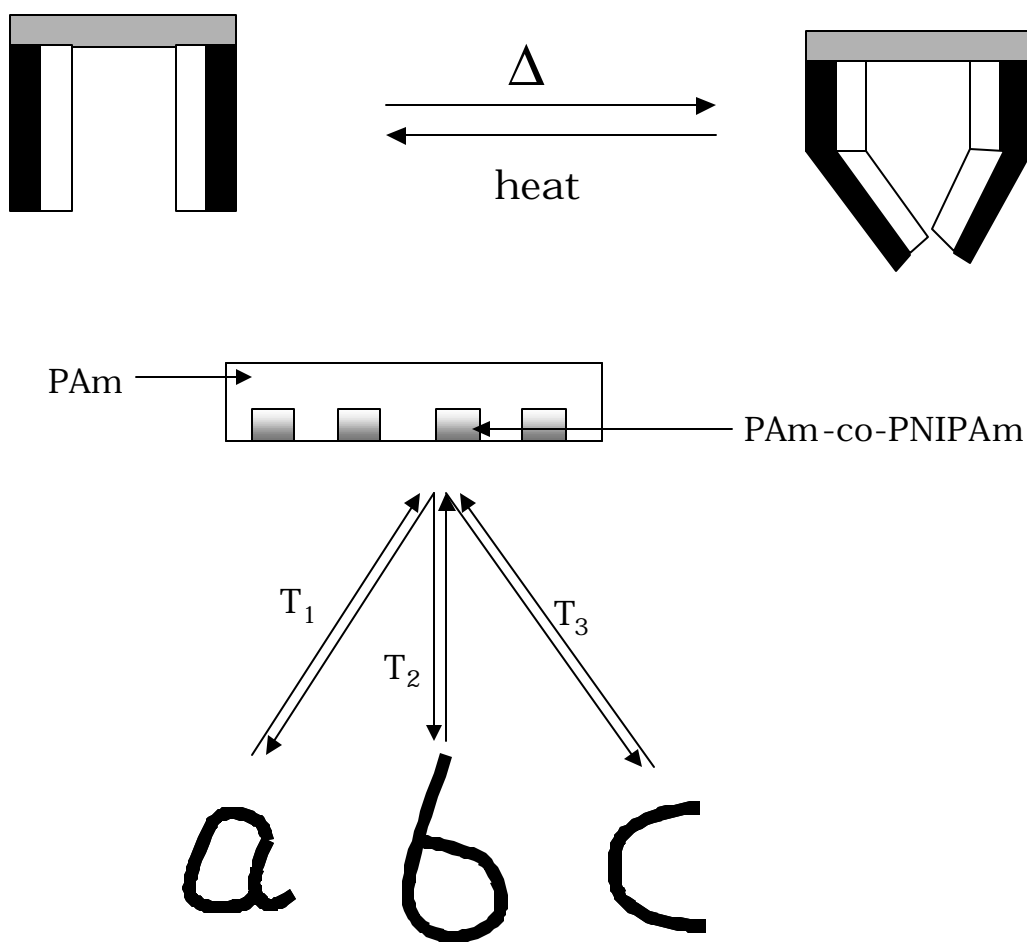


**Figure 2.12:** Shape memory gels

### **2.6.3 Self assembly in gels:**

Amphiphiles such as surfactants and lipids can form a variety of structures such as micelles, vesicles etc in aqueous solutions. Self-assembly occurs due to a combination of the hydrophobic and hydrophilic interactions such that the hydrophobic attraction induces the molecules to associate, while the hydrophilic attraction forces them to remain in contact with water.

Amphiphilic polymers having both hydrophilic and hydrophobic groups are well known for self-assembly in aqueous media. Synthetic polymer gels are amorphous in nature and not reported to have any particular ordered structure. However, a supramolecular self-organization in amphiphilic hydrogels has been reported by Osada and his coworkers (Matsuda *et al.*, 1994, 2000; Osada *et al.*, 1995). A copolymer gel of AAC with SA (stearyl acrylate), HA (hexadecyl acrylate) and DA (dodecyl acrylate) have shown an ordered structure both in the swollen as well as in the collapsed state wherein the hydrophobic long alkyl side group seemingly align perpendicular to the polymer back bone. Osada *et al.* (1995) have also observed the formation of higher order aggregates, resulting out of an interaction between the positively charged surfactant molecules and polyelectrolyte gels. The formation of crystalline aggregates in the gels was very much dependent on the concentration and size of the alkyl chain length of the surfactant. To our knowledge this is the only example of self-assembly at a molecular level in a synthetic hydrogel.

### **2.6.4 Mobility**

Mobility is a characteristic feature of all living organisms. Movement in living organisms is due to the isothermal conversion of chemical energy



into mechanical energy as exemplified by muscular, flagellar and ciliary movement. Such a highly efficient energy conversion mechanism has also been incorporated in synthetic hydrogels in which the contraction and expansion of the gels can be monitored by an external trigger such as an electric field. For example, Osada *et al.* (1992, 1993) have demonstrated electrically driven mobility in gels wherein the poly (2-acrylamido-2-methyl-1-propane sulfonic acid) gel doped with n-dodecyl pyridinium chloride surfactant) moved through a bath of an electrolyte solution. A ratchet type "gel looper" can "crawl" along a bar when a 20V voltage is supplied. They also showed that a gel bar made of polyacrylate material can bend backward and forward by the application of an alternating electric field. Here, water and ions migrate towards the electrode bearing a charge opposite to the charge in the gel, and this coupling of electro-osmosis and electrophoresis is thought to be responsible for the chemo-mechanical behaviour.

Since a gel piece can exert a force on swelling, smart gels have found potential applications such as actuators, artificial muscles, and fingers of robots. For example, Toshio Kurachi *et al.* have developed a mechanical hand having four "smart gel fingers" which can pick up and hold a quail egg. An artificial "fish" that swims with the help of the flapping action of its tail made out of an electrically responsive polymer has also been reported. The conceptual design, kinematics and dynamics of swimming robotic structures using ionic polymer gels muscles is elegantly summarized by Shahinopoor (1992). These smart materials in future may lead to the construction of self-regulating, self-sensing intelligent soft gel based machines.

The present work describes two more characteristics of smart gels namely, self-organization and self-healing, which brings them closer to being truly bio mimicking.

# Chapter 3

## OBJECTIVES AND SCOPE

Smart polymers, which mimic biological systems by using the same types of fundamental molecular interactions, have been creatively used in a number of novel applications including molecular sensors, actuators, artificial muscles, valves, controlled drug delivery systems, etc. The present work attempts to investigate the effects of hydrophobic interactions on certain interesting phenomena in lightly cross-linked hydrogels.

We present here a study of three seemingly different sets of problems namely, volume-phase transition (VPT) in thermoreversible gels, metal complexation in hydrogels, and self-organization and self-healing in hydrogels. These phenomena, however, have a common fundamental basis on which they rest namely, the balance of hydrophobic and hydrophilic interactions between the polymer network and the absorbed solvent. Each phenomenon has been addressed in a different chapter of the thesis. We define below the objectives and scope of the each of the three problems.

The first problem deals the effect of hydrophobic and hydrophilic interactions on the volume phase transition of a new copolymer gel. The objective of our study was to test the fundamental details of the Lattice-Fluid-Hydrogen-Bond (LFHB) model, which predicts that a **critical** balance of hydrophobic and hydrophilic interactions is required for a hydrogel to exhibit a discontinuous volume phase transition in the experimentally observable range. The motivation for such a study was to understand why only certain gels show discontinuous VPT and to provide clues for designing

new gels that can potentially show such a transition. There have been several studies in the literature that elucidate the effects of hydrophobic and hydrophilic groups on the VPT of thermoreversible gels. However, most of these studies have been carried out on poly (N-isopropylacrylamide) (PNIPAm) gel or its copolymers because of its easily measurable VPT. Although such studies demonstrate how the variation of hydrophobic and hydrophilic interactions can modulate the VPT, they do not directly answer the question of why only some gels such as PNIPAm show a distinct VPT.

The LFHB model provides an answer to this question. It predicts that a gel that contains a critical balance of the two interactions could, in principle, show a discontinuous VPT. We have attempted to test this hypothesis experimentally by arguing that a copolymer gel made from hydrophobic and hydrophilic monomers, whose homopolymers do not show a VPT, could show a discontinuous VPT at a critical composition of the comonomers. The scope of our study involves investigations on several compositions of one pair of comonomers viz, the hydrophobic N-t-butyl acrylamide (NtBAm) and the hydrophilic 2-acrylamido-2-methyl-1- propane sulfonic acid (AMPS). We also show that the LFHB model predictions quantitatively fit our experimental data.

The second problem we investigate is that of the influence of metal complexation on the effective hydrophobicity of hydrogels and also the influence of hydrophobicity on the metal complexation itself. The motivation of our study is linked to the understanding of the importance of polymer-metal complexation on catalysis, water treatment and possible understanding of metal-complexation in biopolymers. A few studies in the literature have shown that volume transition temperature of thermoreversible PNIPAm copolymer gels is altered in presence of metal-salt

solutions. The shift in the transition temperature was mainly attributed to an extra attraction created by the metal ions between the polymers. We believe that a more fundamental reason for the change in VPT lies in the way the hydrophobic-hydrophilic balance is modulated by metal complexation. We investigate this hypothesis by studying the effect of trace amounts of metal-complexation on the VPT of the N-t-BAm-co-AMPS gel. A complimentary problem is that of the influence of hydrophobicity on metal complexation. Our motivation was to understand the structure of polymer-metal complexes formed from gels of varying degrees of hydrophobicity. Such a study might give valuable insights into designing catalysts or understanding complexation in biopolymers. We have investigated the metal uptake of a series of hydrogels of acrylic acid and acryloyl amino acids of different alkyl chain lengths ( $n = 0$  to 7) simultaneously with an investigation of the structure of the coordination complex using electron spin resonance spectroscopy (EPR).

During the course of our investigations on metal-complexation in acryloyl amino acid gels, we discovered two interesting phenomena namely, a macroscopic shape-organization of gels and healing of gel pieces. The last section of this thesis presents an investigation of these two novel phenomena. The motivation for our study arises from our belief that a demonstration of self-organization and self-healing attributes in gels would further narrow the gap between synthetic bio-mimicking hydrogels and biopolymers. In this study we have investigated the process of macroscopic reorganization of a dried hydrophobic polymer gel from an initial cylindrical shape to a hollow spherical shape on complexation with certain transition metal ions. Further, we show that separate pieces of a gel can heal via metal complexation across the weld line. This is interesting because lightly

cross-linked gels are otherwise incapable of healing due to the restricted reptative motion of cross-linked chains across a weld line. The study describes the strength of healed joints and investigates possible healing mechanisms.

Smart hydrogels have been long recognized as ideal model systems for understanding biomimicking processes. Indeed, intelligent gels demonstrate sensitive-responsiveness, selectivity, shape memory and self-mobility, all of which are important attributes of biological systems. Our work adds two more new features to the bio-mimicking properties of gels.

# Chapter 4

## MOLECULAR TAILORING OF THERMOREVERSIBLE GELS

*"If you can dream it you can do it"*

*-Walt Disney*

### 4.1 Introduction

Certain non-ionic polymer hydrogels, which contain hydrophilic and hydrophobic functional groups, have been known to show a discontinuous or a continuous volume phase transition with temperature. The mechanism of temperature induced macroscopic volume transition in hydrogels has been extensively investigated experimentally (for example, Inomata *et al.*, 1990; Otake *et al.*, 1990; Schild *et al.*, 1990; Shibayama *et al.*, 1994, 1996) and theoretically (for example, Walker *et al.*, 1987; Otake *et al.*, 1989; Prange *et al.*, 1989; Marchetti *et al.*, 1990; Lele *et al.*, 1995). It has been shown that the macroscopic volume transition phenomena in hydrogels are mainly linked to the breakage of hydration layers (Otake *et al.*, 1990) or to the rearrangement of hydrophilic hydrogen bonds in the polymer water mixture (Walker *et al.*, 1987) or to the combination of these two effects (Lele *et al.*, 1995). These aspects have been extensively discussed in chapter two.

In the case of PNIPAm gel, the monomer itself has a unique hydrophilic-hydrophobic balance such that the gel can show LCST behaviour in the experimentally observable temperature range. Other similar hydrophobic gels that have been studied include N-methyl acrylamide, N-ethyl acrylamide (Seker *et al.*, 1998), N-n-propylacrylamide, N-cyclopropylacrylamide (Inomata *et al.*, 1990). However, it is perhaps not

necessary for a single monomer to have a balance of hydrophilic and hydrophobic interactions so that its gel will show a discontinuous volume transition. Previous research in our group has shown that a critical balance of hydrophilic and hydrophobic interactions is necessary for the occurrence of discontinuous volume transition in gels (Lele *et al.*, 1995). In this chapter we present an experimental validation for this prediction. We propose a hypothesis that a copolymer gel, which has an appropriate balance of hydrophilic and hydrophobic interactions, could show a distinctly observable LCST behaviour. Indeed copolymerization has been widely used to alter the hydrophilic-hydrophobic interactions in thermoreversible gels (Feil *et al.*, 1993; Katakai *et al.*, 1996; Shibayama *et al.*, 1996; Lele *et al.*, 1997; Badiger *et al.*, 1998). However, there are no reported efforts to synthesize a thermoreversible gel from two monomers whose individual homopolymers do not show any LCST in the observable temperature range. Such a study would clearly demonstrate the molecular level causes which manifest into a macroscopic volume phase transition (VPT).

More specifically, we report on the VPT in hydrogels prepared by copolymerising a highly hydrophilic monomer namely, 2-acrylamido-2-methyl-1-propane sulfonic acid (AMPS) with a highly hydrophobic monomer namely, N-tertiary-butylacrylamide (N-t-BAm). We show that the homopolymers of these two monomers do not show any LCST, however at a critical composition, the copolymer gel shows a discontinuous LCST type volume transition. We quantify the experimental observations using Lattice Fluid Hydrogen Bond (LFHB) model. We also show that a small change in the hydrophobic functional group can also significantly alter the VPT behaviour, which again highlights the critical nature of the hydrophilic-hydrophobic balance required for a discontinuous VPT.



## 4.2 Theory

The free energy change associated with the swelling of a dry gel, which is immersed in a solvent, is given by

$$\Delta G = \Delta G_{mix} + \Delta G_{el} \quad (4.1)$$

Here,  $\Delta G_{mix}$  is the free energy of mixing of the polymer network with the solvent, and  $\Delta G_{el}$  is the elastic free energy stored in the gel. In the following we will summarize the extended LFHB theory as applied to a binary mixture of solvent (component 1) and a copolymer gel (component 2) made from comonomers A & B. The total free energy of the system is given as the sum of the free energies of mixing and the elastic free energy of an affine network. The elastic free energy  $\Delta G_{el}$  is given by the theory of rubber elasticity as

$$\Delta G = \frac{3}{2} \left( \frac{\mathbf{n}_e}{V_o} \right) \left\{ \left( \frac{V}{V_o} \right)^{2/3} - 1 - \frac{1}{3} \ln \left( \frac{V}{V_o} \right) \right\} \quad (4.2)$$

where,  $\mathbf{n}_e$  is the moles of elastically active chains in the gel,  $V$  is the volume of the gel and  $V_o$  is the volume at synthesis at a given temperature and pressure. The free energy of mixing is calculated from a mean field assumption in which the mers of the two components 1 and 2 are randomly placed on a lattice. For the mixture of  $n_1$  molecules of component 1 and  $n_2$  molecules of component 2 ( $N = n_1 + n_2$ ), the mer length ( $r$ ), the characteristic mer volume ( $\mathbf{n}^*$ ), and the characteristic mean-field mer-mer interaction energy ( $\mathbf{e}^*$ ) are given by

$$\frac{1}{r} = \frac{\mathbf{f}_1}{r_1} + \frac{\mathbf{f}_2}{r_2} \quad (4.3)$$

$$\mathbf{n}^* = \mathbf{f}_1 \mathbf{n}_1^* + \mathbf{f}_2 \mathbf{n}_2^* \quad (4.4)$$

$$\mathbf{e}^* = \mathbf{f}_1^2 \mathbf{e}_1^* + \mathbf{f}_2^2 \mathbf{e}_2^* + 2\mathbf{f}_1 \mathbf{f}_2 \mathbf{z}_{12} (\mathbf{e}_1^* \mathbf{e}_2^*)^{0.5} \quad (4.5)$$

Here,  $\mathbf{f}$  is the volume fraction,  $r_i$  is the number of lattice sites occupied by a molecule of component  $i$ ,  $\mathbf{n}_i^*$  is the characteristic mer volume of component  $i$  and  $\mathbf{e}_i^*$  is the characteristic mer-mer interaction energy for component  $i$ . A pure component  $i$  is thus characterized by three parameters  $r_i$ ,  $\mathbf{n}_i^*$  and  $\mathbf{e}_i^*$ .  $\mathbf{z}_{12}$  is the binary interaction parameter between components 1 and 2. The characteristic parameters of the pure random copolymer are obtained from Eqs. (4.3) to (4.5) by assuming that the copolymer can be considered as a random mixture of the two homopolymers A and B, which form the copolymer A-B and that the interaction parameter between the two homopolymers  $\mathbf{z}_{AB}$  is unity. In using Eqs. (4.3) to (4.5) for the copolymer, the subscripts 1 and 2 are replaced by A and B representing the two homopolymers. The volume fraction of the mers of two homopolymers are calculated as

$$\mathbf{f}_i = \frac{w_i / \mathbf{r}_i^*}{\sum_i w_i / \mathbf{r}_i^*} \quad (4.6)$$

where  $w_i$  is the weight of the component ( $i = A, B$ ) and  $\mathbf{r}_i^*$  is its characteristic density.

In a mixture of the copolymer and water, the binary interaction parameter  $\mathbf{z}_{12}$  is calculated as

$$\mathbf{z}_{12} = \mathbf{z}_{1A} \mathbf{f}_A + \mathbf{z}_{1B} \mathbf{f}_B \quad (4.7)$$

where the binary interaction parameter between water and the two homopolymers A and B are in general given as

$$\mathbf{z}_{12} = a_i T + b_i; \quad i = A, B \quad (4.8)$$

The binary interaction parameter between the copolymer and water can be considered as simulating the "effective hydrophobicity" of the copolymer since the hydrophilic part of the interactions is considered separately in the hydrogen bonding terms in the mean -field frame work of the LFHB theory.

Let there be  $i(i=1,m)$  types of proton donors and  $j(j=1,n)$  types of proton acceptors in the system of a gel and a solvent. The total number of donors and acceptors is given by

$$N_i^d = \sum_k d_i^k n_k \quad \text{and} \quad N_a^j = \sum_k a_j^k n_k \quad (4.9)$$

where  $d_i^k$  and  $a_j^k$  are the number of donors of type  $i$  and acceptors of type  $j$  in component  $k$ . If  $N_{ij}$  is the total number of hydrogen bonds formed between an  $i-j$  donor-acceptor pair, then the number of undonated protons of type  $i$  and unaccepted protons of type  $j$  are given by

$$N_{io} = N_i^d - \sum_j N_{ij} \quad (4.10)$$

and

$$N_{oj} = N_a^j - \sum_k N_{kj} \quad (4.11)$$

If  $E_{ij}^0$ ,  $S_{ij}^0$  and  $V_{ij}^0$  are changes in the energy, entropy and volume due to the formation of an  $i-j$  hydrogen bond, then the fraction of such  $i-j$  bonds formed is given by

$$\mathbf{n}_{ij} = \left[ \mathbf{n}_d^i - \sum_k \mathbf{n}_{ik} \right] \left[ \mathbf{n}_a^j - \sum_k \mathbf{n}_{kj} \right] \exp\left(-\frac{G_{ij}^0}{RT}\right) \quad (4.12)$$

where,

$$\mathbf{n}_{ij} = \frac{N_{ij}}{rN}; \quad \mathbf{n}_d^i = \frac{N_d^i}{rN}; \quad \mathbf{n}_a^j = \frac{N_a^j}{rN}$$

$$G_{ij}^o = E_{ij}^o + PV_{ij}^o - TS_{ij}^o \quad (4.13)$$

The free energy of mixing in the LFHB model can be calculated from the mixing rules given by Eqs.(4.3)-(4.5) and the hydrogen bonding fractions are given by Eq. (4.13). The details of the free energy of mixing terms are described in Lele *et al.* (1995). From the free energy of mixing and the elastic free energy of Eq. (4.1), the chemical potential of water in the gel phase can be calculated as

$$\begin{aligned}
\frac{\mathbf{m}_1^G}{RT} = & \ln\left(\frac{\mathbf{f}_1}{\mathbf{w}_1}\right) + \left(1 - \frac{r_1}{r_2}\right) \mathbf{f}_2 + r_1 \tilde{\mathbf{r}} \mathbf{f}_2^2 \mathbf{c}_{12} \\
& + r_1 \left\{ -\frac{\tilde{\mathbf{r}}}{\tilde{T}_1} + \frac{\tilde{P}_1 \tilde{v}}{\tilde{T}_1} + (\tilde{v} - 1) \ln(1 - \tilde{\mathbf{r}}) + \frac{1}{r_1} \ln \tilde{\mathbf{r}} \right\} \\
& + r_1 \sum_i^m \sum_j^n v_{ij} - \sum d_i^1 \ln \frac{v_d^i}{v_{io}} - \sum a_j^1 \ln \frac{v_a^j}{v_{oj}} \\
& + \left\{ r_1 \left( \frac{v_e}{V_0} \right) v_1^* \tilde{v} \left[ \left( \frac{V_0}{V} \right)^{1/3} - \frac{1}{2} \left( \frac{V_0}{V} \right) \right] \right\}
\end{aligned} \tag{4.14}$$

where,

$$\mathbf{c}_{12} = \frac{\mathbf{e}_1^* + \mathbf{e}_2^* - 2\mathbf{z}_{12}(\mathbf{e}_1^* \mathbf{e}_2^*)^{1/2}}{RT} \tag{4.15}$$

and  $\tilde{\mathbf{r}}$  is the reduced density of the mixture which is related to the reduced pressure  $\tilde{P} = \frac{P}{P^*}$  and reduced temperature  $\tilde{T} = \frac{T}{T^*}$  by the equation of state

$$\begin{aligned}
\tilde{\mathbf{r}}^2 + \tilde{P} + \tilde{T} \left\{ \ln(1 - \tilde{\mathbf{r}}) + \tilde{\mathbf{r}} \left[ 1 - \left( \frac{1}{r} - \sum_i^m \sum_j^n v_{ij} \right) \right] \right\} \\
+ \frac{v_e}{V_0} \tilde{T} v^* \left[ \left( \frac{V_0}{V} \right)^{1/3} - \frac{1}{2} \left( \frac{V_0}{V} \right) \right] = 0
\end{aligned} \tag{4.16}$$

In the first line of Eq. (4.13), the first two terms are the combinatorial entropy contribution and the third term is the energetic (effective hydrophobic) contribution. The term in the second line represents the effect

of the pure component properties, while those in the third line represent the hydrogen bonding contribution. The fourth line represents the elastic energy contribution.

The equilibrium swelling capacity of the gel,  $q = 1/f_2$ , can be calculated from the condition that the swelling pressure of the gel at equilibrium is equal to zero. Thus,

$$p = m_1^G - m_1^0 = 0 \quad (4.17)$$

where  $m_1^0$  is the chemical potential of pure water outside the gel. The solution of equation (4.16) requires solving eq. (4.2) to eq. (4.15) simultaneously. These are the main equations constituting the model.

The model parameters for a copolymer gel-water mixture include nine pure component parameters (three for each component), one binary interaction parameter ( $z_{12}$ ), three hydrogen bonding parameters ( $E_{ij}^0, S_{ij}^0, V_{ij}^0$ ) for each  $i-j$  type of hydrogen bond, and the crosslink density ( $n_e/V_0$ ). Parametric values are discussed in the Results and Discussion section.

### 4.3. Experimental section

#### 4.3.1 Materials:

The hydrophilic monomer, 2-acryloylamido-2-methyl-1-propane sulfonic acid (AMPS) was purchased from Fluka. The hydrophobic monomers N-tertiary-butylacrylamide (N-t-BAm) and N-isopropyl acrylamide (NIPAm) were obtained from Aldrich Chemical Company Inc. and Polysciences Inc. (Warrington, PA, USA), respectively. In addition, the crosslinking agent N, N'-methylene bis-acrylamide (Bis-Am) was also procured from Aldrich Chemical Company Inc USA. The solvent Dimethyl

sulfoxide (DMSO), AR grade, was obtained from S.d. Fine chemicals, Mumbai, India. The initiator "azo bis isobutyronitrile" (AIBN) was procured from SAS Chemical Co., Mumbai, India. All chemicals were used as such without further purification. Deionized distilled water was prepared in the laboratory using standard procedures.

#### **4.3.2 Synthesis of gels:**

We have synthesize copolymer gels by copolymerising Nt-BAm or NIPAm monomers with AMPS monomer as per the feed composition tabulated in Tables 4.1 and 4.2. The copolymerization was carried out in DMSO using Bis-Am as cross-linker and AIBN as free radical initiator. The reaction scheme is shown in Figure 4.1. The desired amounts of monomers, with defined mol ratios, cross-linking agent and initiator were taken in a beaker and dissolved in DMSO with constant stirring under nitrogen gas bubbling. The reaction mixtures were poured into test tubes and sealed. The reaction was carried out at 65°C for 24 hrs. The cylindrical gels so obtained were immersed in water for 48 hrs in order to wash away the unreacted reactants. During this time fresh water was added frequently. The washed gels were dried in an oven at 50°C to constant weight. A series of copolymer gels, AMPS-co-N-t-BAm and AMPS-co-NIPAm, were prepared with different mol ratios to study the effect of the concentration of the hydrophobe on swelling behavior. All the gels were clear and transparent except the N-t-BAm homopolymer gel, which was opaque. The gels prepared with 10 mol % and 20 mol % cross-linker were very soft and difficult to handle. Therefore in the present work, all gels were prepared by using 30 mol % cross-linking agent.

Sample Code	Mole Ratio	Crosslinker (Moles)	Initiator (Moles)	Solvent (ml)
Bu-AMPS(10/0)	N-t-BAm/AMPS (0.01/0.0)	Bis-Am $3 \times 10^{-3}$	AIBN $4.87 \times 10^{-4}$	DMSO 23
Bu-AMPS(10/1)	N-t-BAm/AMPS (0.01/0.001)	Bis-Am $3.3 \times 10^{-3}$	AIBN $4.87 \times 10^{-4}$	DMSO 23
Bu-AMPS(10/2)	N-t-BAm/AMPS (0.01/0.002)	Bis-Am $3.6 \times 10^{-3}$	AIBN $4.87 \times 10^{-4}$	DMSO 23
Bu-AMPS(10/5)	N-t-BAm/AMPS (0.01/0.005)	Bis-Am $4.5 \times 10^{-3}$	AIBN $4.87 \times 10^{-4}$	DMSO 23
Bu-AMPS(5/10)	N-t-BAm/AMPS (0.005/0.01)	Bis-Am $4.5 \times 10^{-3}$	AIBN $4.87 \times 10^{-4}$	DMSO 23
Bu-AMPS(1/10)	N-t-BAm/AMPS (0.001/0.01)	Bis-Am $3.3 \times 10^{-3}$	AIBN $4.87 \times 10^{-4}$	DMSO 23
Bu-AMPS(0/10)	N-t-BAm/AMPS (0.0/0.01)	Bis-Am $3.0 \times 10^{-3}$	AIBN $4.87 \times 10^{-4}$	DMSO 23
N-t-Bam	N-tertiary -butylacrylamide			
AMPS	2-acrylamido-2-methyl-1-propane sulfonic acid			
Bis-Am	N,N-methylene bisacrylamide			
AIBN	Azo bis isobutyronitrile			
DMSO	Dimethyl sulfoxide			

**Table 4.1:** Feed composition of the AMPS-co-N-t-BAM gels

Sample Code	Mole Ratio	Crosslinker (Moles)	Initiator (Moles)	Solvent (ml)
ip-AMPS(10/0)	NIPAm/AMPS (0.01:0.0)	Bis-Am $3.0 \times 10^{-3}$	AIBN $4.87 \times 10^{-4}$	DMSO 23
ip-AMPS(10/1)	NIPAm/AMPS (0.01:0.001)	Bis-Am $3.3 \times 10^{-3}$	AIBN $4.87 \times 10^{-4}$	DMSO 23
ip-AMPS(10/2)	NIPAm/AMPS (0.01:0.002)	Bis-Am $3.6 \times 10^{-3}$	AIBN $4.87 \times 10^{-4}$	DMSO 23
ip-AMPS(10/5)	NIPAm/AMPS (0.01:0.005)	Bis-Am $4.5 \times 10^{-3}$	AIBN $4.87 \times 10^{-4}$	DMSO 23
ip-AMPS(5/10)	NIPAm/AMPS (0.05:0.001)	Bis-Am $4.5 \times 10^{-3}$	AIBN $4.87 \times 10^{-4}$	DMSO 23
ip-AMPS(1/10)	NIPAm/AMPS (0.01:0.001)	Bis-Am $3.3 \times 10^{-3}$	AIBN $4.87 \times 10^{-4}$	DMSO 23
ip-AMPS(0/10)	NIPAm/AMPS (0.0/0.001)	Bis-Am $3.0 \times 10^{-3}$	AIBN $4.87 \times 10^{-4}$	DMSO 23
NIPAm	N-isopropylacrylamide			
AMPS	2-acrylamido-2-methyl-1-propane sulfonic acid			
Bis-Am	N,N-methylene bisacrylamide			
AIBN	Azo bis isobutyronitrile			
DMSO	Dimethyl sulfoxide			

**Table 4.2:** Feed composition of the AMPS-co-NIPAm gels



**Figure 4.1:** Reaction scheme for the synthesis of copolymer gels

### **4.3.3 Characterization of the copolymer gels:**

#### **Swelling Measurements (SWR)**

Dry gel samples of known weight were immersed in excess quantity of distilled water and kept in sealed containers, which were placed in a temperature-control bath (Julabo F25) with  $\pm 1^\circ\text{C}$  accuracy until equilibrium was reached, which took approximately 96 hrs. The samples were removed and blotted dry. The swelling ratio of the copolymer gels was determined gravimetrically. The equilibrium weight of the swollen samples at each temperature was determined. The swelling ratios of the copolymer gels were calculated from the ratio of the weight of the equilibrated gel to the dry weight.

$$Q = \text{Weight of the equilibrated gel (Ws)} / \text{Dry weight of the gel (Wd)}.$$

On an average the swelling measurements were repeated thrice at each temperature. The percentage error was found to be 0.3 to 1%.

#### **Measurement of elasticity**

A compression rig (Figure 4.2) fitted to an Instron Universal Testing Machine (model 4204) was used to obtain compression-strain data on swollen specimens having dimensions 25 mm length and 12 mm diameter. The samples were prepared using a mould of 25 mm length and 12 mm diameter. The solutions were poured into the moulds and then polymerized at  $50^\circ\text{C}$  for 24 hrs as discussed in section 4.3.2. The gels were washed after removing from the mould and then dried to get pure gel with constant weight. A load cell of 1 kN was fitted to the instrument and the tests were done at a crosshead speed of 10mm/min.

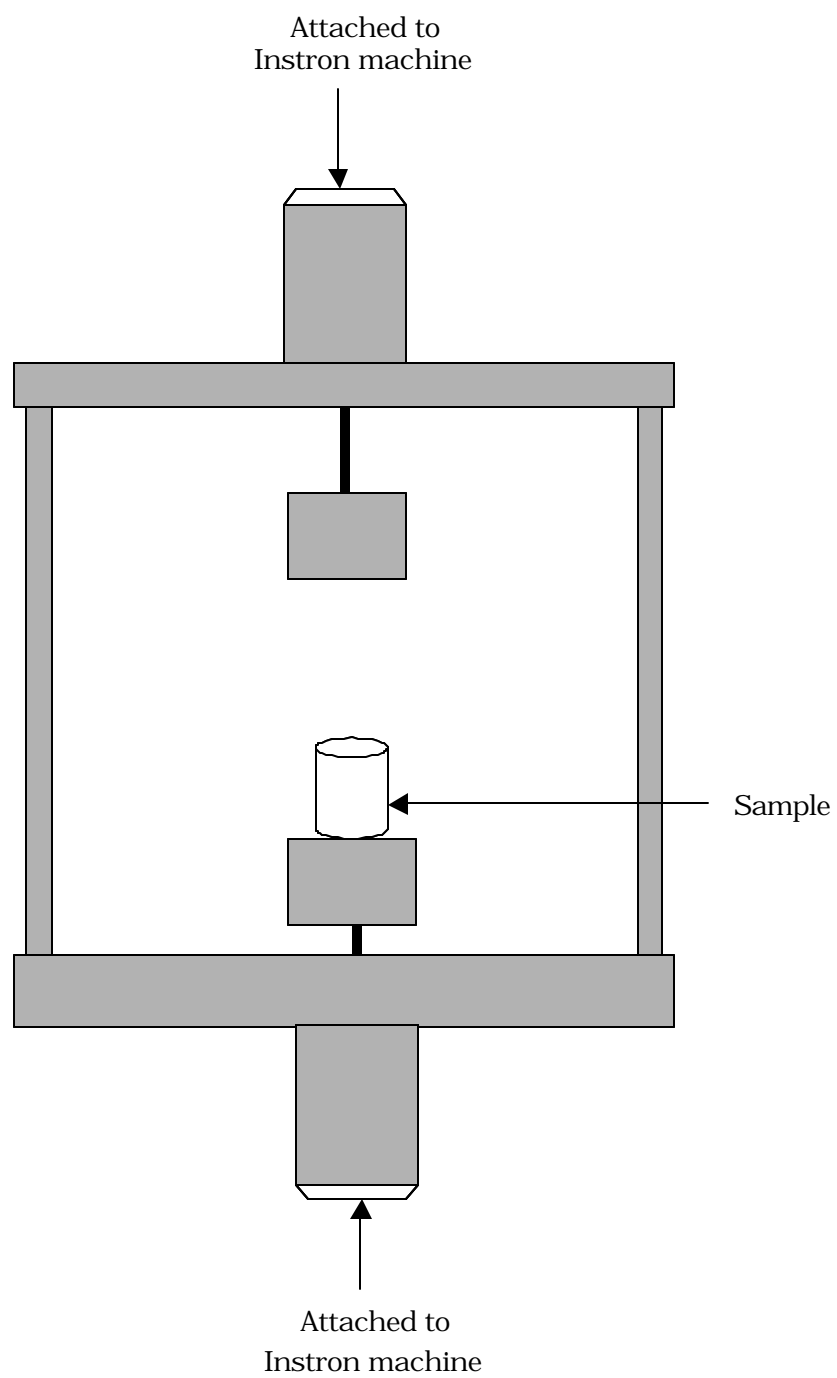


**Figure 4.2:** Schematic of the compression rig used to measure the compression modulus of the gel samples.

We have used the swollen samples (at the equilibrium swelling) for the measurement directly without immersing them in water while doing the tensile experiments. The tests were completed in 3 min and no water was evaporated at the experimental temperature (25°C) during the experimental time period. Water was not squeezed out of the gel during the compression tests. It clearly indicates that the water molecules are hydrogen bonded to the polymer unlike they stay within the pores in the case of sponge.

Figure 4.3 shows the typical stress-strain curve obtained for Bu-AMPS (10/1). The modulus is calculated from the linear part of the curve as shown in the figure.

## **FTIR**

The infrared absorption spectra of the copolymer gels were measured by Shimadzu model 3000 FT-IR spectrophotometer. The dried samples were pelletized with KBr powder and the transparent pellets were used for scanning.

## **4.4 Results and Discussion**

### **4.4.1 Theoretical hypothesis**

Figure 4.4 shows the qualitative predictions of the LFHB model for the swelling behavior of copolymer gels in which one of the monomers is highly hydrophilic while the other is highly hydrophobic. The homopolymer gel of the hydrophobic monomer remains completely collapsed in water in the temperature range of 5°C to 100°C as shown by curve 1, whereas the homopolymer of the highly hydrophilic gel shows a UCST (Upper Critical Solution Temperature) type swelling behavior, i.e., an increase in swelling with temperature, in the same temperature range as shown by curve 2.

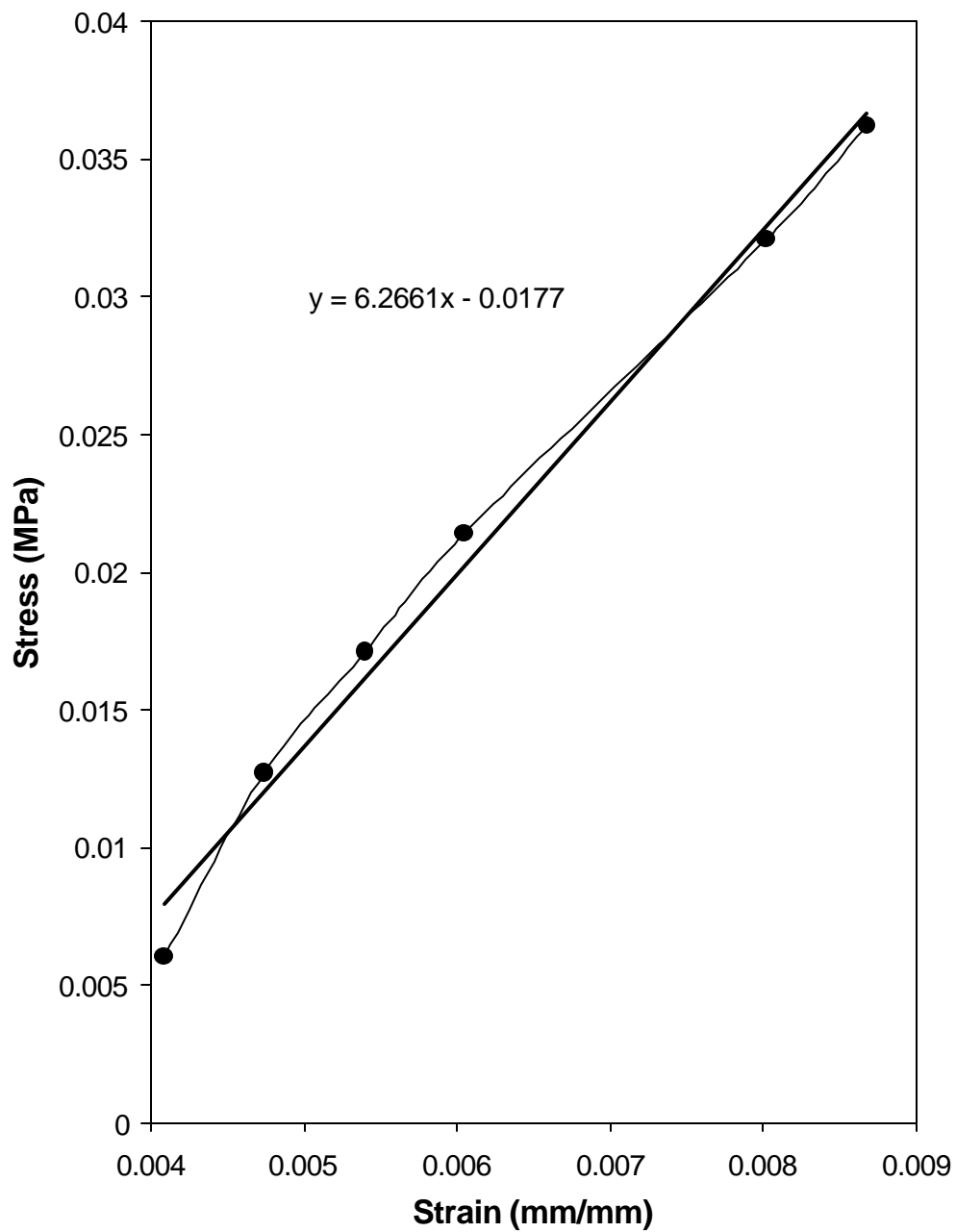


**Figure 4.3:** Stress-strain curve for Bu-AMPS (10/1)

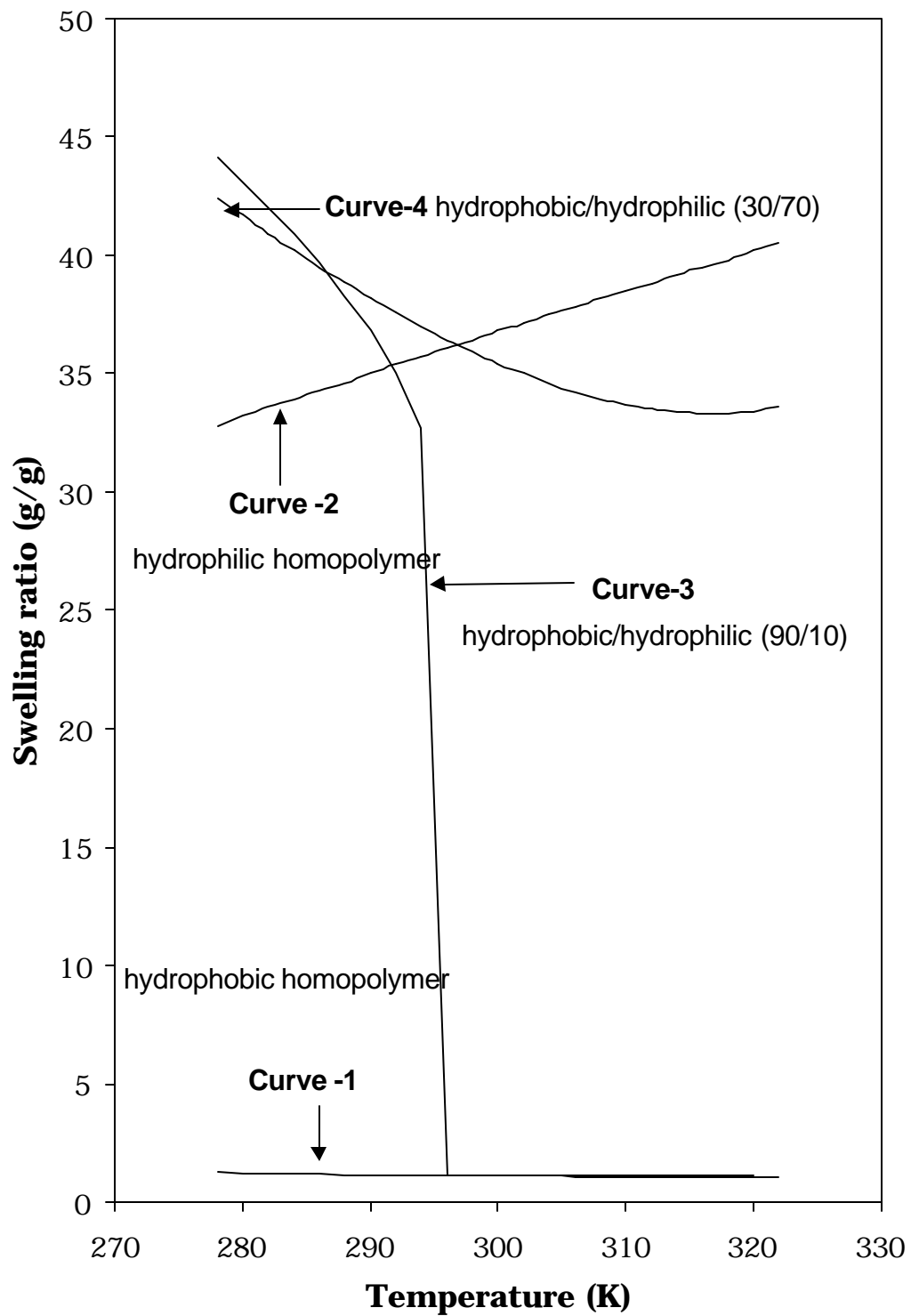


**Figure 4.4:** Qualitative predictions of the LFHB model for the swelling behaviour of copolymer gels

Thus, neither of the homopolymers show a first order discontinuous LCST type volume transition or a continuous LCST type volume transition within the temperature range, 5°C to 100°C. However, at an intermediate composition of these two monomers, the LFHB model predicts a discontinuous LCST-type swelling behavior for the copolymer gel as shown by curve 3. This suggests a novel method for synthesizing thermoreversible gels. It proposes that if a proper balance of hydrophilic and hydrophobic interactions is reached in a copolymer gel, it should exhibit a first order discontinuous volume transition. As the hydrophilicity increases the hydrophilic-hydrophobic balance is disturbed and consequently the LCST behaviour is lost. At a higher hydrophilic monomer composition, the decrease in swelling with temperature (LCST-type behaviour) is balanced by the increase of swelling with temperature (UCST-type behaviour), resulting in a swelling plateau as shown by curve 4. At still higher hydrophilic monomer content the swelling behavior changes to UCST type, i.e., the swelling ratio increases with temperature. Thus the model predicts qualitatively different types of swelling behaviors such as a collapsed state, discontinuous LCST type, continuous LCST type, swelling plateau, and UCST type swelling behaviors with respect to temperature. The predictions of the LFHB model were quantified experimentally and the results are discussed in the following sections.

#### **4.4.2 Experimental Results**

##### **4.4.2.1 Structure of the copolymers**

The FT-IR spectra of the copolymer gels and homopolymer gels are given in Figures 4.5 and 4.6. The spectrum of PAMPS homopolymer shows

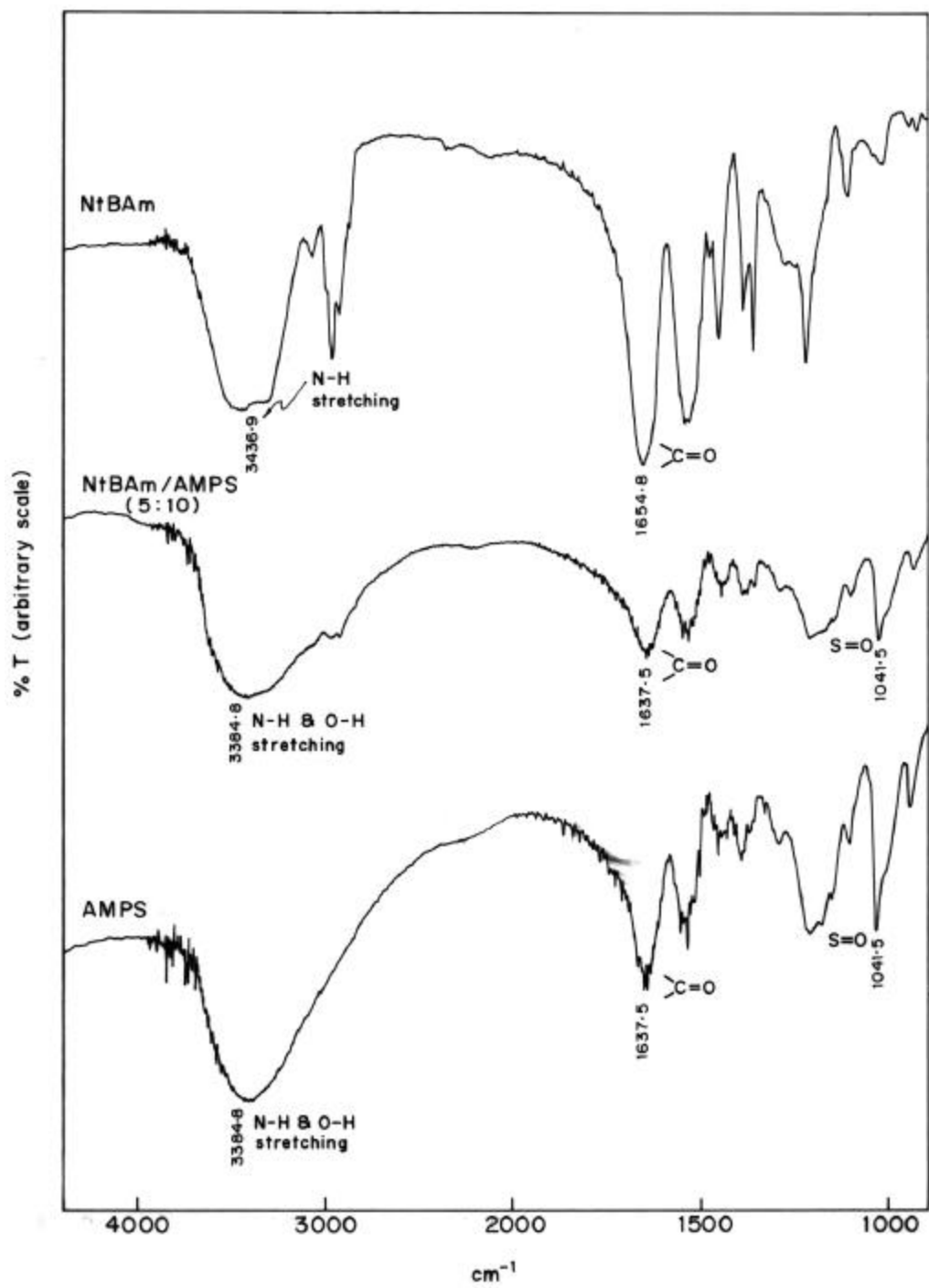


**Figure 4.5:** FT-IR spectra of N-t-BAm-co-AMPS gels



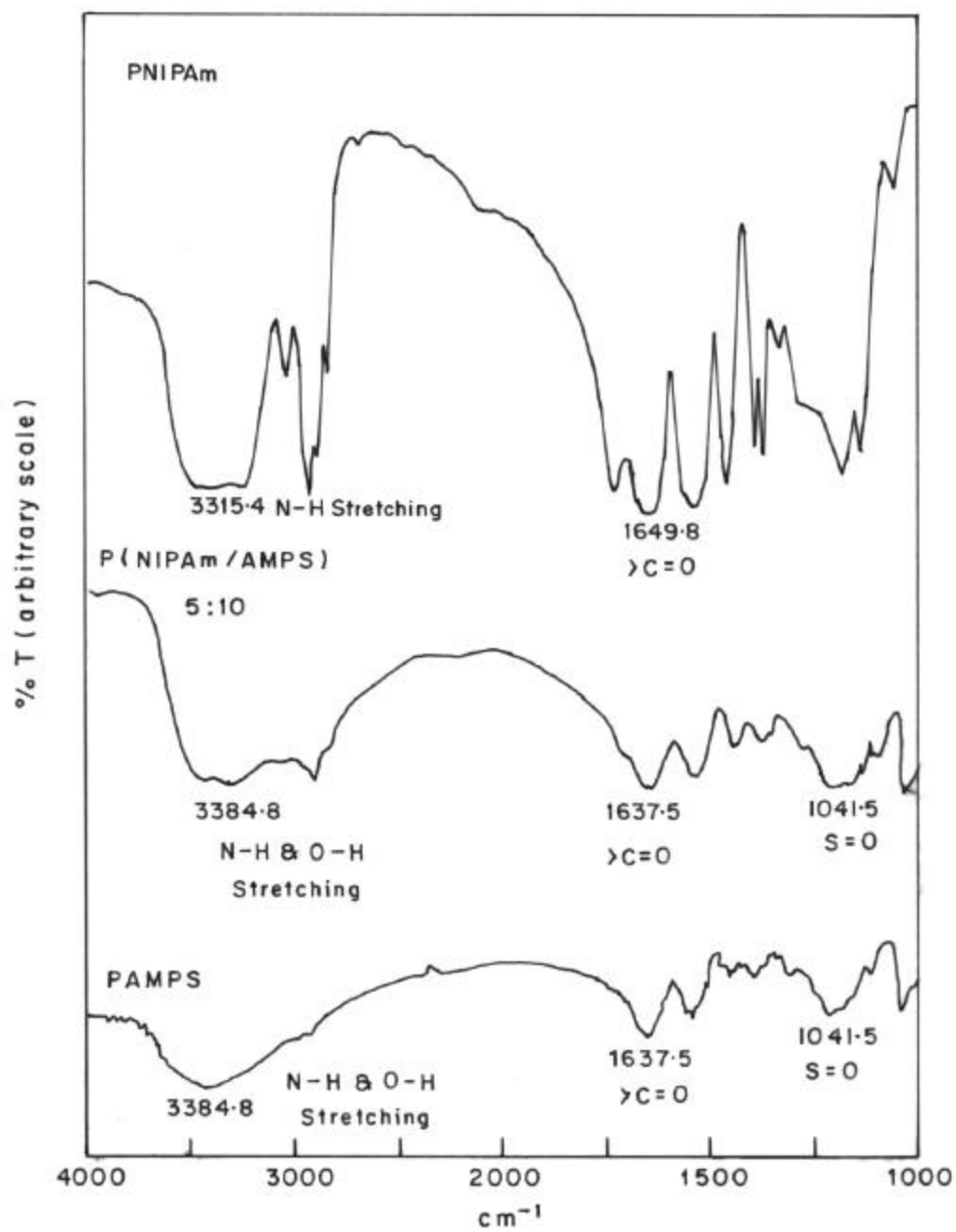


**Figure 4.6:** FT-IR spectra of NIPAm-co-AMPS gels

sharp peaks at 1160 and 3350  $\text{cm}^{-1}$  indicating the presence of S=O and OH group in the polymer gels. The broad peak observed at  $\sim 3350$  may be either due to the -OH group or due to the -NH group. However, the absence of the peak corresponding to the S=O group as well as C=O group clearly indicates that the broad peak observed in the spectrum of N-t-BAm as well as NIPAm at  $\sim 3300$  might be due to the moisture or due to the -NH stretching. Nevertheless, the spectrum of the copolymer gels shows the characteristic peaks of both the monomers. This clearly indicates the incorporation of both the monomers in the copolymer gel..

#### **4.4.2.2 Swelling behaviour of NtBAm-co-AMPS copolymer gels**

Figure 4.7 presents the swelling behavior of a series of copolymer gels in which AMPS is used as the hydrophilic monomer and N-t-BAm is used as the hydrophobic monomer. The lines through the experimental points are the trend lines and are drawn for the sake of clarity. As shown in the figure, the swelling capacity of the pure PAMPS gel increased with increase in temperature (UCST type swelling behavior). The pure poly (N-t-BAm) gel did not swell in water in the temperature range studied. In fact, it did not swell in water till the freezing point. However, when a small amount of AMPS comonomer (0.1 mole) was copolymerized with N-t-BAm (1mole), the swelling behavior of the copolymer gel changed qualitatively from that of the homopolymer gels as indicated in Figure 4.7.

The copolymer gel Bu-AMPS (10/1) (1 mole of N-t-BAm and 0.1 mole of AMPS) showed a sharp discontinuous LCST type swelling-collapse phenomena in water as the temperature was raised from 14°C to 16°C. The discontinuous nature of this transition is demonstrated in Figure 4.8, which shows the co-existence of a swollen and a collapsed phase at 15°C.

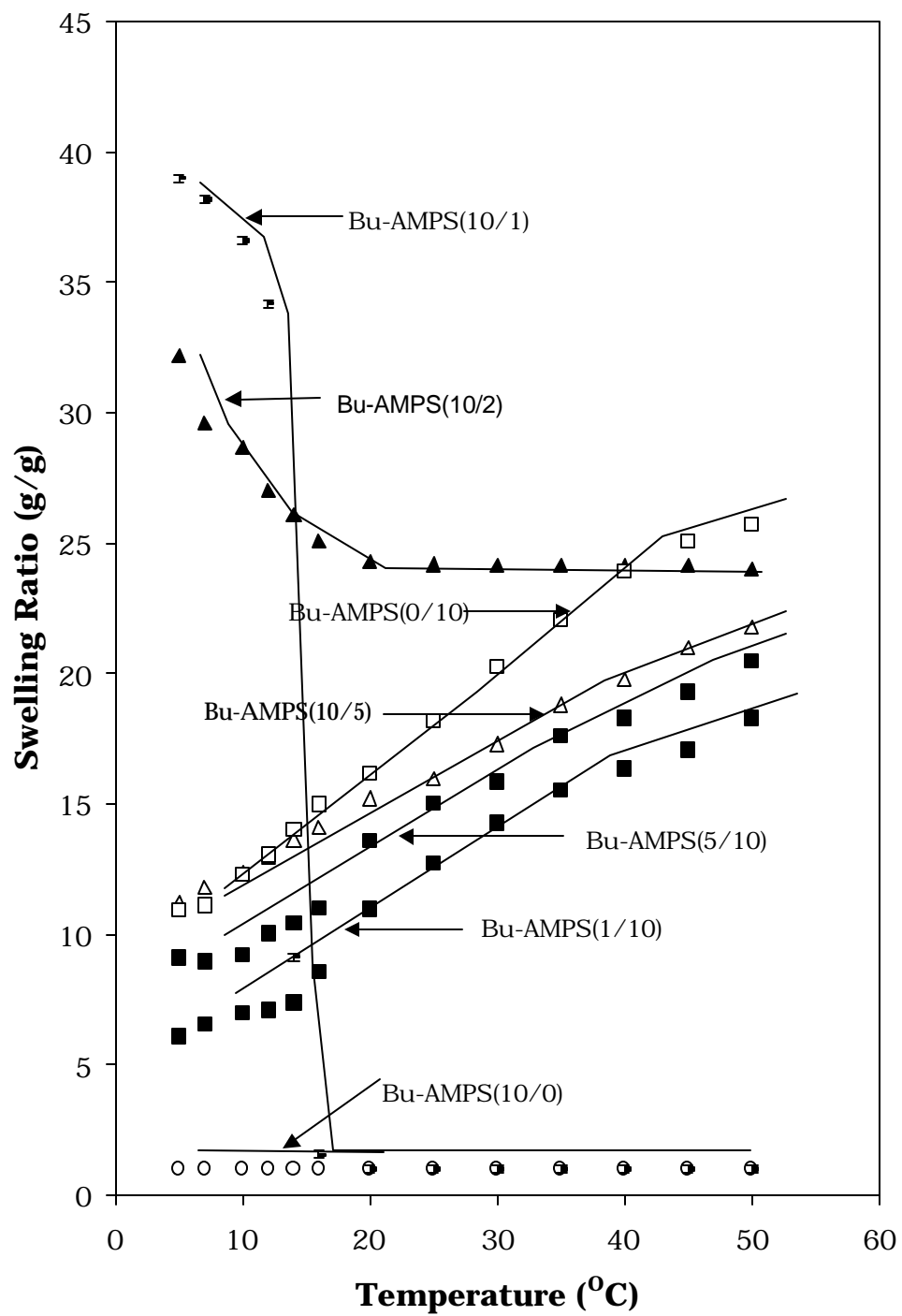


**Figure 4.7:** Swelling behavior of AMPS-co-N-t-BAm copolymer gels

**Figure 4.8:** Coexistence of a swollen and a collapsed phase at the transition temperature

With a further slight increase in the AMPS content of the copolymer gel such as in the case of Bu-AMPS (10/2) the discontinuous nature of the transition was completely lost. A continuous decrease in swelling was observed with increasing temperature. Another significant observation was that the copolymer gel, Bu-AMPS (10/2), showed a swelling plateau at higher temperatures. With further increase in the content of AMPS comonomer, no volume transition phenomenon was observed in the temperature range of 5°C to 100°C. In fact all the copolymer gels with higher AMPS content showed a UCST type-swelling behavior. The experimentally observed swelling behaviour has striking resemblance to the theoretical predictions shown in Figure 4.4 suggesting validity of the hypothesis.

The discontinuous volume transition exhibited by the Bu/AMPS (10/1) was reversible in nature. For example, the collapsed gel reverted back to the swollen phase while lowering the temperature from 16 to 14°C. Again, while increasing the temperature from 14 to 16°C, the gel attained the collapsed phase.

#### **4.4.2.3 Swelling behavior of NIPAm-co-AMPS copolymer gels**

Figure 4.9 shows the effect of temperature on the equilibrium swelling ratio of the NIPAm (N-isopropylacrylamide) based copolymer gels. The lines through the points are trend lines drawn for the sake of clarity. Pure poly (NIPAm) gel was found to undergo a sharp volume transition at 32°C in which the swelling ratio of the gel decreased from 10 g/g to 1 g/g. A significant change in swelling behavior was observed with the incorporation of a small amount of the hydrophilic comonomer.

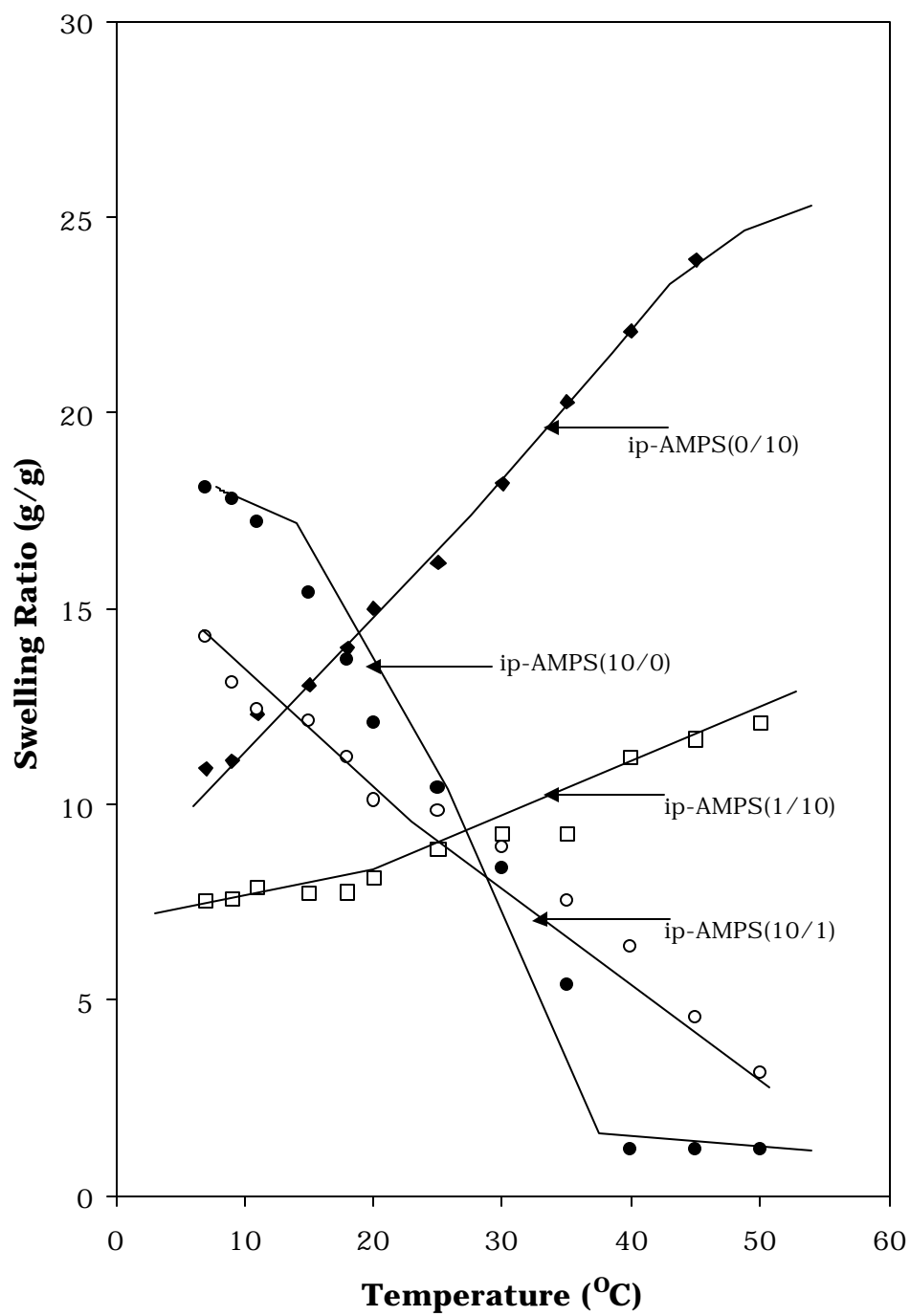


**Figure 4.9:** Swelling behavior of AMPS-co-NIPAm copolymer gels

The ip-AMPS (10/1) gel (NIPAm 1.0 mol and AMPS 0.1 mol) showed a continuous LCST type swelling behavior. The sharp volume transition seen in PNIPAm gel was lost with the incorporation of small amount of AMPS.

As shown in the above figure, in all other compositions, as the AMPS content increases, the LCST behavior disappeared and the swelling capacity increased with temperature (UCST type swelling behavior). This shows that subtleties of hydrophilic-hydrophobic balance play a vital role in determining the volume transition phenomenon of the copolymer gels.

#### **4.4.2.4 Effect of comonomer structure on Volume transition phenomenon**

On comparing the N-t-BAM copolymer gels with the NIPAm gels, it is seen that the more hydrophobic Nt-BAM homopolymer gel did not swell in water while the PNIPAm gel showed a distinct LCST type volume transition. When the monomers are copolymerized with AMPS at 1.0:0.1 mole ratio, the N-t-BAM copolymer gel showed a distinct discontinuous volume transition, whereas the NIPAm based homopolymer gel showed a continuous transition at the same composition. The chemical structures of the hydrophobes are given in Figure 4.1 and the only difference between the N-t-BAM and NIPAm is that in N-t-BAM, there is an additional methyl group.

#### **4.4.2.5 Effect of modulus on swelling behavior**

The experimental data in Figures 4.7 & 4.9 indicates that as the hydrophilic (AMPS) content in the gel increases, the equilibrium swelling capacity decreases, which counter intuitive. This is surprising since the swelling capacity of the gel is expected to increase with increase in the hydrophilic content. Figure 4.10 shows the compression modulus of the

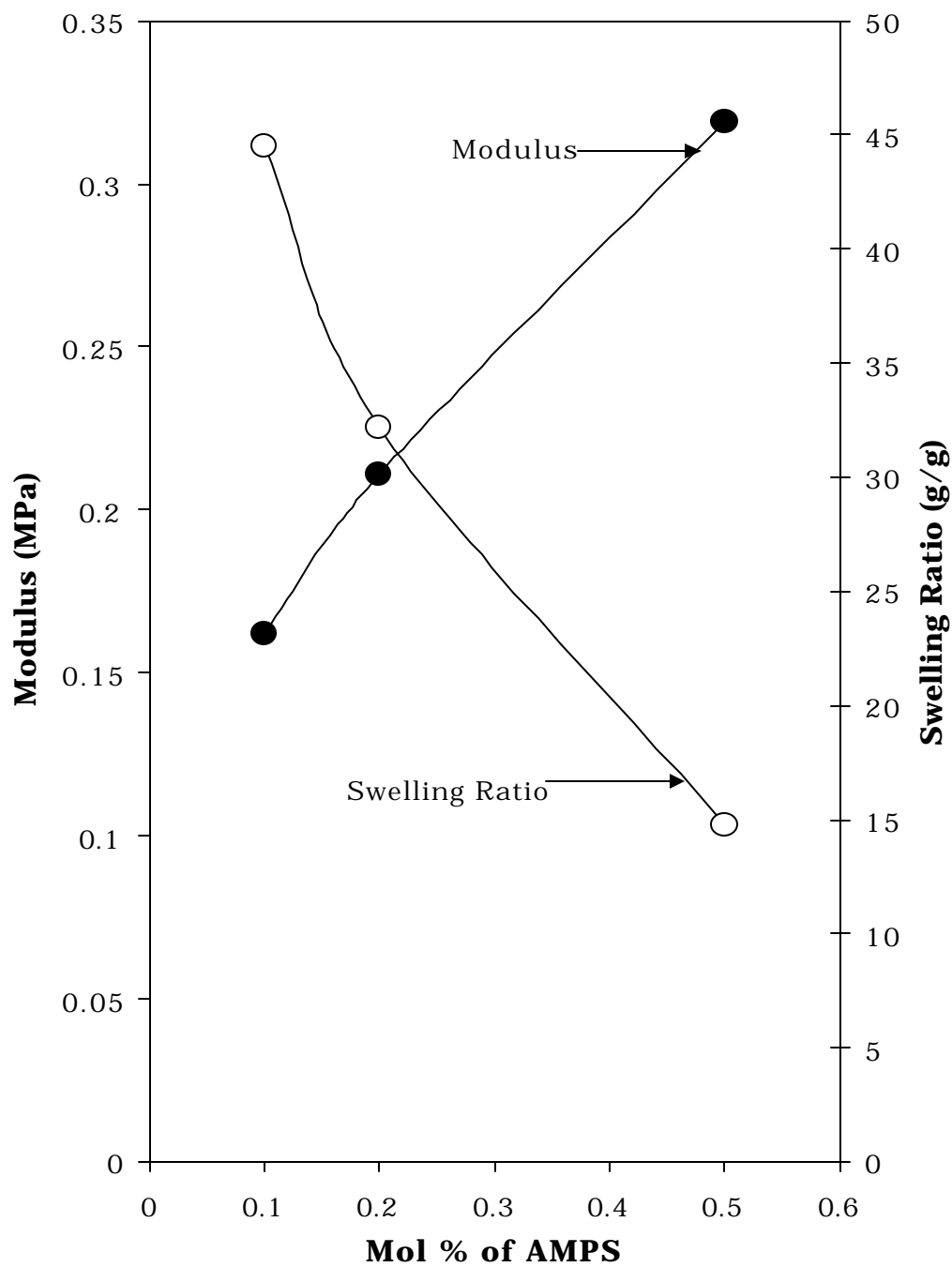


**Figure 4. 10:** Correlation between AMPS content, modulus and swelling behavior of the copolymer gels



copolymer gels as a function of the AMPS content. It is seen that the modulus of the gels increases with AMPS content, which implies an increase in the crosslink density of the gels. Since our synthesis procedure for copolymer gels does not provide any control over the crosslink density, it appears that the incorporation of the crosslinking agent (bisacrylamide) into the polymerizing network is enhanced in the presence of the hydrophilic AMPS monomer. Alternatively, the higher crosslink density may be due to a combination of covalent crosslinks from bis-Am and physical crosslinks from inter polymer hydrogen bonds such as those reported by Bensberg *et al.* (1997) and Cho *et al.* (1997).

We examined the copolymer gels by FT-IR spectroscopy to check the presence of interpolymer hydrogen bonding interactions, if any, in the copolymer gels. As seen in Figure 4.5, no shift in peaks was observed for the hydrogen bonding groups (C=O, -NH, -OH, S=O) in the copolymer gel. This observation suggests that the presence of interpolymer hydrogen bonding interactions in the copolymer gels is negligible. Hence the increase in crosslink density with AMPS content can be considered to be mainly due to covalent crosslinks formed by greater or more effective incorporation of bisacrylamide in the gel. The calculations from the LFHB model also indicate that the contribution of physical crosslinks is negligible. From the experimentally determined modulus, we have calculated the crosslink density of the copolymer gels by using equation (4.18). For fully swollen Bu-AMPS (10/1) and Bu-AMPS (0/10) the crosslink density values were determined to be 60 and 240 gmol/cm<sup>3</sup>, respectively.

$$\mathbf{s} = \mathbf{n}_e kT \left( \mathbf{a} - \frac{1}{\mathbf{a}^2} \right) \quad (4.18)$$

The theoretical crosslink density values of the Bu-AMPS (10/1) and Bu-AMPS (0/10) were estimated to be 280 and 260 gmol/cm<sup>3</sup> respectively. Crosslink densities of the gels were theoretically calculated from the stoichiometric amount of Bis-Am added to the system using the equation (4.19). The actually determined crosslink density values are less than those estimated theoretically. It is well known that the crosslink density is always lower than that calculated theoretically because of the presence of imperfections such as dangling chain ends, steric hindrance, and incomplete conversion of the crosslinking agent during the reaction.

$$\frac{n_e}{V_0} = \frac{(\text{functionality}) \times (\text{mol of Bis-Am in 1 g gel})}{\text{Vol. of 1 g gel (as measured at equilibrium)}} \quad (4.19)$$

#### 4.4.3 Simulation results

##### 4.4.3.1 Model parameters

The hydrogen bonding parameters used for all calculations in this paper are reported in Table 4.3. For the copolymers, the LFHB model requires pure component P-V-T properties of the homopolymers, which are not reported in the literature for the N-t-BAm, NIPAm and AMPS polymers. However, Lele *et al.* (1995, 1997, 1998) have reported successful predictions of the VPT in PNIPAm homopolymer and copolymer gels by assuming the PVT properties of poly (methyl methacrylate) for PNIPAm. The success for the LFHB predictions of VPT in hydrogels lies in the fact that the swelling behaviour of the hydrogels do not depend very significantly on the values of the pure component parameters. As discussed in Chapter two, the contributions of the pure component properties become significant only at very high pressure and temperature near the critical point of the solvent. Since VPT in hydrogels is seen at near-ambient temperature and pressure,

it is expected that the pure component properties will not significantly affect the predictions. In this work we have assumed the pure component values of poly (methyl methacrylate) for AMPS and NIPAm homopolymers, and those of poly (n-butyl methacrylate) for the N-t-BAm homopolymer. These values have been reported by Sanchez and Lacombe (1976, 1977, 1978). The rationale for the choice of poly (n-butyl methacrylate) parameters for N-t-BAm is that it is more hydrophobic than poly (methyl methacrylate) whose parameters have been used for poly (NIPAm). Table 4.4 gives the pure component properties assumed for poly (NIPAm), poly (AMPS) and poly (N-t-BAm). The calculations of the hydrogen bonding terms in the chemical potential require solving nine simultaneous equations represented by Eq. (4.10) for three pairs of donors and acceptors. The donors and acceptors along with their hydrogen bonding energies, entropies and volume changes are listed in Table 4.3.

The parameters corresponding to the hydrogen bonding between the terminal sulfonic acid group on the AMPS monomer and the hydroxyl group of water are assumed to be such that hydrogen bonding is more favourable than that between the amide and water. The values of crosslink density of the gels required for quantitatively fitting the experimental data are calculated from the modulus values and are given in Table 4.5. It is seen that Bu-AMPS (10/1) has lower crosslink density and thereby maximum swelling as observed experimentally. The effective hydrophobicity of the copolymer gel is represented by  $\mathbf{z}_{12}$ . The binary interaction parameter required for fitting the experimental swelling data are listed in Table 4.5. A lower value of  $\mathbf{z}$  indicates higher hydrophobicity.

H bonding parameters	Donors →			
	Acceptors ↓	-NH $d_1^2 = 8,6,94,56$	-OH $d_2^1 = 2$	-SO <sub>3</sub> H $d_3^2 = 0,1,4,43$
$E_{ij}^0 (J / gmol)$		-3.24x10 <sup>3</sup>	-16.0x10 <sup>3</sup>	-3.24x10 <sup>3</sup>
$S_{ij}^0 (J / gmolK)$	-C=O $a_1^2 = 8,6,94,56$	-9.9	-25.8	-10.0
$V_{ij}^0 (cm^3 / gmol)$		-0.85x	-0.85	-0.85
$E_{ij}^0 (J / gmol)$		-12.5x10 <sup>3</sup>	-16.595x10 <sup>3</sup>	-25.00x10 <sup>3</sup>
$S_{ij}^0 (J / gmolK)$	-OH $a_2^1 = 2$	-17.8	-26.6	-10.6
$V_{ij}^0 (cm^3 / gmol)$		-0.85	-4.2	-0.85
$E_{ij}^0 (J / gmol)$		-12.5x10 <sup>3</sup>	-25.00x10 <sup>3</sup>	-12.5x10 <sup>3</sup>
$S_{ij}^0 (J / gmolK)$	-SO <sub>3</sub> H $a_3^2 = 0,2,8,86$	-7.8	-10.0	-7.8
$V_{ij}^0 (cm^3 / gmol)$		-0.85	-0.85	-0.85

$a_3^2 = d_3^2 = 0$  for Bu-AMPS (10/0) and ip-AMPS (10/0)

$a_1^2 = d_1^2 = 8, 6, 94$  and  $56$  for Bu-AMPS (10/1), Bu-AMPS (10/2), ip-AMPS (10/1), ip-AMPS(10/0)

$a_3^2 = 2,8$  and  $86$  for Bu-AMPS (10/1), Bu-AMPS (0/10) and ip-AMPS (10/1)

$d_3^2 = 1, 4$  and  $43$  for Bu-AMPS (10/1), Bu-AMPS (0/10) and ip-AMPS (10/1)

**Table 4.3:** Hydrogen bonding parameters

Component	P* (Mpa)	T* (K)	$\rho^*$ (kg/cm <sup>3</sup> )	MW (g/mol)
PN-t-BAm	503	699	1269	1000
PNIPAm	503	699	1269	10000
PAMPS	431	627	1125	1000
Water	475	578	853	18

**Table 4.4:** Molecular parameters

Gel	Components	$\zeta$	( $v_e/v_0$ )(gmol/cm <sup>3</sup> )
Bu-AMPS(10/0)	N-t-BAm	1.451-1.8x10 <sup>-3</sup> T	200
Bu-AMPS(10/1)	N-t-BAm	1.451-1.8x10 <sup>-3</sup> T	60
	AMPS	1.0-0.0x10 <sup>-3</sup> T	
Bu-AMPS(0/10)	AMPS	1.0-0.0x10 <sup>-3</sup> T	240
ip-AMPS(10/0)	NIPAm	1.5-1.56x10 <sup>-3</sup> T	60
ip-AMPS(10/1)	NIPAm	1.5-1.56x10 <sup>-3</sup> T	120
	AMPS	1.0-0.0x10 <sup>-3</sup> T	

**Table 4.5:** Binary interaction parameters and crosslink density

It is seen from the values of  $z$  that the effective hydrophobicity of all gels is slightly temperature dependent and that the value of  $z$  at any temperature decreases with increasing hydrophobicity of the comonomer. It is found that  $z$ , along with the hydrogen bonding energies and entropies, and the number of donors and acceptors together determine the volume transition behavior of the gels.

#### **4.4.3.2 Swelling behaviour AMPS-co-NtBAm copolymer gels**

Figure 4.11 shows a quantitative comparison between the experimental swelling behavior of the N-t-BAm-co-AMPS gels and LFHB model calculations. The lines are the calculations of the LFHB model. The model successfully predicts a first order volume phase transition at 15°C for the Bu-AMPS (10/1) copolymer gel. However, the LFHB model could not predict quantitatively the swelling behavior of Bu-AMPS (10/2). The model predicted a discontinuous volume transition at a higher temperature for Bu-AMPS (10/2), where as the experimental swelling data show a swelling plateau as a function of temperature. The LFHB model predicted a swelling plateau for the copolymer gel at a higher composition with a higher AMPS content as shown in the Figure 4.11.

#### **4.4.3.4 Swelling behaviour of NIPAm-co-AMPS copolymer gels**

Figure 4.12 shows the experimental and predicted swelling behaviour of NIPAm-AMPS copolymer gels. The lines are the calculations of the extended LFHB theory. Both the model as well as the experimental observations showed a sharp volume transition for the PNIPAm homopolymer gel.

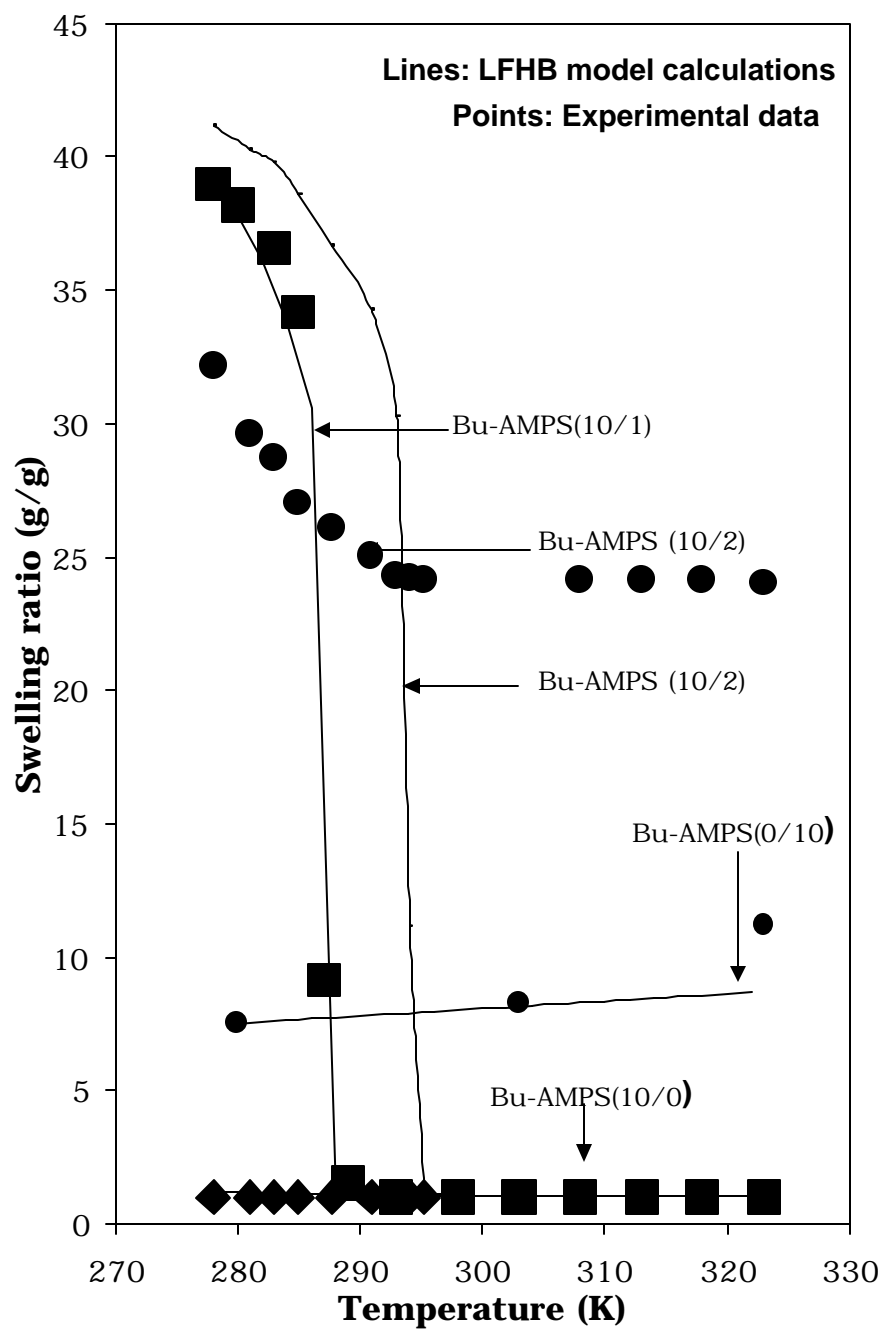


**Figure 4.11:** Quantitative comparison of experimental data with the model calculations for AMPS-co-N-t-BAm copolymer gels

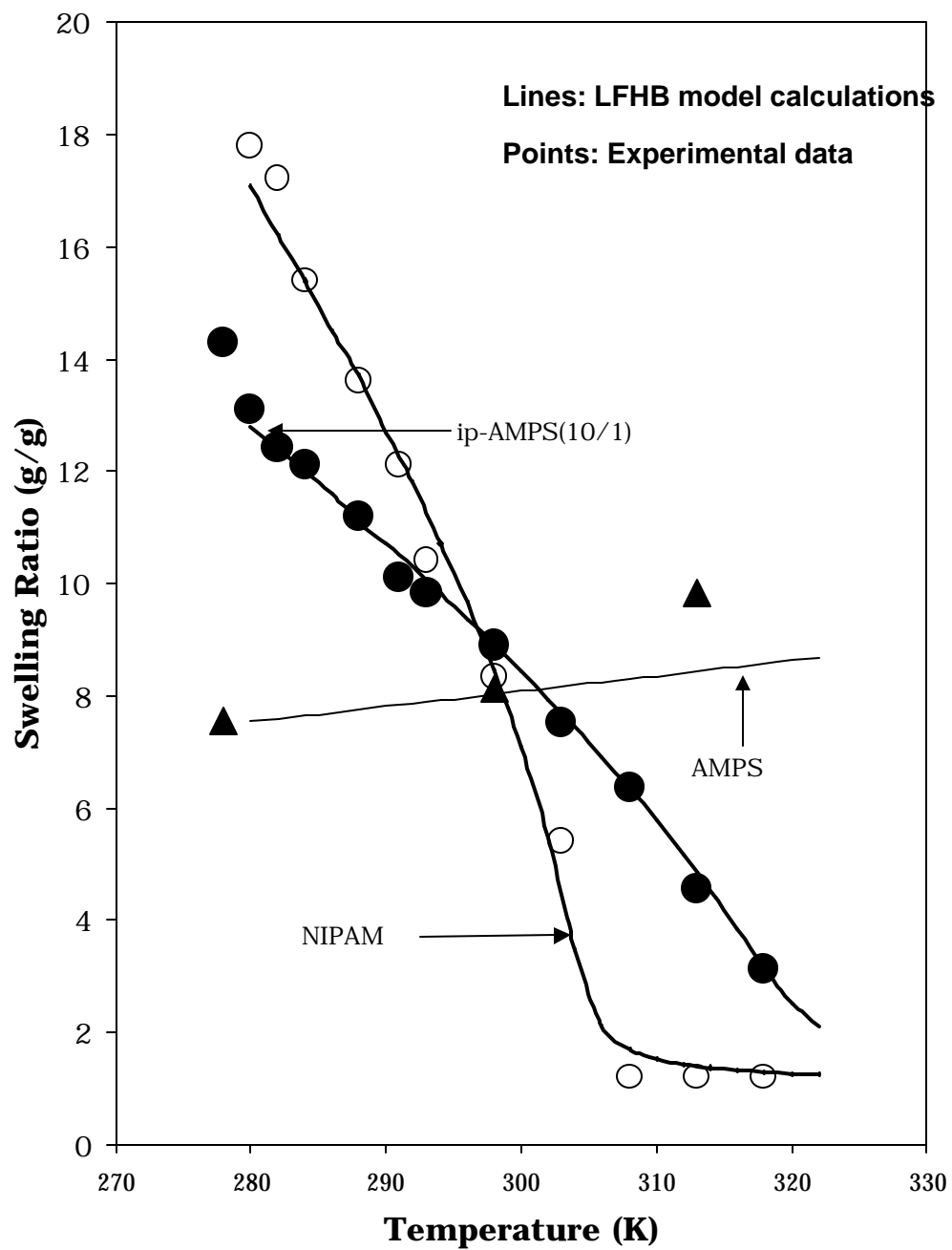


**Figure 4.12:** Quantitative comparison of experimental data with the model calculations for AMPS-co-NIPAm gels



But a slight increase in hydrophilicity by copolymerising NIPAm with AMPS (1 mole of NIPAm with 0.1 mole of AMPS) qualitatively changed the swelling behavior of the gel. The model calculations are very well matched with the experimental observations.

#### **4.5 Conclusions**

A new thermoreversible copolymer gel is synthesized from a highly hydrophilic monomer (AMPS) and a highly hydrophobic monomer (N-t-BAm) such that their homopolymers do not show any LCST phenomenon in the observable range of temperature. At a critical hydrophilic hydrophobic balance the copolymer gel showed a discontinuous volume transition at 15°C with the co-existence of swollen and collapsed states. A subtle change in the hydrophilic hydrophobic balance by increasing the hydrophilic content resulted in the loss of the LCST phenomenon. The hydrophilic-hydrophobic balance in the gel was altered by either changing the composition of the comonomers or by substituting the N-t-BAm with another hydrophobic monomer N-isopropylacrylamide (NIPAm). The experimental observations clearly indicate the importance of a critical balance of hydrophilic and hydrophobic interactions as a pre-requisite for LCST polymers as predicted by LFHB model.

# Chapter 5

## METAL COMPLEXATION IN SMART GELS

### 5.1 Introduction:

Metal complexation is a process by which certain inorganic metal ions coordinate with organic functional groups through ionic bonds, coordination bonds and ion dipole interactions to form organo-metallic hybrids, which have many interesting properties and applications. Metal complexed polymers could have applications in wastewater treatment, in improving thermal properties of polymers and in the area of catalysis. Recently metal- complexed stimuli responsive polymer gels have been used to produce smart catalysts, which combine the advantages of homogeneous catalysis with those of heterogeneous catalysis (Bergbreiter *et al.*, 1998a; Case *et al.*, 1998a). In this chapter we present a study of two interrelated phenomena: (a) the effect of hydrophobicity of gels on the structure of polymer-metal complexes, and (b) the effect of metal complexation on the volume phase transition (VPT) of thermoreversible hydrophobic gels.

The catalytic function of polymer-metal compounds depends on the structure of the coordination complex. Examples of such hybrids include protein supported copper complexes, which are well known catalysts for biological functions (Solomon, 1994). There have been very few scientific studies on investigating the structure of gel-metal hybrids. Kruczala *et al.* (1999) reported two types of monomeric Cu(II)-polyacrylic acid acids in which the  $\text{Cu}^{2+}$  was complexed with one or two carboxylic acid groups on the polymer chains. El-Sonbati *et al.* (1994) reported the formation of

binuclear Cu(II) complexes with poly(5-vinylsalicyledene-2-aminopyridine). Schlick *et al.* (1989) reported the formation of Cu(II)-Cu(II) dimer in Nafion membranes. In this chapter we report on the effect of hydrophobicity of polyelectrolyte gels on the coordination complex formed with transition metal ions.

It is well known that monovalent and polyvalent metal ions decrease the swelling capacity of polyelectrolyte gels due to the “screening” effect. Similarly, multivalent transition metal ions also decrease the swelling capacity of hydrogels; however, this is due to the formation of additional crosslinks in the gel through coordination complexation of the ions with the network chains. Transition metal ions have also been reported to decrease the VPT temperature of thermoreversible gels (Tanaka *et al.*, 1996). This was rather vaguely attributed to an ‘additional interaction’ between the metal ions and the polymer. We report in this chapter a detailed investigation on the effect of metal complexation on the VPT phenomenon.

## **5.2 Experimental Section:**

### **(a) Effect of metal complexation on VPT**

The effect of metal complexation on VPT was investigated using Bu-AMPS (10/1) gel. The metal ions used for complexation were Cr(VI), Cu(II) and Co(II).

### **(b) Effect of hydrophobicity on structure of the complex.**

The influence of hydrophobicity of polymeric gels on their ability to form complex with transition metal ions were investigated using a series of polymeric gels of acrylic acid and acryloyl amino acids containing carboxyl group. The metal ion used for the complexation was Cu(II).

### 5.2.1 Materials:

Acrylic acid (AAC), and 8-amino caprylic acid were obtained from Aldrich chemical Company Inc. USA. Thionyl chloride was obtained from S.d. fine chemicals, Mumbai, India. The purest available metal salts  $\text{CrO}_3$ ,  $\text{CoCl}_2$ , and  $\text{CuCl}_2$ , were procured from S.d.fine chemicals, Mumbai, India and all were used to prepare metal ion solutions. 4-amino butyric acid and 6-amino caproic acid were obtained from SRL, Mumbai, India. Details about the other materials such as AMPS, N-t-BAM, DMSO, Bis-AM etc were given in chapter four section 4.3.1. Deionized distilled water was prepared in the laboratory using standard procedures.

### 5.2.2 Synthesis of Acryloyl chloride:

Acryloyl chloride was synthesized by reacting acrylic acid with thionyl chloride. A mixture of 40.1-ml (0.6M) acrylic acid along with 3-ml dimethyl formamide and 5g hydroquinone were taken in a round bottom flask. 46-ml (0.6M) freshly distilled thionyl chloride was added drop wise over a period of 2-3 hrs. After complete addition of thionyl chloride, the reaction mixture was maintained at  $60^\circ\text{C}$  for six hours with continuous stirring. The flask was then kept overnight at room temperature. Pure Acryloyl chloride was distilled at  $70-71^\circ\text{C}$  under normal conditions after adding 3 more gram hydroquinone to the mixture.

### 5.2.3 Synthesis of monomers:

The hydrophobic monomers, acryloyl amino acids having carboxylic acids groups, were synthesized by reacting the respective amino acids with acryloyl chloride as discussed below. The structure of the monomers is shown in Figure 5.1.

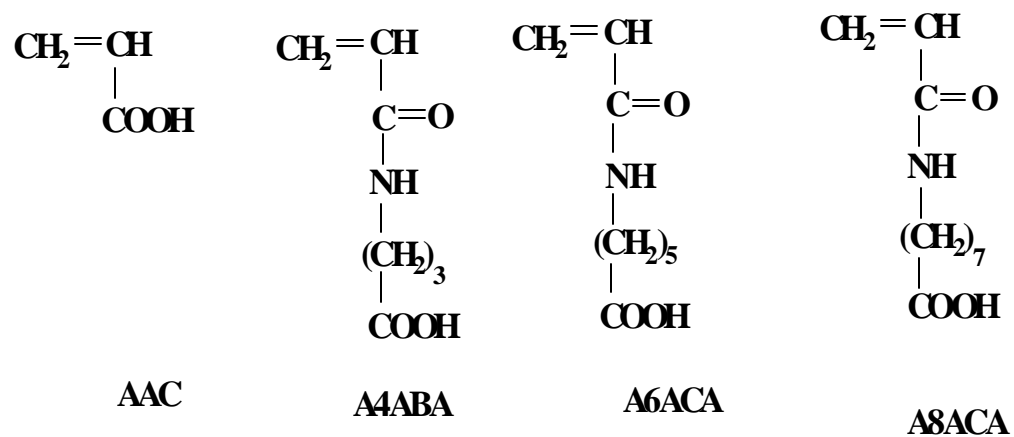


**Figure 5.1:** Structure of the monomers used to prepare the gels

**Acryloyl-4-amino butyric acid (A4ABA):**

A clear solution of 0.1M (10g) 4-amino butyric acids in 80 ml distilled water along with 0.1M (4 g) sodium hydroxide was taken in a 250 ml beaker. The solution was stirred with a magnetic needle at 5-10°C. To this solution 0.1M (9 ml) acryloyl chloride in 9 ml dichloromethane was added drop wise. The pH of the solution was monitored through out the experiment using a digital pH meter. The pH of the solution was dropped down with the addition of acryloyl chloride and is maintained between 7.5 to 7.8 by adding sodium hydroxide solution till the reaction was completed. Unreacted monomer along with acryloyl chloride and dichloromethane was removed by extracting the reaction mixture with ethyl acetate. The clear aqueous layer was acidified to pH 5.0 using hydrochloric acid and then extracted with ethyl acetate. The product in the ethyl acetate layer was dried with anhydrous sodium sulfate and concentrated in rotavapor. The product was precipitated out using pet ether. Redissolving in ethyl acetate and reprecipitating in petroleum ether did further purification of the product.

Melting point: white powder with melting point 91°C.

IR (Nujol): 3278 (-NH and -OH stretching), 2950 and 2957 (-CH stretching), 1701 (-CO stretching of COOH) 1643 (-CO stretching of -CONH<sub>2</sub>), 1540cm<sup>-1</sup> (-NH bending)

<sup>1</sup>H NMR (D<sub>2</sub>O): δ2.3 (-CH<sub>2</sub>COO), δ1.8 (-CH<sub>2</sub>), δ3.3 (-CH<sub>2</sub>-N), δ4.8 (HOD), δ5.8 (-CH<sub>2</sub>=CH), δ6.2ppm (-CH<sub>2</sub>=CH)

**Acryloyl-6-amino caproic acid (A6ACA):**

A6ACA monomer was prepared by reacting 6-amino caproic acid with acryloyl chloride using the same procedure described in the case of A4ABA monomer

Melting point: white powder with melting point 77.1°C

IR (Nujol): 3284 (-NH and -OH stretching), 2978 and 2852 (-CH stretching), 1697 (-CO stretching of COOH), 1650 (-CO stretching of CONH<sub>2</sub>), 1622 (-C=C stretching), 1546cm<sup>-1</sup> (-NH bending)

<sup>1</sup>H NMR (CDCl<sub>3</sub>): δ2.3 (CH<sub>2</sub>COO), δ1.7 (-CH<sub>2</sub>)<sub>2</sub>, δ1.4 {-(CH<sub>2</sub>)<sub>2</sub>-CH<sub>2</sub>}, δ3.3 (-N-CH<sub>2</sub>), δ5.6 (-CH<sub>2</sub>=CH), δ6.2ppm (CH<sub>2</sub>=CH)

**5.2.4 Synthesis of gels:****AMPS-co-N-t-BAm copolymer gel**

The copolymer gel, Bu-AMPS (10/1) was prepared by free radical polymerization in an organic medium (DMSO) using AIBN as an initiator as described in chapter four section 4.3.2. The structure of the monomers is given in chapter four.

**Acrylic acid homopolymer gels:****Unionized AAc gels**

Poly-AAc gels were prepared by free radical polymerization of AAc monomer in aqueous medium using Bis-Am as crosslinker and APS as an initiator in the presence of N, N, N', N'-tetramethylethylenediamine (TEMED) as an accelerator. 0.01 mole of AAc (0.72 g) was dissolved in 20 ml water along with 10 mole percent of Bis-Am (0.001moles, 0.154g). The reaction mixture was stirred using a magnetic stirrer at room temperature.

Nitrogen gas was bubbled through the solution. 40mg ammonium persulfate along with 60 $\mu$ l TEMED were added. The homogeneous solution was poured into glass test tubes and sealed. The polymerization was carried out at 50°C. After 24 hrs the gel rods were removed and washed. Ten such washings were done using fresh water during 72 hrs of time. The washed gels were dried at 50°C.

**Partially ionized AAc gels:**

Partially ionized AAc gels were prepared from partially ionized AAc monomer, which was prepared by reacting 0.01M (0.72g) AAc monomer with 0.005M (0.2g) sodium hydroxide. The procedure for the gel synthesis was the same as for non-ionized AAc gel.

**Fully ionized AAc gels:**

Completely ionized AAc gels were prepared from completely ionized AAc monomer using the same synthesis procedure as before. Completely ionized AAc monomer was prepared by reacting 0.01M (0.72g) AAc monomer with 0.01M (0.4g) sodium hydroxide.

**Acryloyl-4-amino butyric acid gels (A4ABA)**

A4ABA gels having different degrees of ionization were prepared following the same procedure used for AAc gels as mentioned earlier.

**Acryloyl-6-amino butyric acid gels (A6ACA)**

A6ACA gels having different degrees of ionization were prepared following the same procedure used for AAc gels.



### **Acyloyl-8-amino butyric acid gels (A8ACA)**

A8ACA gels were prepared following the same procedure used for AAc gels.

The pH of the “unionized gel” was 2.6. The “unionized” gel is the acid form of the gel, which means that carboxyl groups exist in non-ionized –COOH state. The “partially ionized” and “completely ionized” gels were prepared by adjusting the pH of the reactants with aqueous NaOH to 7.6 and 12.1, respectively. In the “partially ionized” gels some of the carboxyl groups exist in their salt form, i.e.,  $-\text{COO}^- \text{Na}^+$  state. However, in the “fully ionized” gel most of the carboxyl groups are in their salt form. This was verified by using excess NaOH to ensure complete ionization of the carboxyl groups and then measuring the swelling capacity of the gel. Ionization increases the swelling capacity of the gel due to the electrostatic repulsion between the charges on the network. After complete ionization of all the carboxyl groups in the gel, the swelling capacity of the gel remains unchanged. The unionized gels were opaque, the partially ionized gels were translucent and the completely ionized gels were transparent.

#### **5.2.5 Complexation of the gels with transition metal ions:**

The complexation of the thermoreversible copolymer gel, Bu-AMPS (10/1), with the metal ions, Cu(II), Co(II) and Cr(III), was done by swelling dried gels in the respective aqueous metal salt solutions for 72hrs followed by washing the equilibrated gel until all the metal ions except the one which are bound to the network were leached out. Washings were done for at least 12 hours at 6°C until the UV-visible spectra of the washed solutions showed no peaks corresponding to the metal ions. About ten such washings were required for complete leaching. The washed complexed gels

were dried in an oven at 50°C to constant weight. The dried Cr(III) complexed gels showed green color, the Co(II) complexed gels showed pink color and the Cu(II) complexed gels showed blue color. Gels of acrylic acid and acryloyl amino acids containing carboxylic groups were complexed with Cu(II) by batch equilibrium method as explained above. No washings were done to remove the absorbed metal ions as the gels were completely collapsed.

### **5.2.6 Characterization of the complexed gels:**

#### **Swelling Ratio measurements:**

Swelling measurements of the thermoreversible gels, pure and metal complexed, were done in double distilled water by immersing the dried gels for typically 72 hours, by which time the gels reached equilibrium swelling. The swollen gels showed only a trace of color due to dilution with water. In the case of acrylic acid gels and acryloyl amino acid gels having carboxylic group, the swelling measurements were done both in metal solutions as well as pure water for 72 hrs till the equilibrium was reached. The swelling ratio of the gels was measured gravimetrically. The degree of swelling (Q) was defined as the weight of solvent uptake per unit mass of dried polymer.

$$Q = \text{Weight of the equilibrated gel (W}_s\text{)} / \text{Weight of the dried gel (W}_d\text{)}$$

#### **Metal-uptake**

Metal uptake of the gels was investigated using Shimadzu UV- 1601 PC UV-visible spectrophotometer. The concentrations of the metal ions before and after complexation were estimated at 810 nm. Different solutions of CuCl<sub>2</sub> having different concentrations were prepared. Corresponding absorptions were measured for each solution. A standard

curve was plotted with concentration against absorbance as shown in Figure 5.2. From this standard curve, the concentration of the unknown salt solution was obtained by measuring the absorbance.

### **Structure of polymer-metal complex**

The metal complexed thermoreversible gels, Bu-AMPS (10/1) both in the collapsed as well as swollen states were characterized by electron paramagnetic resonance (EPR) using a Bruker EMX spectrometer at  $\nu = 9.7\text{GHz}$ . EPR spectra were observed for all the complexed gels at ambient temperature except for the thermoreversible Bu-AMPS (10/1) gels in the swollen state. EPR spectra of the complexed gels were recorded in the temperature range 77 - 298 K by using a Bruker EMX spectrometer operating at X and Q band frequencies. A field modulation of 100 kHz was used. The microwave frequency was calibrated with a frequency counter fixed in the microwave bridge Bruker ER 041 XG-D and the magnetic field was calibrated using a Bruker ER 035 M NMR Gaussmeter. Spectral editing and simulations were done by using the Bruker WINEPR and Simfonia software packages.

## **5.3 Results and Discussion**

### **5.3.1 Effect of metal complexation on VPT**

As shown in chapter four, the copolymer gel Bu-AMPS (10/1) exhibits a discontinuous LCST behaviour. We also observed that a slight change in this balance alters the LCST behaviour of the gel quantitatively. To understand the effect of metal complexation on VPT we have complexed the gel Bu-AMPS (10/1) with the transition metal ions and studied their swelling behaviour.

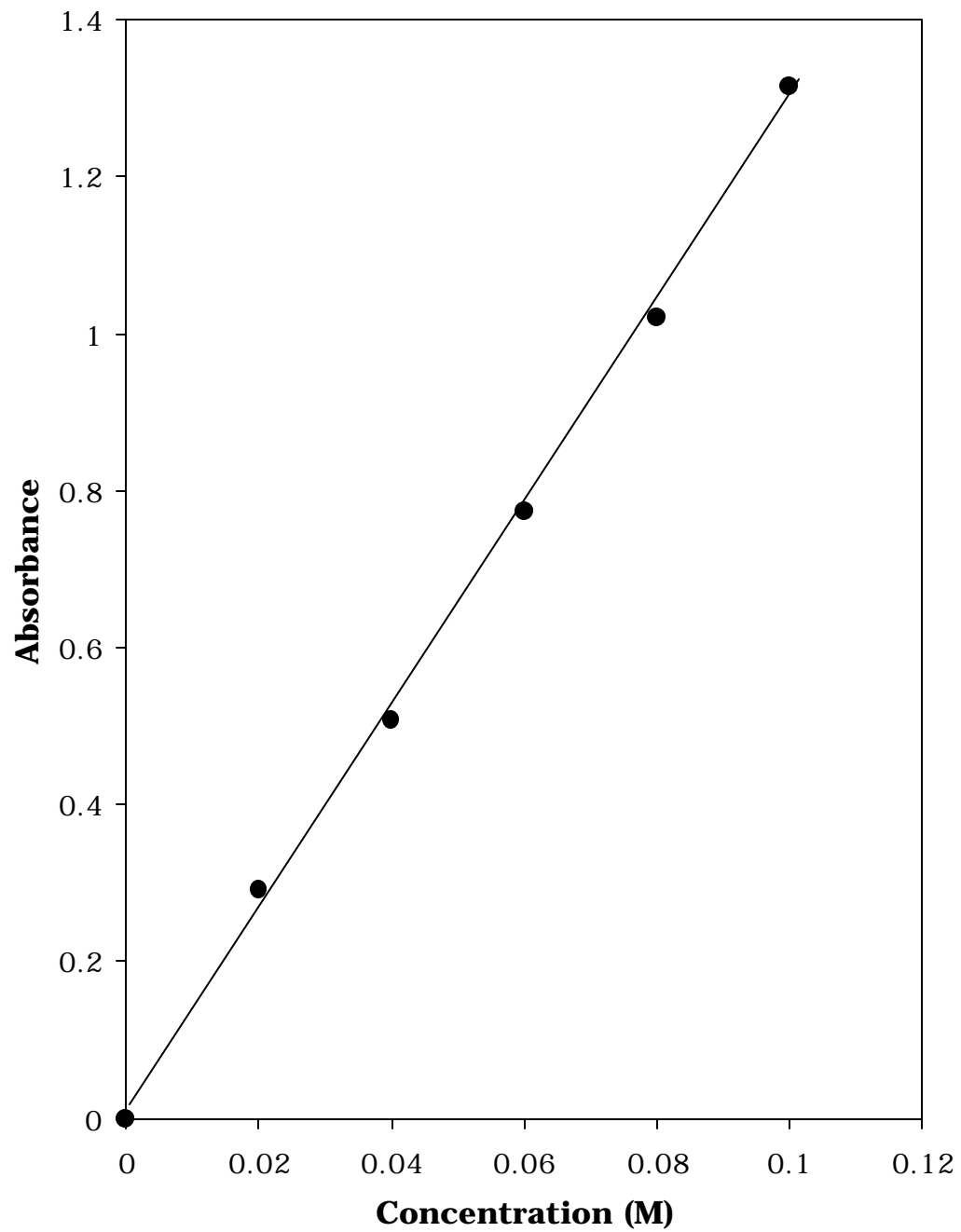


**Figure 5.2:** Standard curve of Cu(II) solution at 810nm

Figures 5.3 and 5.4 show the EPR spectra for the dried and the swollen Cu(II)-complexed gels respectively. Similar spectra were observed for the Cr(III) and the Co(II)-complexed gels. For the swollen and the dried gels, the EPR measurements were done at 5°C and 25°C, respectively. The spin Hamiltonian parameters for the collapsed state ( $g_{\parallel} = 2.385$ ,  $g_{\perp} = 2.045$  and  $A_{\parallel}(\text{Cu}) = 122.6\text{G}$ ) correspond to a tetrahedrally distorted square planar geometry for Cu(II) as shown in Figure 5.5. For the Cu(II) ions in a free mobile state one could observe an isotropic resonance at  $g_{\text{iso}} = (g_{\parallel} + 2g_{\perp})/3$ . However, the anisotropic spectrum observed for the swollen state ( $g_{\parallel} = 2.241$  and  $g_{\perp} = 2.147$ ) clearly suggests that the Cu(II) ions in the swollen gels are complexed with the polymer probably through  $\text{SO}_3\text{H}$  groups. The lesser "g" anisotropy ( $\Delta g = g_{\parallel} - g_{\perp}$ ) for swollen gels compared to the collapsed state is consistent with the restricted mobility of the paramagnetic unit in the swollen state.

The effect of the complexation of metal ions on the swelling behavior of the washed copolymer gel is shown in Figure 5.6 as a function of temperature. As shown in the figure, all the metal-complexed gels showed lower equilibrium swelling capacity than the uncomplexed gels. The decrease in the swelling capacity can be attributed to the increase in the overall crosslink density of the gel introduced due to complexation with the metal ions. More importantly, the volume transition temperature of the complexed gel was reduced by about 4 to 6°C. For example, the VPT temperature of pure gel was 15°C, while that of the Cr(VI) complexed gel was observed to be 11°C. The volume transition observed for the complexed gels was very sharp and could be discontinuous in nature.

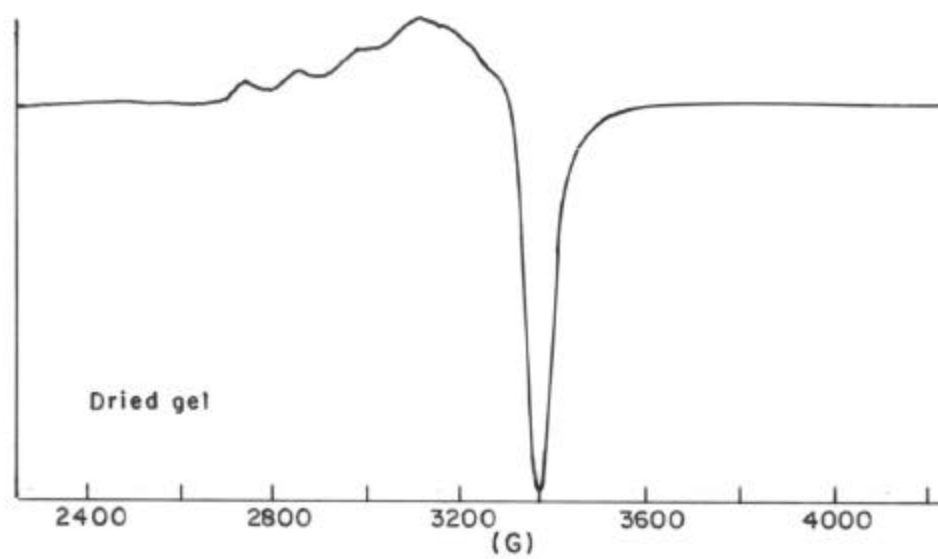


**Figure 5.3:** EPR spectra for the Cu(II)-complexed (N-t-BAm-co-BisAm-co-AMPS) gel in the dried states

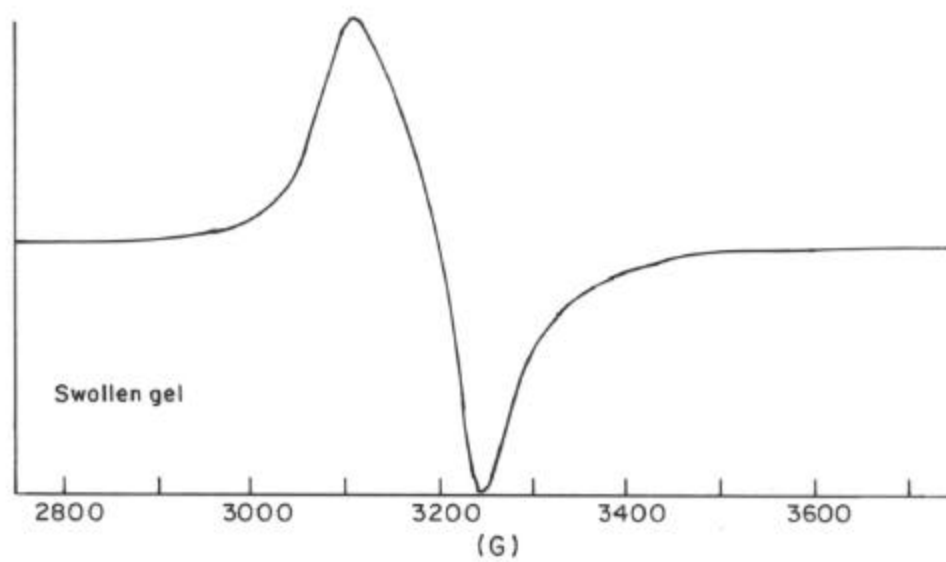


**Figure 5.4:** EPR spectra for the Cu(II)-complexed (N-t-BAm-co-BisAm-co-AMPS) gel in the swollen states

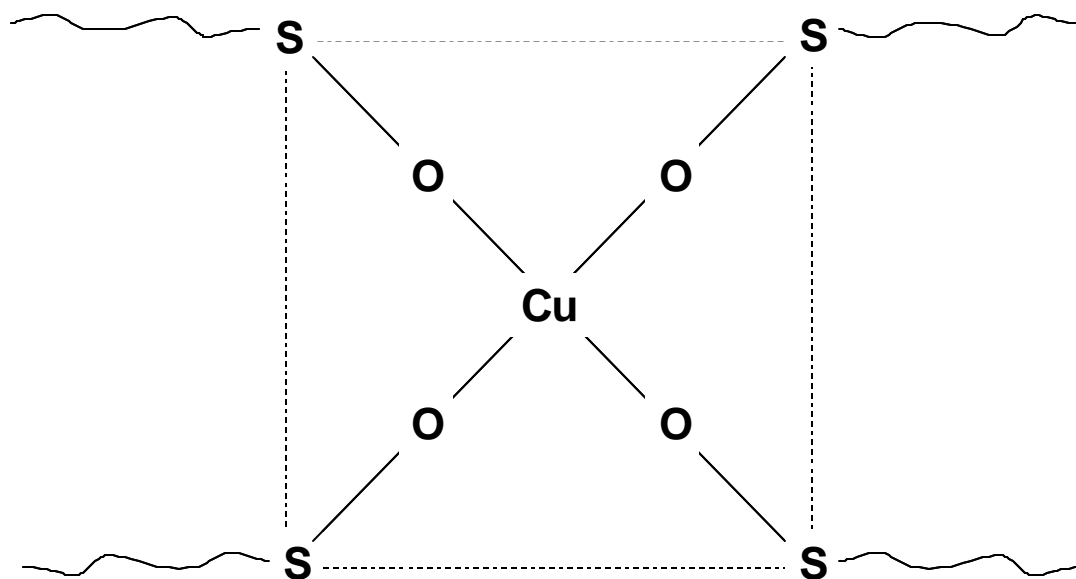


**Figure 5.5:** Probable structure of the Cu(II) complexed gel



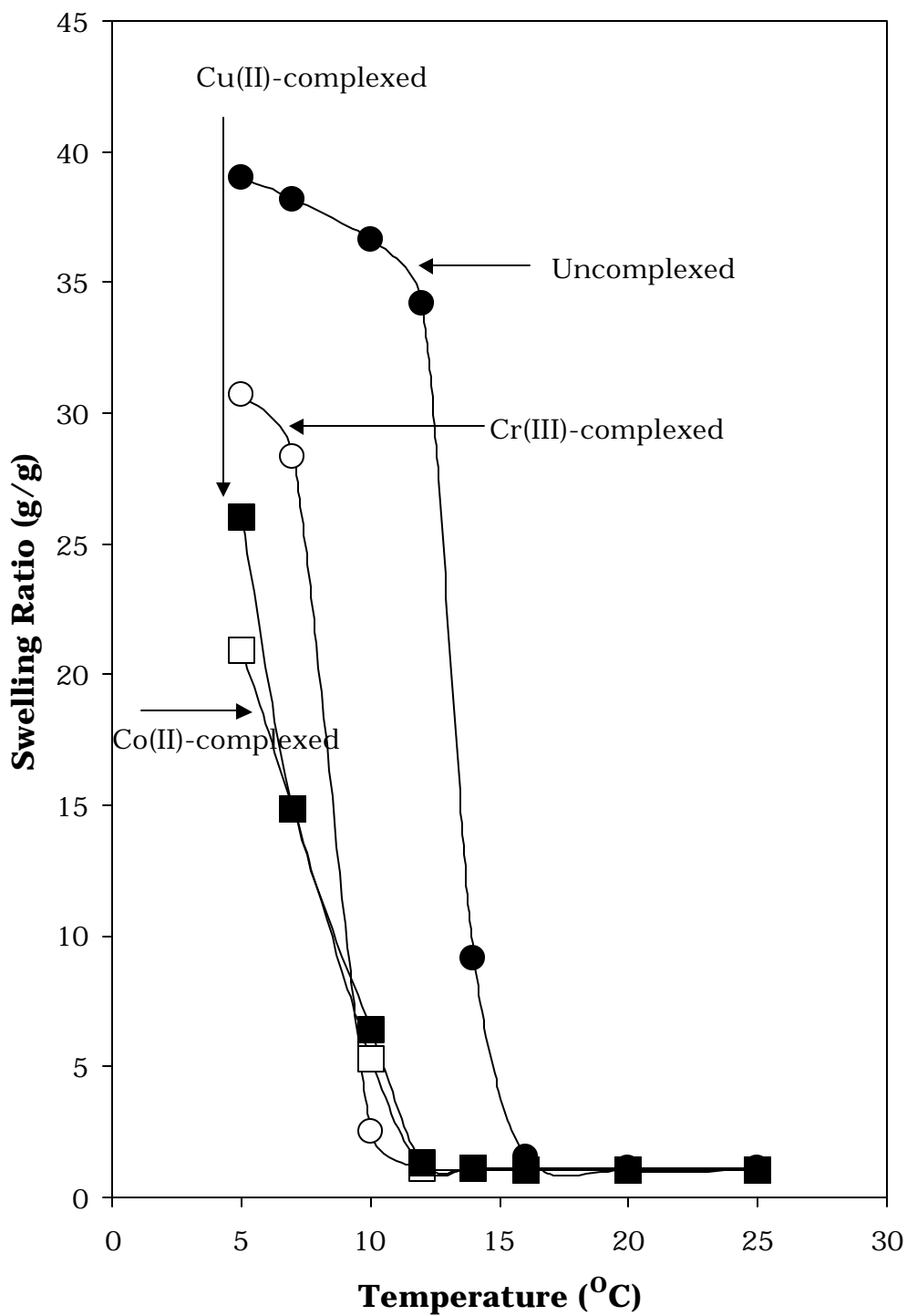


**Figure 5.6:** Effect of metal complexation on the swelling behaviour of the thermoreversible gels

However, co-existing phases were not observed for these gels [metal complexed Bu-AMPS (10/1)] at a single temperature (transition temperature) unlike the pure Bu-AMPS (10/1) gel.

It is clear from the EPR measurements that the hydrophilic sulfonic-acid groups on the macromolecular chains are engaged in complexation with the metal ions and hence are not freely available to the water molecules. We propose that this will result in a decrease in the effective hydrophilicity of the network and indirectly enhances the overall hydrophobicity. It is well known that an increase in hydrophobicity of a gel decreases its VPT temperature (see discussions in section 2.4.2 of Chapter 2 and the references cited there). Hence the volume transition temperature of the complexed gels decreases.

Tanaka *et al.* (1996) have observed a similar shift in the volume transition temperature of N-isopropylacrylamide-co-acrylic acid (NIPAm-co-AAc) gel immersed in copper chloride solution. The shift in the transition temperature was attributed to an extra attraction created by the copper ions between the polymers. The authors reported that NIPAm-co-AAc gel absorbed the copper ions in the collapsed and released the copper ions in the swollen states. Our experimental data and interpretations differ considerably from the work of Tanaka *et al.* (1996). First, we have studied the swelling behaviour of complexed gels in pure water, whereas Tanaka *et al.* (1996) have studied the volume transition of gels in salt solutions. Further, we have shown through detailed EPR measurements that our gel complexes with the metal ions in the collapsed state as well as in the swollen state.

The metal uptake of the gel was found to be  $2.1 \times 10^{-4}$  gmol/g of the gel. This means that only a trace amount of metal ions were incorporated to

the gel sample. This is mainly attributed to the small amount of AMPS in the copolymer gel and that of the N-t-BAm does not pick up any metal ions. Hence the hydrophobic copolymer gel does not pick up much metal ions. Our data show that a subtle change in the hydrophilic-hydrophobic balance caused by complexation of hydrophilic  $-\text{SO}_3\text{H}$  groups with the trace amounts of metal ions can result in significant shift in volume transition temperature of N-t-BAm-AMPS-Bis-Am terpolymer gels. Another interesting feature of our results is that trace amounts of metal can behave as yet another stimuli for inducing volume transition in gels. A gel, which can undergo volume transition on complexation and which can change its color in the presence of ppm levels of transition metal ion might find application as sensors for trace metal-ion impurities.

### **5.3.2 Effect of hydrophobicity on metal complexation**

When a weakly crosslinked gel is immersed in an aqueous solution of  $\text{CuCl}_2$  (0.1 M), the Cu(II) ions bind to the polymeric network and the gel attains a collapsed state as indicated by the swelling behavior tabulated in Table 5.1. The gel, which is equilibrated with the salt solution of the metal ion, contains, in general, two types of metal ions, those complexed with the polymer chain and those simply osmotically absorbed along with the solvent (water) in the gel matrix. The metal ions absorbed by the polymer network can be estimated by assuming that the concentration of metal ions outside the solution is equal to the concentration of metal ions inside the gel (Lee *et al.*, 1998) We have calculated the amount of metal ions that are complexed with the polymeric network by subtracting the absorbed quantity of metal ions from the total metal uptake.

gel	swelling ratio in water <sup>(a)</sup> (g/g)	swelling ratio in CuCl <sub>2</sub> <sup>(a)</sup> (g/g)	amount of Cu(II) complexed (gmols/g)	% COOH groups complexed <sup>(b)</sup>	mono-meric species <sup>(c)</sup>	dimeric species <sup>(c)</sup>
AAc(H)	4.4	2.3	1.2x10 <sup>-4</sup>	1.6	✓	✓
AAc(Na/H)	16.3	4.9	1.7x10 <sup>-3</sup>	24	✓	
AAc(Na)	24.8	4.8	1.3x10 <sup>-2</sup>	26	✓	
A4ABA(H)	1.1	1.0	5.0x10 <sup>-5</sup>	1.6	✓	✓
A4ABA(Na/H)	24.9	1.1	9.3x10 <sup>-4</sup>	28	✓	✓
A4ABA(Na)	98.8	1.0	9.9x10 <sup>-4</sup>	30	✓	
A6ACA(H)	1.0	1.0	5.4x10 <sup>-5</sup>	1.8	✓	✓
A6ACA(Na/H)	147.0	1.9	2.4x10 <sup>-4</sup>	32	✓	
A6ACA(Na)	230.0	1.0	9.8x10 <sup>-4</sup>	36	✓	✓
A8ACA(Na)		1.0	9.8x10 <sup>-4</sup>	40	✓	✓

(a) Swelling measurements made 4 h after immersion in salt solution.

(b) %complexation = 
$$\frac{100(\text{gmols of metal ion complexed})}{\text{gmols of COO}^- \text{ on dry gel}}$$

(c) EPR studies

**Table 5.1:** Swelling behaviour of Polyacid gels in water and CuCl<sub>2</sub> solutions

The amount of metal ions absorbed into the polymer network was calculated using the following equation.

$$AD = C_0V_1 \quad (5.1)$$

where  $AD$  is the moles of metal ions absorbed,  $C_0$  is the concentration of the metal solution outside the gel and  $V_1$  is the amount of water picked up by gel.  $V_1$  can be estimated from the swelling capacities reported in Table 5.1. In all gel systems it was observed that very small amount of metal ions was absorbed by the polymer network while most of the metal ions were coordinated with or “adsorbed” on the chains. Evidently, the gels collapse in the presence of the metal ions, which serve additional “crosslinks” through interchain complexation. The swelling ratio of the acid form of the gels (i.e., unionized gels) in pure water decreased with the alkyl chain length as shown in Table 5.1. This is expected since the linear polymers having longer alkyl side chains are more hydrophobic and hence absorb less water. However, the salt form of the gels (i.e., ionized gels) showed a reverse trend in that the swelling ratio increased with the alkyl chain length. This seemingly anomalous swelling behaviour of the ionized gels could be possibly due to two reasons: The first reason pertains to the cross-link density of the gels. Since we do not have a direct control over the crosslink density during polymerization, it is possible that gels with longer alkyl side chains happen to have lower crosslink density and hence swell more. The other possible reason could be that the longer flexible side chains place the ionic charges at a finite distance away from the main chain because of which the polymer chains are forced to adopt a more “open” configuration in order to overcome the electrostatic repulsion, hence the higher swelling capacity.

The fraction of carboxyl group involved in complexation is defined as the ratio of the actually complexed metal ions to the stoichiometrically defined maximum possible amount of complexation. Our experimental data in Table 5.1 indicates that as the alkyl chain length of the gel increases the percentage of COOH groups involved in complexation increases. These findings are similar to those of Sasaki *et al.* (1998) who observed that the binding of  $\text{Ca}^{2+}$  to the polymer gel increased with the “hydrophobicity” of the gel. This was attributed to the cooperative effect of hydrophobicity and metal binding. The complexation of the metal ions with the carboxylic groups increases the overall hydrophobicity of the system since the metal complexed carboxyl groups are not available to the water molecule. This complexation-induced hydrophobicity drives the polymer chains to attain a compact conformation and in turn enhances the metal binding to the polymer chains.

It may also be noted that the fraction of carboxyl groups involved in complexation is low for the unionized gels and high for completely ionized gels for the same alkyl chain length. This is simply due to the fact that the ionized carboxyl ions can coordinate with the Cu(II) ions much more effectively than the unionized carboxyl group.

X-band EPR spectra of the complexed polyacrylic acid gels of different degrees of ionization (AAc(H), AAc(Na) and AAc(H/Na)) at 298 K are shown in Figure 5.7. In general, two types of Cu(II), dimeric and monomeric, species were detected in the EPR spectra. The signals denoted by D around 230, 4800 and 6075 G correspond to dimeric Cu(II) species while those denoted by M1/M2 in the region 2690 - 3600 G are attributed to monomeric species.

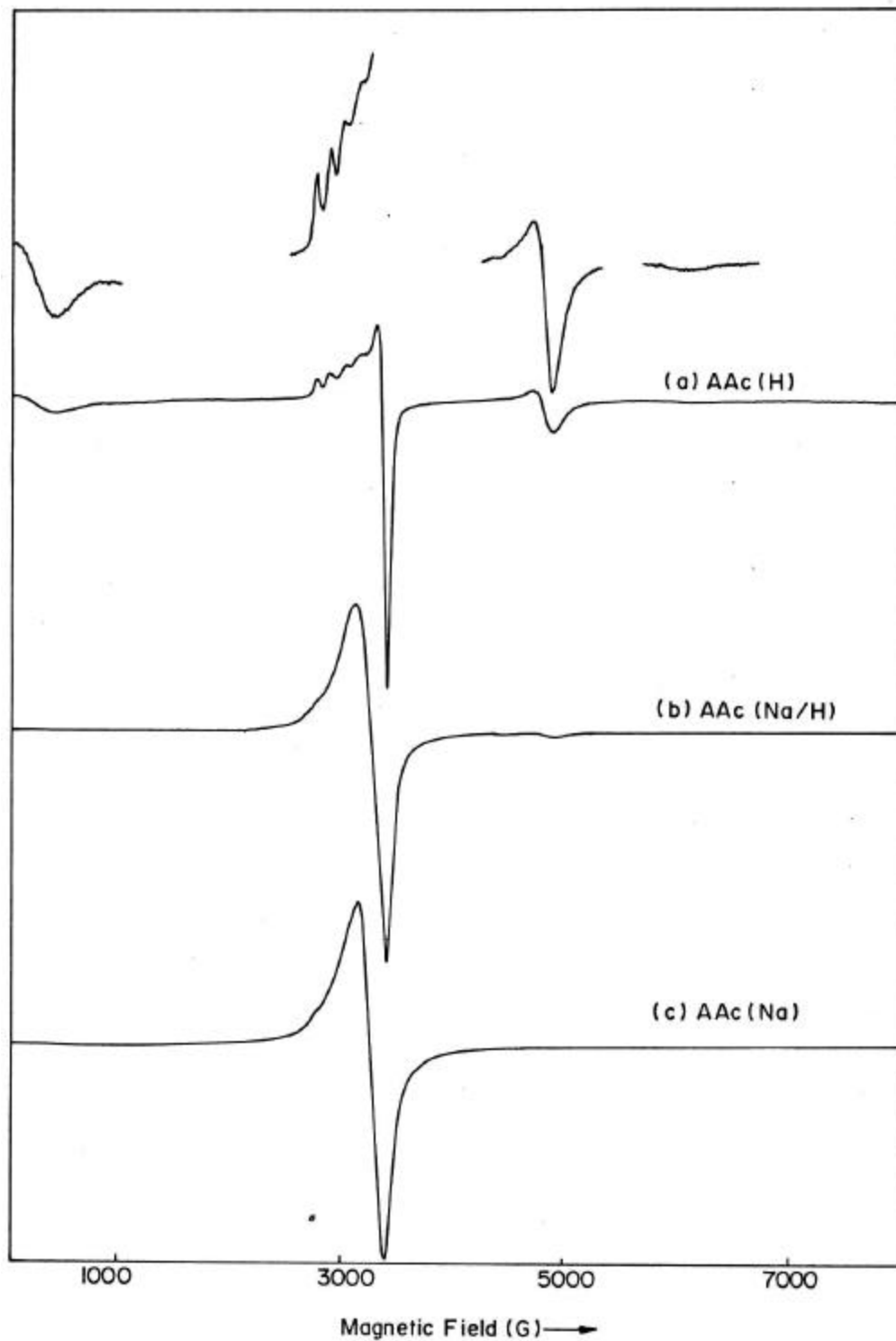


**Figure 5.7:** EPR spectra of Cu(II)-AAc gels as a function of degree of ionization at 298 K.

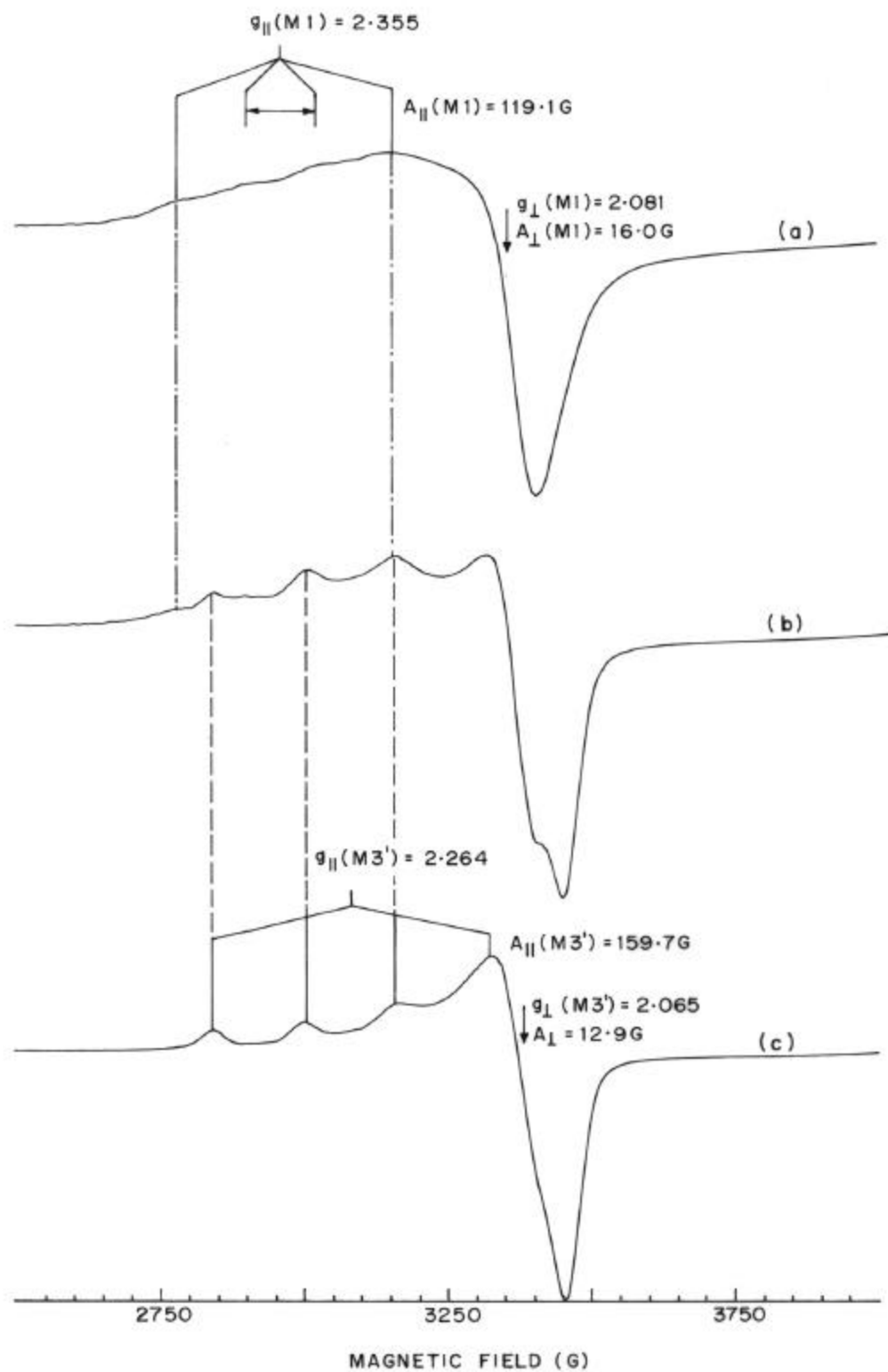
The nature of the EPR spectrum i.e., the intensities of the dimer signals and the spectral characteristics of the monomeric species are dependent on the degree of ionization. The resolved parallel hyperfine features of the monomeric species in AAc(H) correspond to a distorted molecular geometry for Cu(II). Only an averaged signal was observed in the complexed gels of AAc(Na) and AAc(H/Na). In other words, the monomeric species in AAc(H) (hereafter referred to as M1) has a geometry different from that in AAc(Na) and AAc(H/Na) (hereafter referred to as M2). The complexed gels of AAc(H/Na) contain a trace amount of yet another monomer species M3.

Figure 5.8 shows the changes in the nature of the EPR spectrum of the monomer as a function of ionization for A6ACA. The monomeric species (M3') in A6ACA(Na/H) is characterized by  $g_{\parallel} = 2.264$ ,  $g_{\perp} = 2.065$ ,  $A_{\parallel} = 159.7$  G and  $A_{\perp} = 12.9$  G while that in A6ACA(Na) (M1) is characterized by  $g_{\parallel} = 2.355$ ,  $g_{\perp} = 2.081$ ,  $A_{\parallel} = 119.1$  and  $A_{\perp} = 16.0$  G. The gel A6ACA(H) contained both types of the monomeric species (M1 and M3'). Hence, the EPR spectra reveal that the structure of the Cu(II) complexed gel changes with the degree of ionization.

The spin Hamiltonian parameters for the monomeric species are listed in Table 5.2. It is apparent that three types of monomeric Cu(II) species are formed, one exhibiting an average signal (M2;  $g_{av} = 2.119$ ) and the other two, M1 and M3/M3', having distorted molecular geometry.

The length of the pendent chain has a pronounced effect on the nature of the copper(II) species. Figure 5.9 reveals this effect on the EPR spectra of the fully ionized gels as a function of alkyl chain length.





**Figure 5.8:** EPR spectra of the monomeric Cu(II) species in A6ACA gels as a function of degree of ionization at 298 K.

Gel	species	$g_{\parallel}$	$g_{\perp}$	$g_{av}$	$A_{\parallel}$ (G)	$A_{\perp}$ (G)
AAc(H)	$M_1$	2.356	2.076		128.8	*
AAc(Na/H)	$M_2$			2.119		
	$M_3$	2.325	2.082		150.5	
AAc(Na)	$M_2'$			2.133		
A4ABA(H)	$M_1$	2.360	2.088		125.2	*
A4ABA(Na/H)	$M_1$	2.358	2.085		119.8	*
A4ABA(Na)	$M_3$	2.328	2.083		150.2	*
A6ACA(H)	$M_1$	2.367	2.082		119.1	16.0
	$M_3'$	2.264	2.071		159.7	12.9
A6ACA(Na/H)	$M_3'$	2.264	2.065		159.7	12.9
A6ACA(Na)	$M_1$	2.355	2.081		119.1	16.0
A8ACA(Na)	$M_1$	2.352	2.081		120.1	*

\* Hyperfine features not resolved.

**Table 5.2:** EPR Spin Hamiltonian Parameters of Cu(II) Complexed Polymer Gel

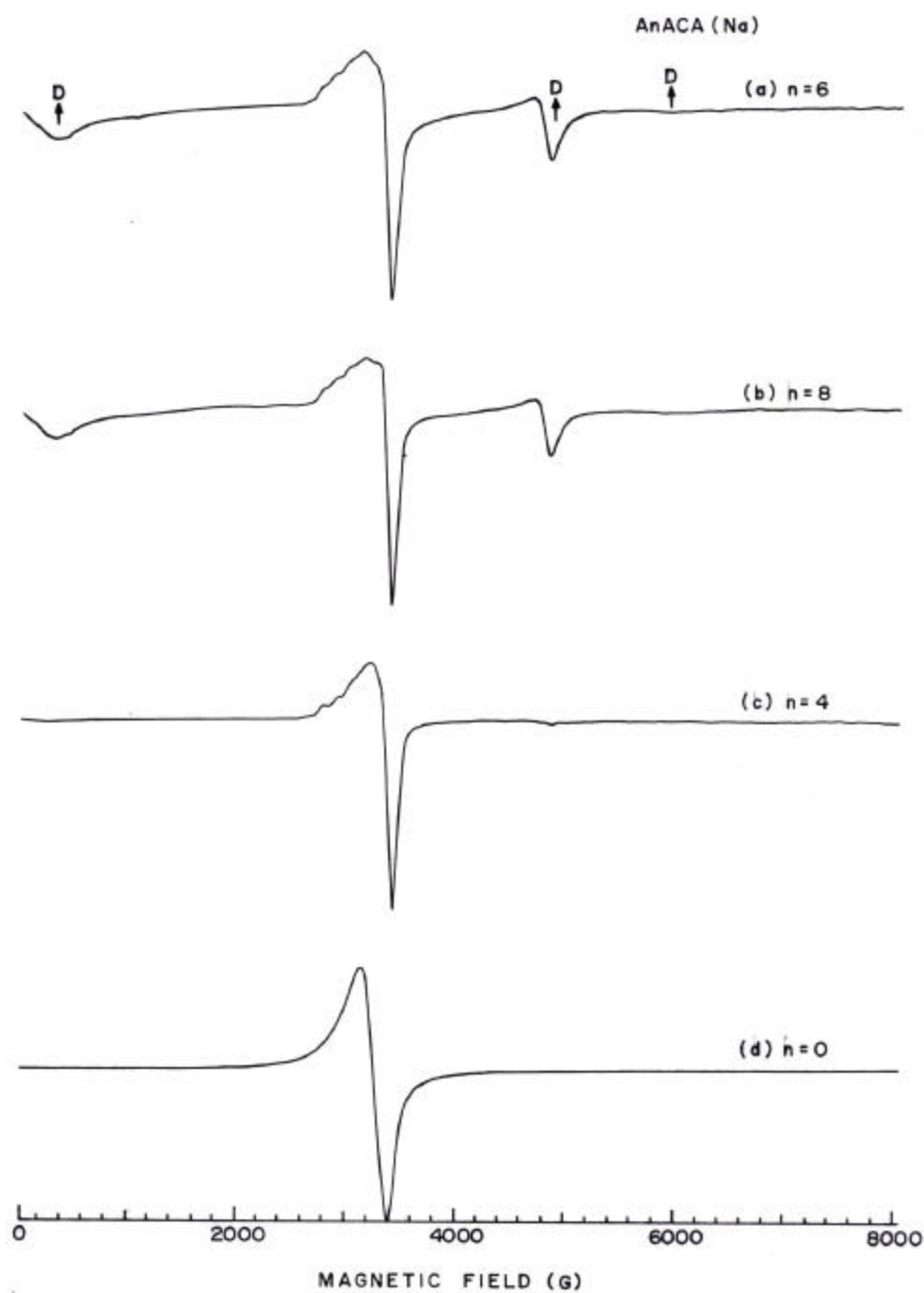
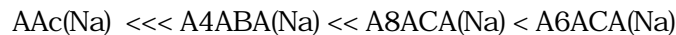


**Figure 5.9:** EPR spectra at 298 K showing the effect of hydrophobic alkyl chain length on the Cu(II) species in the completely ionized Cu(II) complexed AAc, A4ABA, A6ACA and A8ACA gels.

As the alkyl chain length increases, larger quantities of copper are seen to be present in the dimeric form (D). The intensity of the dimer signals in the fully ionized gels increases with the chain length in the order



The gel A6ACA (Na) appears to have an optimal alkyl chain length to form the maximum amount of dimer species (D).

The spectrum of the dimer species at X-band ( $\nu = 9.75 \text{ GHz}$ ) corresponds to axial symmetry, in which zero field splitting is larger than the microwave quantum ( $h\nu$ ). It is interesting to note from the Q-band ( $\nu \approx 35 \text{ GHz}$ ) spectra that the dimer spectrum (Figure 5.10a) matches well with that of dimeric copper acetate,  $\text{Cu}(\text{CH}_3\text{COO})_2 \cdot 2\text{H}_2\text{O}$  complex (Figure 5.10b) wherein four acetate groups bind the two Cu(II) ions to form a dimeric copper complex. This observation clearly indicates that on complexation four strands of the polymer rearrange to form the Cu-Cu dimer species in the polymer gel.

Variable temperature studies on A6ACA(Na) in the range 77 - 298 K indicated that the intensity of dimer signals decreased as shown in Figure 5.11 and the monomeric signals were better resolved and more intense at lower temperatures. This is agreement with the antiferromagnetic coupling between the two copper(II) ions of the dimeric species. Tentative structures of different Cu(II) complexed gels are proposed in Figure 5.12. The spin Hamiltonian parameters, especially  $g_{\parallel} = 2.264$  and  $A_{\parallel} = 159.7 \text{ G}$ , suggest a distorted geometry around copper with oxygens or amide nitrogen as the coordinating ligands. However, studies with polyacrylamide and poly-N-isopropylacrylamide gels did not reveal any complexation with Cu(II) ions indicating that the the amide nitrogen is most probably not involved in complexation.

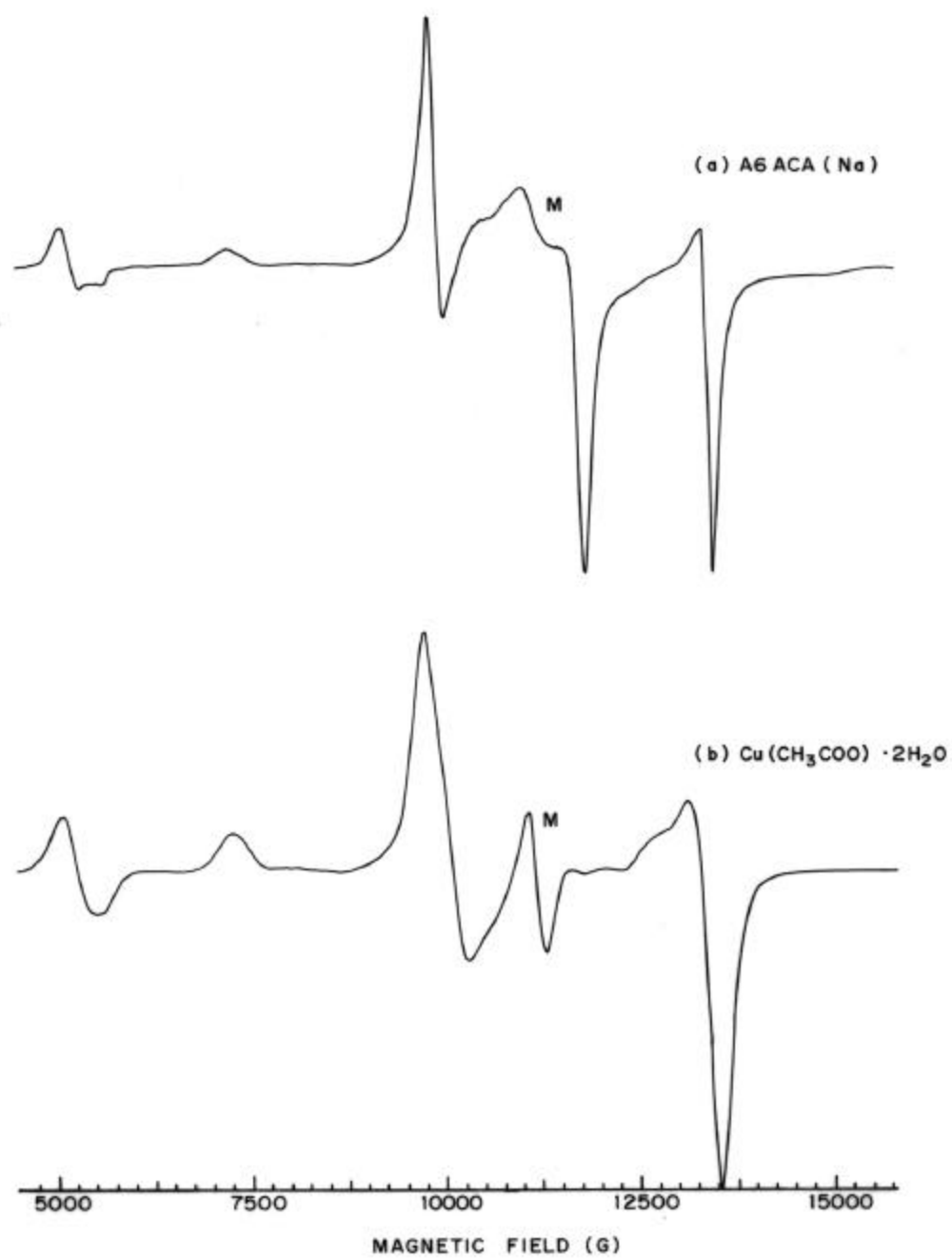


**Figure 5.10:** EPR spectra at Q-band frequency of (a) A6ACA gel and (b) dimeric copper acetate monohydrate at 298 K.

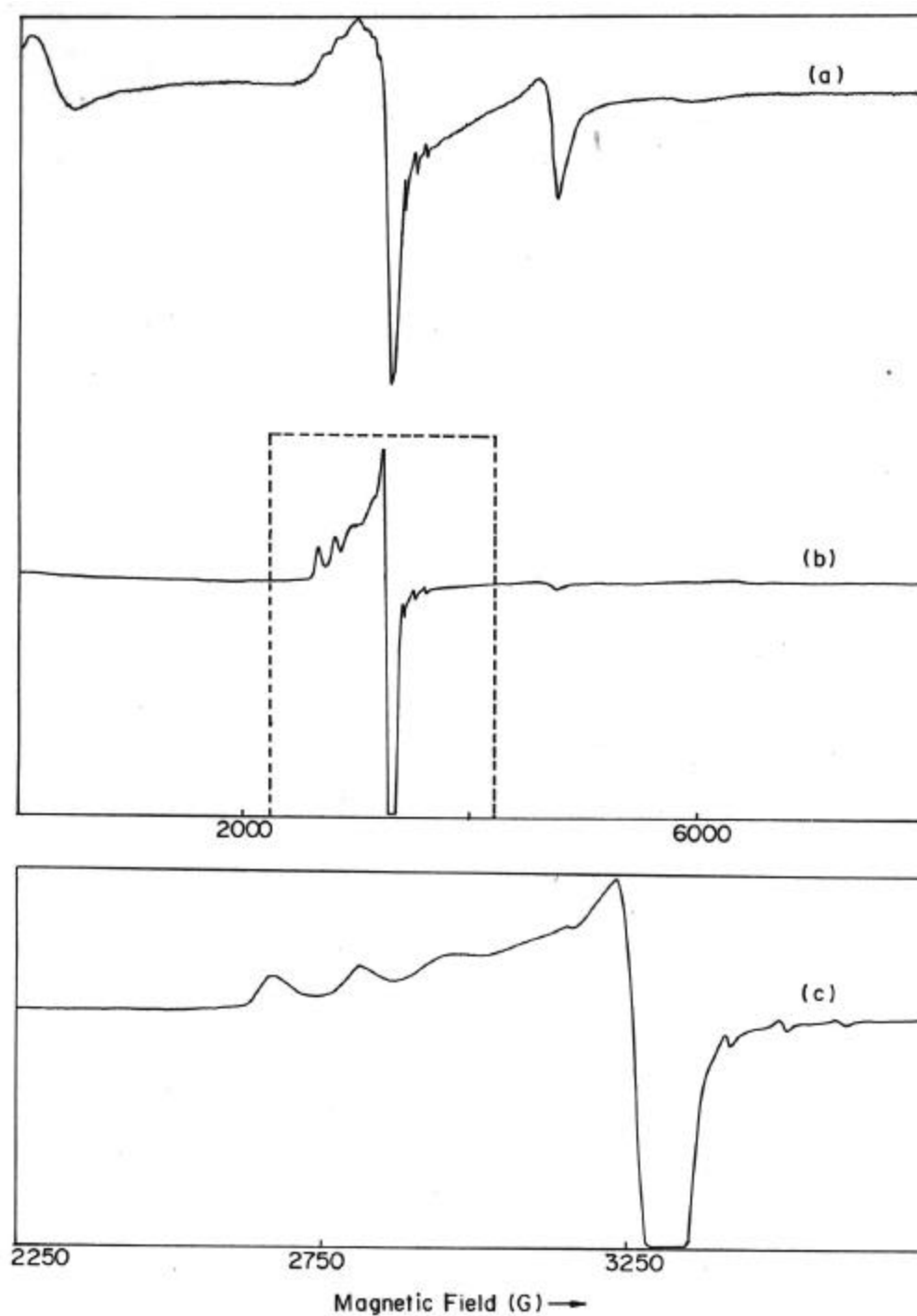


**Figure 5.11:** EPR spectra of Cu(II) complexed A6ACA(Na) gels at (a) 298 K and (b) 80 K, and (c) dotted portion of (b) in expanded scale.

**Figure 5.12:** Structures of monomeric and dimeric Cu(II) species in metal ion complexed gels.

The formation of dimer species is also dependent on the degree of ionization. In the case of acrylic acid gels, as shown in Figure 5.7, the dimer species is relatively more abundant in AAc(H) compared to that in gels AAc(H/Na) and AAc(Na). Cu(II) in AAc(Na) is present mostly as a monomeric species. Thus as hydrophobicity decreases the tendency to form dimeric species also decreases. In the case of the hydrophobic A4ABA gels, dimeric Cu(II) species was observed in the unionized as well as in the partially ionized gels. Further, in the case of more hydrophobic A6ACA gels the dimeric Cu(II) species was found even in the completely ionized forms. These observations clearly suggest that an “optimum hydrophobicity” (i.e., a balance of hydrophilic and hydrophobic interactions) of the polymeric gel is required to form dimeric species with Cu(II) ions. The data in Table 5.1 shows that swelling does not determine the structure of the Cu(II) complexes. For example, both the acid as well as the salt forms of the Cu(II) complexed A6ACA gels showed dimers irrespective of their swelling behavior. Moreover, we have also observed that A6ACA gels of two different crosslink densities viz., 10% and 30%, showed identical EPR spectra consistent with identical structures of the Cu(II) complexes, although their swelling capacities were 230 g/g and 60 g/g, respectively. Thus, we conclude that the structure of the complex is not determined by the crosslink density, but is certainly influenced by the hydrophobic-hydrophilic balance of the polymer.

#### **5.4 Conclusions**

We have investigated the effect of alkyl chain length on metal complexation using a series of homopolymer gels having different alkyl chain lengths varying from zero to seven. The nature of the Cu(II) complexes



as well as the number of COOH groups involved in complexation were strongly dependent on alkyl chain length or hydrophobicity of the gel. The EPR analysis showed two types of complexes, dimeric and monomeric. The present work gives an insight into the role of hydrophobic-hydrophilic balance on the molecular structure of the Cu(II) complexed polyacids. It is known that encapsulation of copper acetate in zeolite cavities enhances the catalytic activity (Chavan *et al.*, 2000) Here we present another innovative way of encapsulating metal complexes within the polymer matrix. In principle, by this method one should be able to design new catalysts for enhanced catalytic activities. These gels could also find applications in water purification, wherein the ability of the gels to form complexes with the divalent metal ions, such as Pb(II), could be used effectively.

# Chapter 6

## SELF-ORGANIZATION IN HYDROGELS

*“Where nature finishes producing its own species man begins in harmony  
with the nature to create an infinity of species “*

*- Leonardo Davinci*

### 6.1 Introduction:

Amphiphilic polymers having proper hydrophilic hydrophobic balance have been attracted much attention because of their resemblance to biological systems as well as their strong tendency for self-organization especially in aqueous environments. Self-organization in amphiphiles occurs mainly because of weak hydrophobic interactions, which causes aggregation of hydrophobic groups to form micelles or vesicles so as to minimize their exposure to water upon dispersion in an aqueous medium (Tanford, 1973).

Self-assembly is a corner-stone phenomenon in biopolymers such as proteins, DNA and lipids. The most important attribute of the chemical structure that drives self-organization in amphiphilic polymers is the balance of hydrophilic and hydrophobic interactions. Micellar polymers are also very well known for their self-organization in aqueous environment by creating plentiful super structures on the mesoscopic level (Laschewsky, 1995). However, the understanding of the detailed nature of the molecular structure of the hydrophobic group on self-organization is surprisingly small.

However, examples of macroscopic self-organization in synthetic materials are rare. Shape memory hydrogels can be considered to be an example of materials that can self-organize into specific shapes in response to an external stimulus (Osada *et al.*, 1995; Hu *et al.*, 1995). The demonstration of shape memory in hydrogels has been restricted to bending of cylindrical pieces of gels in response to thermal, electrical or magnetic stimuli. Shape memory gels maintain their cylindrical nature and simply bend along the length to form different shapes.

In this chapter we report a different type of self-organization in a hydrogel, wherein a cylindrical piece of gel transforms into a completely hollow spherical or ellipsoidal object, dependent upon the original aspect ratio ( $L/D$ ) of the cylindrical gel piece, in the presence of specific transition metal ions. The self-organized gels show similarities with amphiphilic molecules that self assemble into micelles or vesicles. The difference, however, is the length scale over which self-organization occurs in these two cases. The unique hollow shape of our gel bears similarities with many hollow objects abundantly found in Nature such as coconut (at a macroscopic level), and amphiphilic siderophores produced by marine bacteria (at a microscopic level), which have been shown to self assemble into a vesicle upon coordination with Fe(III) (Martinez *et al.*, 2000). It is also noted that when turnip is dried, sometimes, it shrinks from the center to the outer layer. However, in turnip, the phenomenon is irreversible unlike what is demonstrated in these gels.

## **6.2 Experimental section**

### **6.2.1 Materials:**

CuCl<sub>2</sub>, PbCl<sub>2</sub>, CdSO<sub>4</sub>, ZnSO<sub>4</sub>, FeCl<sub>3</sub> etc were procured from S. d. fine chemicals and all of them were used to prepare the salt solutions as they received. The details of the other chemicals such as A6ACA, A4ABA etc were described in chapter 5 section 5.2.1.

### **6.2.2 Synthesis of Gels:**

The gels used in this work were synthesized from acrylic acid and acryloyl derivatives of amino acids, which contain a hydrophobic alkyl chain (of length = n) and a terminal hydrophilic carboxyl group. Specifically we have used acrylic acid (AAC, n= 0), acryloyl-4-amino butyric acid (A4ABA, n=3), acryloyl-6-amino caproic acid (A6ACA, n=5) and acryloyl-8-amino caprylic acid (A8ACA, n=7). Gels were prepared by free radical polymerization of aqueous solution of the monomers in the presence of N, N'-methylene bisacrylamide as the crosslinker. Polymerization was done in deionized double distilled water at 40°C using ammonium persulfate as initiator. The gels were washed thoroughly and then dried to give approximately 0.5 cm diameter cylindrical samples. The general structure of the monomers is shown in Figure 5.1. The details about the monomer synthesis as well as the gel synthesis were given in chapter 5, sections 5.2.3 and 5.2.4 respectively. Metal complexation studies were done using non-ionized, partially ionized and fully ionized gels. The ionization of the gels was done by using NaOH.

### **6.2.3 Complexation of the gels with metal ions**

Complexation of the gels with  $\text{Cu}^{2+}$ ,  $\text{Pb}^{2+}$ ,  $\text{Cd}^{2+}$ ,  $\text{Zn}^{2+}$  and  $\text{Fe}^{3+}$  was carried out by placing the dried cylindrical gels in dilute aqueous solutions of 0.1M, 0.05M and 0.001M  $\text{CuCl}_2$ ,  $0.1 \times 10^{-4}$ M  $\text{PbCl}_2$ , 0.1 M  $\text{CdSO}_4$ , 0.1 M  $\text{ZnSO}_4$ , 0.1M  $\text{FeCl}_3$ . Detailed procedure is given in chapter 5 section 5.2.5

### **6.2.4 Swelling measurements of the gels in metal salt solutions.**

A6ACA dried gels of known weights were placed in respective metal ions at room temperature. The swelling ratio of the gels was recorded gravimetrically as a function of time. More details about the swelling measurements were given in chapter 4 section 4.3.3.

### **6.2.5 EPR measurements**

EPR spectra of the complexed gels were recorded at 298K by using Bruker EMX spectrometer operating at X and Q-band frequencies. The spectral editing was done by using WINEPR software package. A detailed description is given in chapter 5 section 5.2.6.

### **6.2.6 Entrapment and Release of Hemoglobin**

Entrapment of hemoglobin was carried out by placing a dried gel piece of fully ionized A6ACA in  $\text{CuCl}_2$  solution containing hemoglobin for 7 days. The hollow gel entrapped the hemoglobin within it, was placed in pure water and the release of hemoglobin was monitored using Shimadzu UV-1601 PC, UV-visible spectrophotometer for a period of time. An immediate release of the entrapped hemoglobin was achieved by leaching out the bound  $\text{Cu(II)}$  ions from the gel matrix. The removal of the  $\text{Cu(II)}$  ions from the gel matrix was carried out by treating the same with  $\text{HCl}$  (pH~2).

The concentrations of the metal ions before and after complexation were estimated at 810nm, whereas that of the hemoglobin was estimated at 460nm. For spectrophotometric estimation, solutions of  $\text{CuCl}_2$  having hemoglobin at different concentrations were prepared and its absorbance was measured to plot the standard curve as shown in Figure 6.1. From this standard curve, the concentration of the unknown salt solution was obtained by measuring the absorbance at 460nm.

### **6.3 Experimental observations**

#### **6.3.1 Metal induced shape transition**

For the fully ionized A6ACA gel an immediate observation was that a 3.5 mm diameter x 1.5 cm long dried cylindrical gel when placed in a 0.1M  $\text{CuCl}_2$  solution slowly transformed itself into an ellipsoidal green colored gel and that of a 5.0 mm diameter x 5.0 mm long cylindrical gel transformed into a completely spherical green colored gel as shown in Figure 6.2. More interestingly, the spherical/ellipsoidal gel was found to have a hollow interior, which developed gradually with time as shown in Figure 6.3. After 12 hours the solid cylindrical gel turned into a solid spherical/ellipsoidal gel having a core-shell morphology in which the hard green colored shell was filled with a soft blue colored core. After 48 hours, the gel showed a partially developed hollow interior enclosed within the hard shell, which had grown at the expense of the soft inner core. At the end of 96 hrs a completely hollow sphere consisting of only a hard shell was formed.

Hollow A6ACA gels were also formed by complexation with Pb (II) and Fe (III) ions as shown in Figure 6.4. Here the shell, which supported the hollow interior, was found to be porous as shown in Figure 6.5.

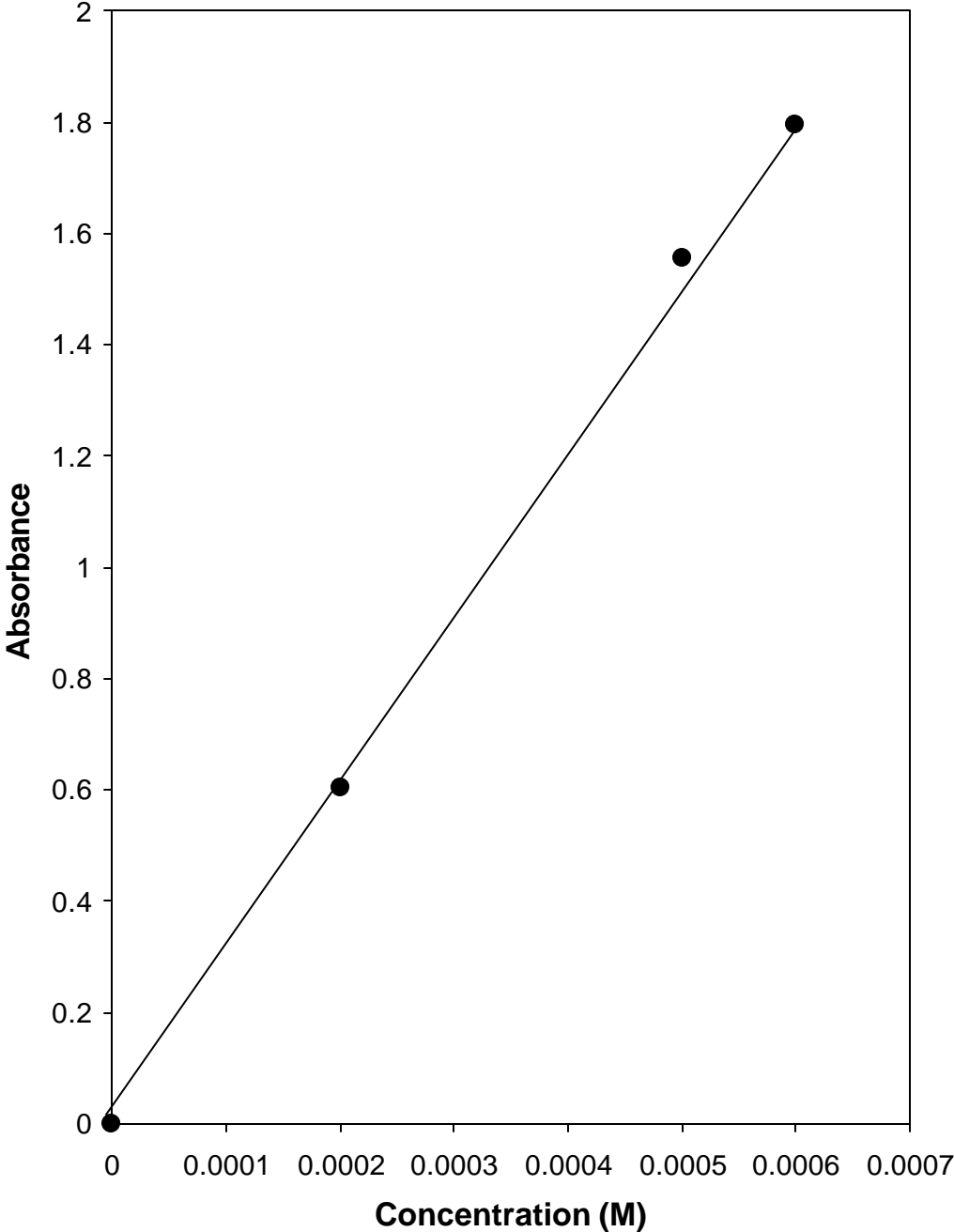


**Figure 6. 1:** Standard curve for hemoglobin at 460nm

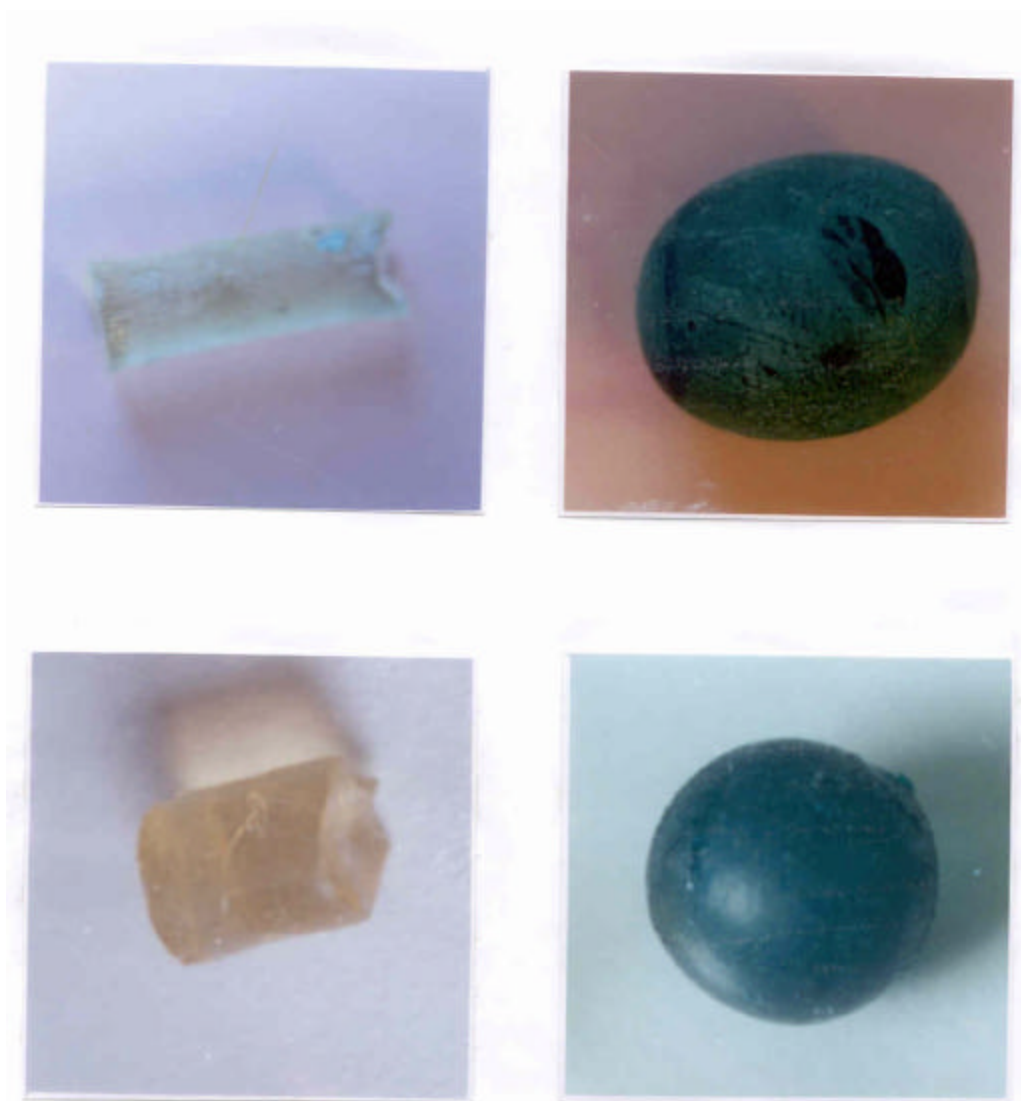


**Figure 6.2:** Morphological change of the A6ACA gel in  $\text{CuCl}_2$  solution



**Figure 6.3:** Development of the hollow interior of the A6ACA copper complexed gel over a period of time

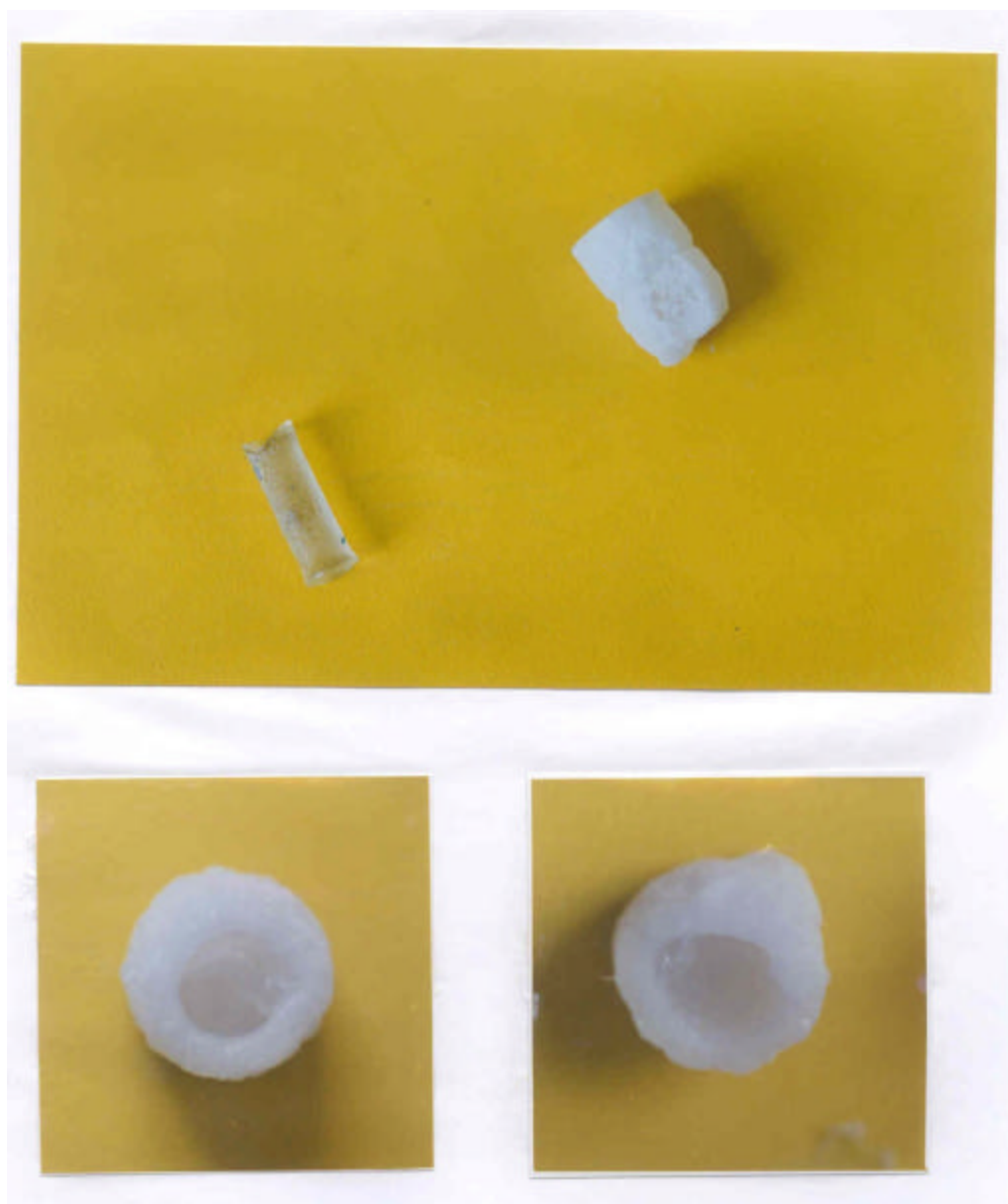


**Figure 6.4:** Morphological change of the A6ACA gel in  $\text{PbCl}_2$  solution

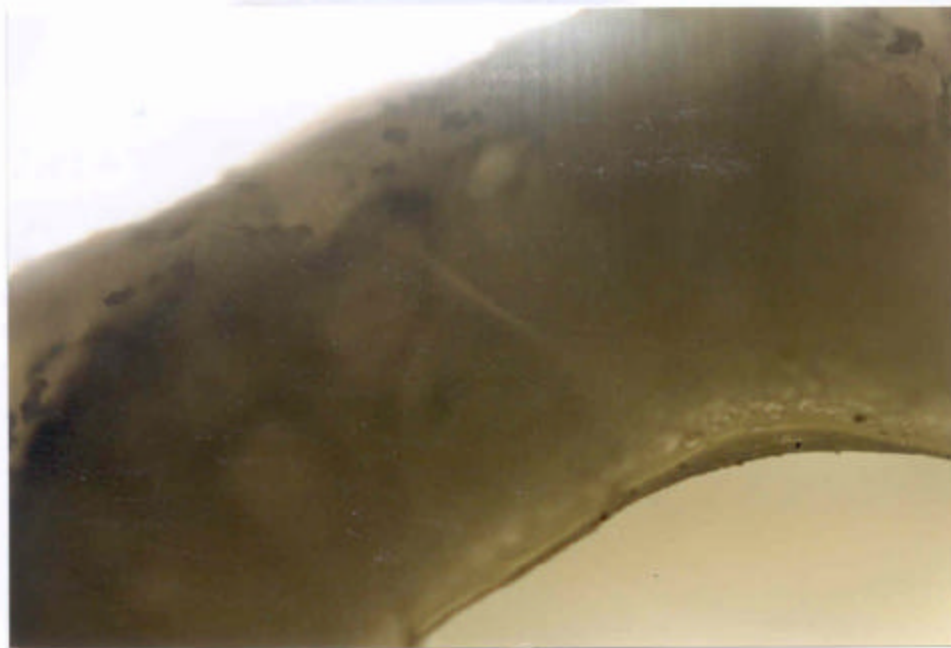


**Figure 6.5:** optical micrograph of the Pb(II) complexed A6ACA gel

Cadmium and zinc complexed A6ACA gel showed an ellipsoidal shape with core (transparent) and shell (opaque) morphology. However, they did not form a hollow interior even after fifteen days. The fully ionized A6ACA gel of 5mm diameter x 1.5 cm long dried cylindrical gel placed in  $\text{CdSO}_4$  solution was transparent for the initial 10 to 12 hrs and then the shell turned to be opaque which supported the soft transparent inner core.

### **6.3.2 Shape memory**

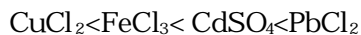
Another interesting aspect of the complexation phenomenon was that the Cu(II), Pb(II) and Fe(III) complexed gels showed a unique shape memory at a macroscopic level as shown in Figure 6.6. For example, the hollow spherical copper complexed A6ACA gel reverted to its original solid cylindrical structure when the complexed copper was leached out using HCl keeping a microscopic rupture line at the centre. For checking the reversibility of the hollow spherical-to-solid cylindrical, the hollow spherical Cu(II) complexed gel was placed in HCl at pH 2. On leaching out the Cu(II) ions, the spherical gel was transformed back into a solid cylindrical gel forming a microscopic rupture line. The solid cylindrical gel was washed with water and then with NaOH to regain the initial ionized state. The ionized gel was dried and again complexed with Cu(II) to get hollow spherical gel. On leaching out the Cu(II) ions with HCl, the hollow spherical gel is transformed back into the original solid cylindrical shape with the rupture line. Interestingly, no further growth in the rupture line was observed.

**Figure 6.6:** Shape memory: The self-organized A6ACA gel reverted back to the original solid cylindrical structure

### 6.3.3 Swelling behaviour of the gel in metal solutions

The swelling ratios of the gels in  $\text{CuCl}_2$  solution were measured gravimetrically. The swelling behavior of A6ACA gel in  $\text{CuCl}_2$  showed several interesting features. It was observed that when a dry A6ACA gel was immersed in  $\text{CuCl}_2$  solution, the gel first swelled to a maximum value and then started collapsing slowly as shown in Figure 6.7. During its initial swelling the cylindrical gel transformed into a solid spherical gel. The hollow interior developed slowly afterwards accompanied by the slow collapse. All the complexed gels were showed a lower swelling ratio in salt solutions. This is attributed to the over all increase in crosslink density due to complexation (a detailed discussion is given in chapter five)

Figures 6.8, 6.9 and 6.10 show the swelling behaviour of A6ACA gels in  $\text{PbCl}_2$ ,  $\text{CdSO}_4$  and  $\text{FeCl}_3$  solutions respectively. As shown in Figure 6.8, the dry A6ACA gel swelled to a maximum and then reached a swelling plateau in  $\text{PbCl}_2$  solution. But, in the case of  $\text{CdSO}_4$  and  $\text{FeCl}_3$  salt solutions, the A6ACA gel swelled to a maximum and then collapsed slowly as shown in Figures 6.9 and 6.10. The time required for the A6ACA gel to swell maximum in the metal salt solutions was varied with the metal ions and is in the following order.



The swelling behavior of the gels in metal salt solutions indicates that the gel swells first in metal salt solution followed by complexation.

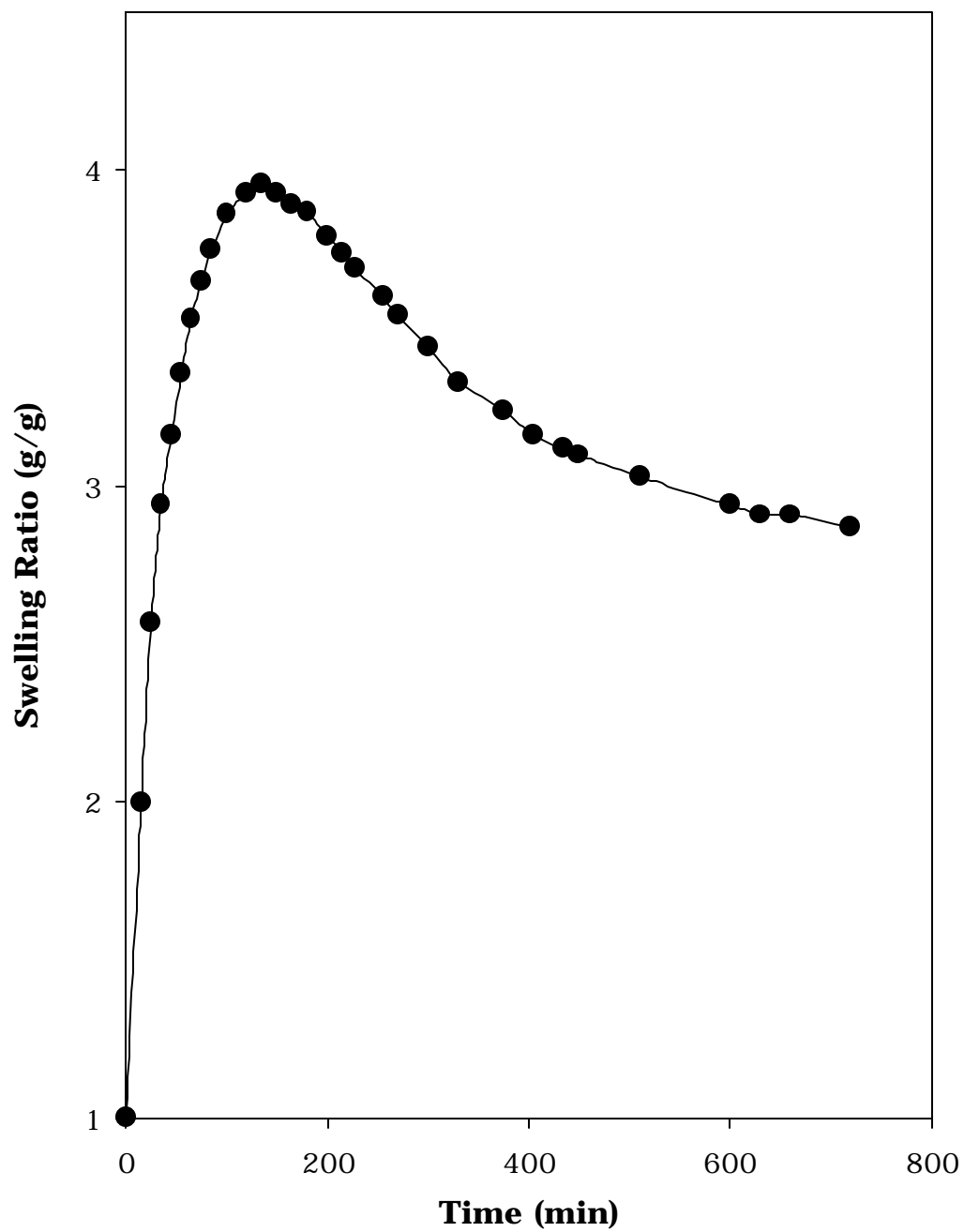


**Figure 6.7:** Swelling behaviour of the A6ACA gel in  $\text{CuCl}_2$  solution

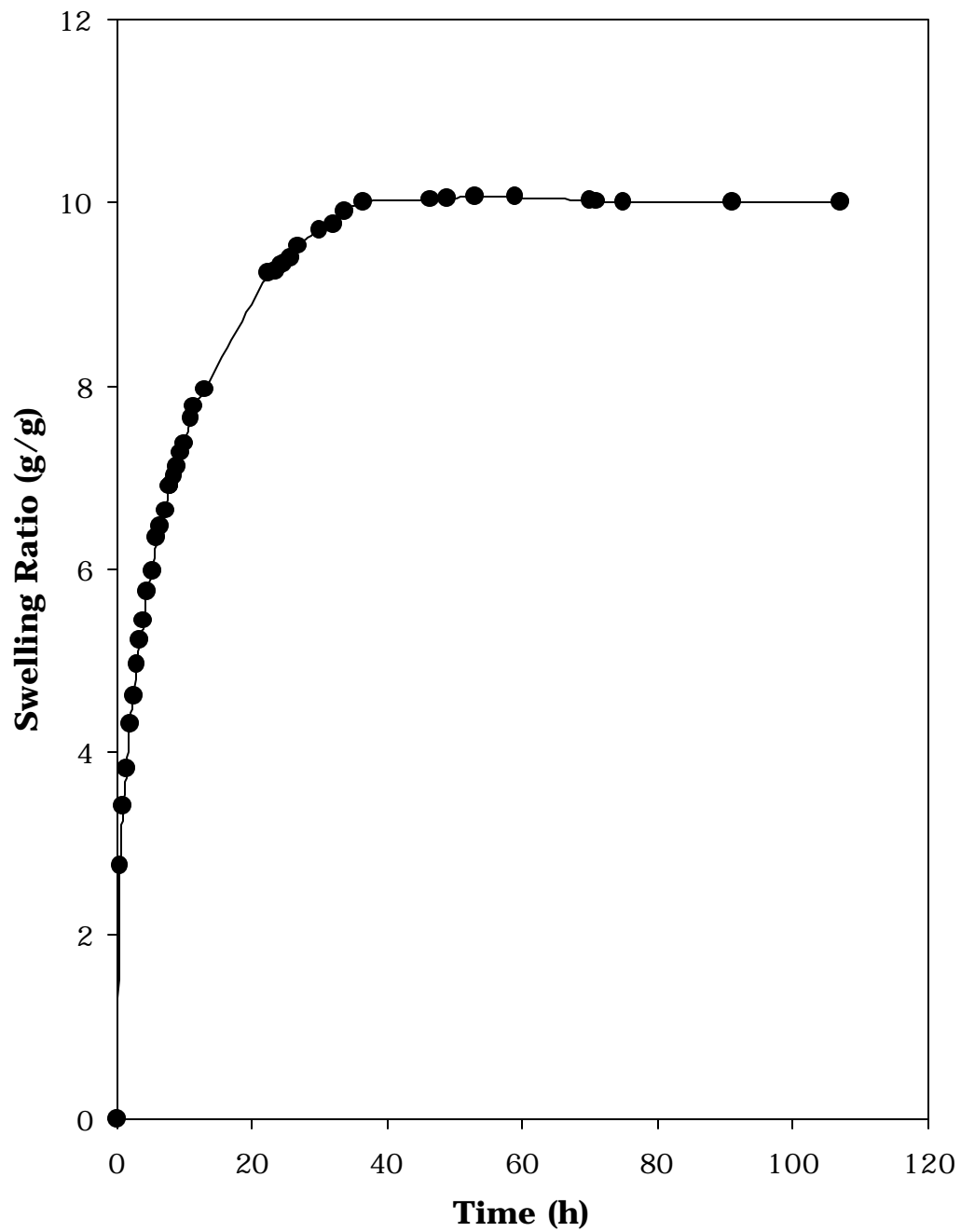


**Figure 6.8:** Swelling behaviour of the A6ACA gel in  $\text{PbCl}_2$  solution



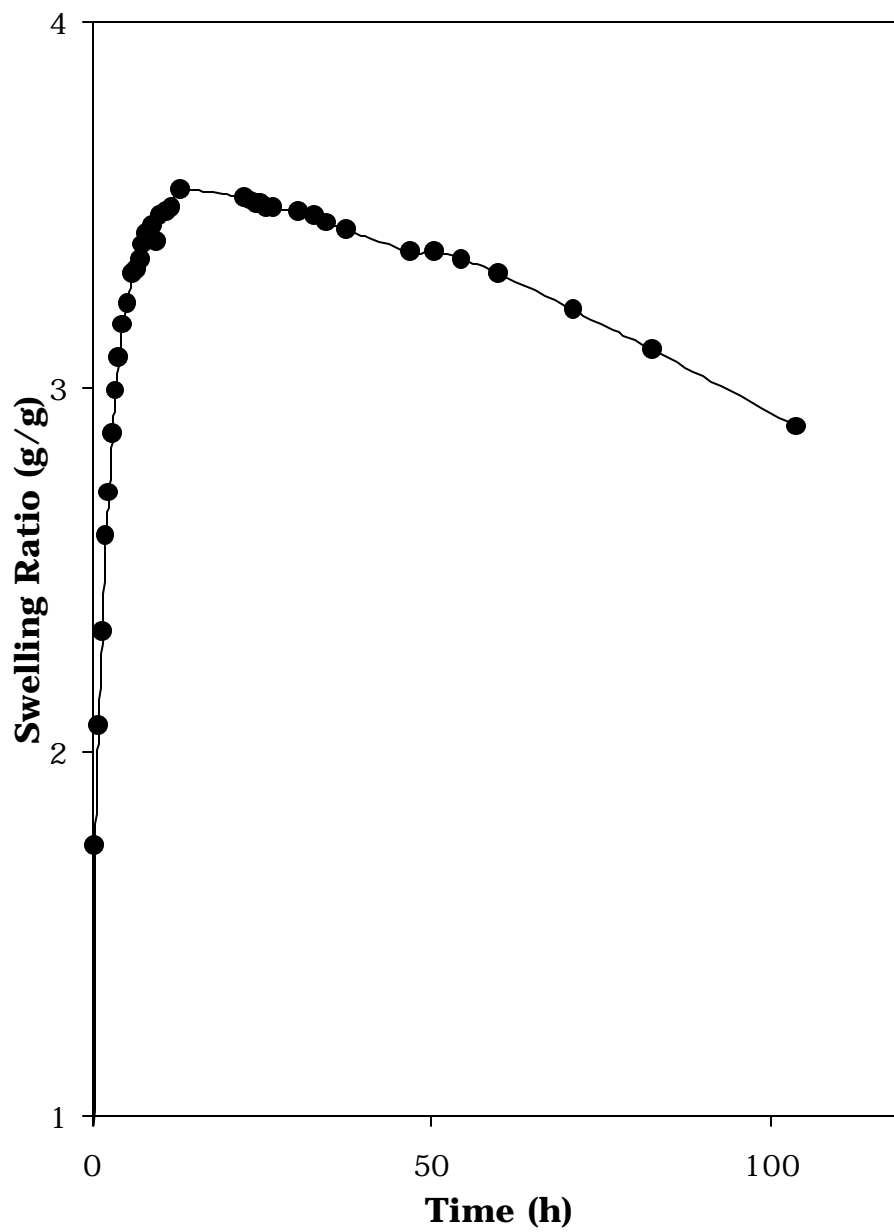


**Figure 6.9:** Swelling behaviour of the A6ACA gel in  $\text{CdSO}_4$  solution

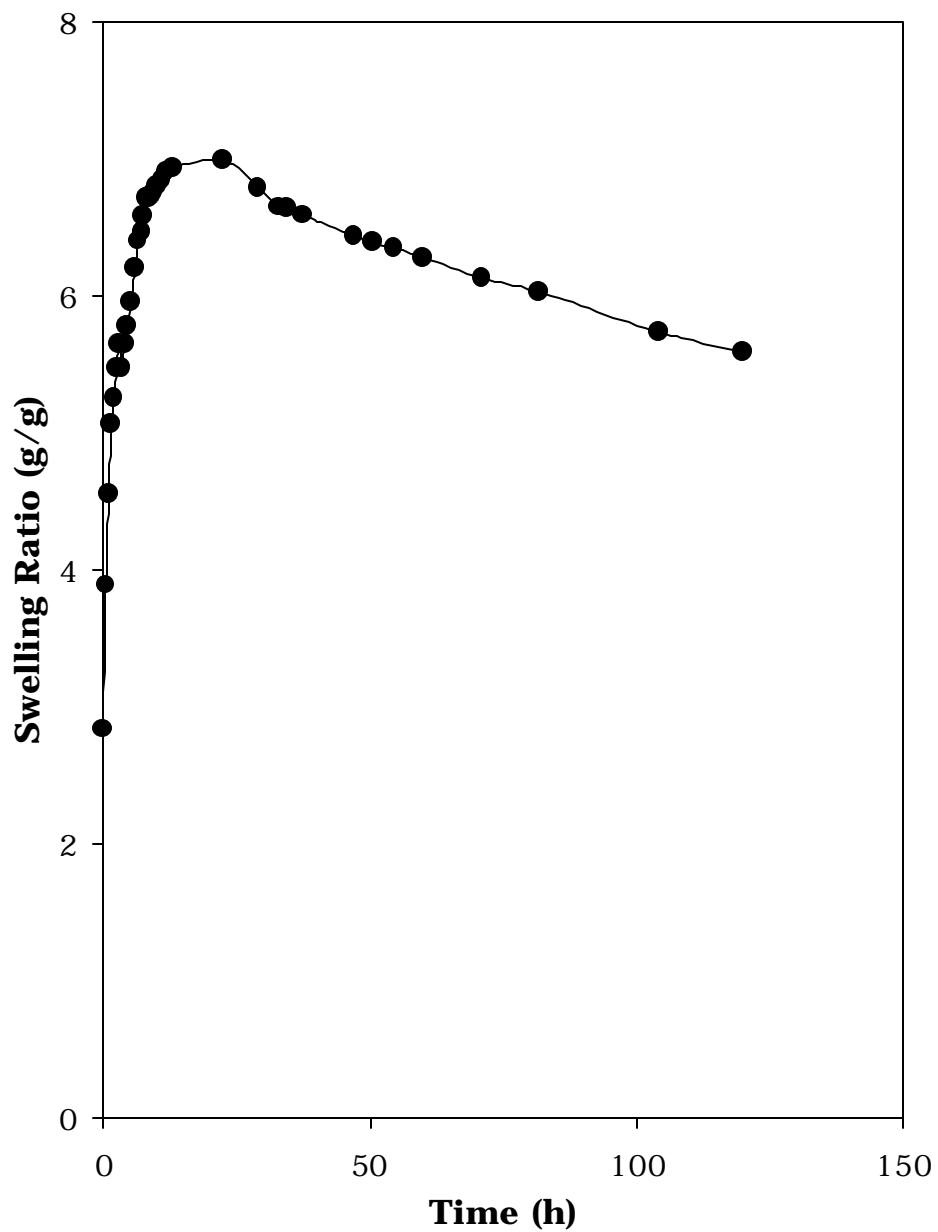


**Figure 6.10:** Swelling behaviour of the A6ACA gel in  $\text{FeCl}_3$  solution

#### 6.3.4 EPR structure

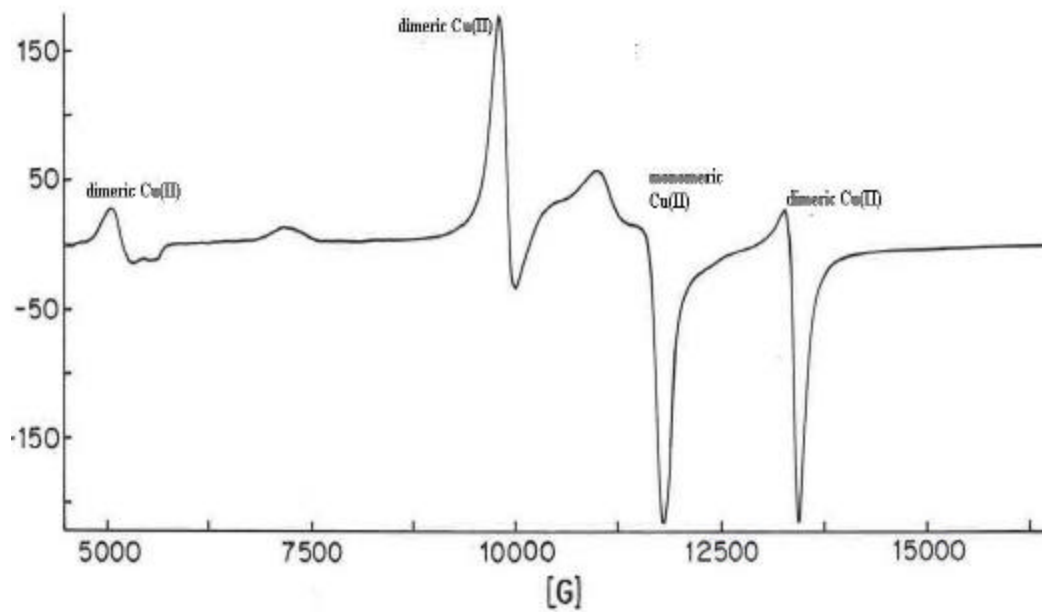
The structure of the complexed gels was investigated using electron paramagnetic resonance spectroscopy (EPR). The EPR spectra of Cu(II)-complexed A6ACA gel showed two types of complexes, dimeric and monomeric as shown in Figure 5.10a. The dimeric species is a much tighter complex than the monomeric species as shown in Figure 5.12. We have done EPR investigation separately on the core and shell of the Cu(II) complexed A6ACA gel to investigate the structure of the complex. We found that the soft blue core contains only monomeric copper complexes, while the hard greenish blue shell contains a mixture of dimeric and monomeric copper complexes as shown in Figure 6.11.

#### 6.4 Results and discussion

The mechanism of formation of hollow interior was investigated by studying the complexation of polymer chains with metal ions together with the swelling behavior of the gel in metal salt solutions. The EPR measurements along with the swelling studies indicate that the gel swells first in the metal solution followed by complexation with metal ions.

The mechanistic picture that emerges from the swelling studies and EPR measurements is as follows. When a dry cylindrical gel is immersed in the  $\text{CuCl}_2$  solution, water molecules and  $\text{Cu}^{2+}$  ions start diffusing inside. The copper ions react with the gel to form a monomeric complex initially, which slowly rearranges into a dimeric complex after sufficient  $\text{Cu}^{2+}$  concentration is available to statistically bring two cupric ions in close proximity. Since the surface of the gel is the first layer to interact with the  $\text{Cu}^{2+}$ , the dimeric complex forms first at the surface.

(a)



(b)

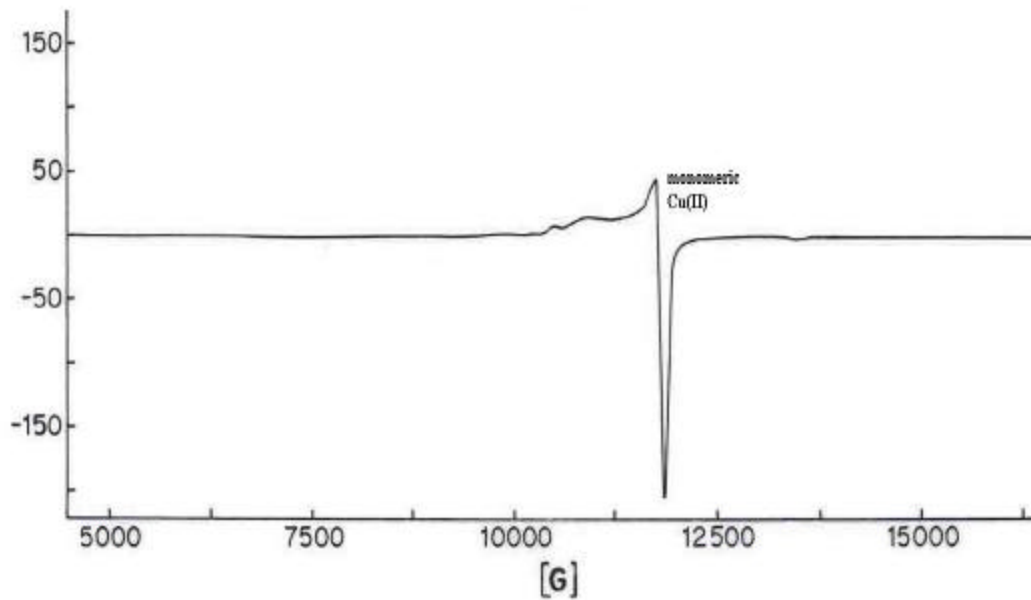


**Figure 6.11:** EPR spectra of the Cu(II) complexed A6ACA gel (a) Hard shell  
(b) Soft core

As discussed in chapter five, a small amount of complexation increases the effective hydrophobicity of the gel. Here the strong dimeric complexation at the surface of the gel renders it effectively hydrophobic, due to which the cylindrical shape reorganizes into a spherical form so as to minimize the surface energy. However, no shape transition such as cylindrical to spherical was observed in the case of Pb(II) complexed gels. In the case of Pb(II) complexed A6ACA, the transformation of smooth surface of the gel to a porous one is attributed to the phase separation. The complexation of the gel with Pb(II) ions enhances the effective hydrophobicity of the system, hence the phase separation.

As reported in the experimental section, the shape transition, into a spherical or ellipsoidal form was very much dependent upon the original L/D ratio of the gel used. It is obvious in a sense that since the sphere is a limiting case of an ellipsoid, the transformation of a cylinder to spherical object will be dependent on the initial aspect ratio of the gel used. As  $\text{Cu}^{2+}$  ions slowly diffuse inside, the monomeric complex in the core of the gel rearranges into dimeric complex whenever a thin layer near the shell attains adequate concentration of  $\text{Cu}^{2+}$  ions. Thus the core material deposits layer by layer on the outer shell. This reorganization results in a hollow interior. Since the process is diffusion-controlled, the time required to self-organize into hollow structures depends on the initial size of the gel. Thus dry gels measuring 5 mm in diameter take about 4 days to form hollow structures, while fine particles measuring about 100  $\mu\text{m}$  can form hollow gels within 5 minutes.

Clearly such a process of macroscopic self-organization would require sufficient mobility of the polymer chains, which in turn will be mainly governed by the initial swelling of the gels. Thus, two conditions

seem to be necessary for the gels to exhibit self-organization: adequate swelling and formation of tighter complexes such as the dimeric species. Absence of any one of these hinders self-organization. The data tabulated in Table 6.1 clearly shows this trend. For example, the copper complexed non-ionized A6ACA gel has dimeric complexes, however the gel does not form a hollow interior due to its inability to swell adequately in the  $\text{CuCl}_2$  solutions. On the other hand, the ionized AAC gels swell considerably in  $\text{CuCl}_2$  solutions but do not form dimeric complexes and therefore do not show a hollow interior. Also, it is obvious that large stresses will be built in the gel during the formation of a hollow interior. The A6ACA copper complexed gel was able to sustain the stresses in contrast to AAC gels, which could not do so and shattered on complexation.

From the shape transition studies it is noted that a small number of covalent bonds would break during the initial formation of the hollow interior. The fine rupture line observed after the gel reverted back to its original solid cylindrical shape indicated that the bonds, which had broken during the hollow formation, could not be healed completely. Thus the shape transition is not microscopically reversible in a true sense. Nevertheless, the formation of a microscopic rupture line during the first transition to a hollow sphere does not hinder the subsequent macroscopic reversibility. Indeed the gel undergoes repeatable reversibility of the shape transition in that the gel does go through a hollow-solid-hollow transitions several times by alternately immersing it in  $\text{Cu(II)}$  and  $\text{HCl}$  solutions. The absence of further growth in the rupture line during the reversibility experiments indicates that the shape transition is truly reversible in all the cases, which follow the first transition.

We wished to clarify that the hollow spherical-to-solid cylindrical transition and its reversibility is driven only by metal complexation and not by pH. We immersed the gel in a low pH phosphate buffer solution (pH~2). During this experiment we found that the hollow gel does not revert back to a solid cylinder. Thus, the hollow sphere-to-solid cylindrical transition and its reversibility is driven only by metal complexation and not by pH. Even EDTA could be used to leach out the Cu(II) and in this case again the hollow spherical object reverted back into a solid spherical object. This clearly suggests that the reversible transition reported here is mainly governed by metal complexation. Thus to achieve a reversible transition one may use any trigger and not necessarily HCl, which can leach out the Cu(II).

It is also interesting to note from Table 6.1 that self organization is exhibited only by those gels having an alkyl chain length of  $n=5$  and above. This indicates that a critical balance of hydrophilic and hydrophobic interactions might be required for the formation of such structures. The formation of hollow gels reported here has some resemblance with an earlier report of pattern formation during shrinking (Matsuo *et al.*, 1992). However, the work reported here is different in many ways. Our work shows that formation of hollow interior due to metal complexation does not occur for all metal ions and for all gels. A balance of hydrophilic and hydrophobic interactions seems to be critical to the formation of hollow interiors in addition to formation of specific coordination structures such as dimers. Further, the gels have a near complete shape memory and can be used for novel applications as discussed below.

Gel	Initial swelling Ratio <sup>(b)</sup> (g/g)	Dimeric Copper complex <sup>(a)</sup>	Monomeric Copper complex <sup>(a)</sup>	Appearance	% Complexation <sup>(c)</sup>
AAC(H <sup>+</sup> )-Cu(II)	1.94	✓	✓	Solid Cylinder	0.8
AAC(Na/H)-Cu(II)	3.35		✓	Shattered	12
AAC(Na <sup>+</sup> )-Cu(II)	4.24		✓	Shattered	13
A4ABA(H <sup>+</sup> )-Cu(II)	1	✓	✓	Solid Cylinder	0.8
A4ABA(Na/H)-Cu(II)	1.2	✓	✓	Solid Cylinder	14
A4ABA(Na)-Cu(II)	3.5		✓	Solid Cylinder	15
A6ACA(H <sup>+</sup> )-Cu(II)	1	✓	✓	Solid Cylinder	1
A6ACA(Na/H)-Cu(II)	3.6		✓	Solid Cylinder	4
A6ACA(Na)-Cu(II)	4.0	✓	✓	Hollow Sphere	18
A8ACA(Na)-Cu(II)	4.12	✓	✓	Hollow Sphere	21
A6ACA(Na)-Pb(II)	10.07	--	--	Hollow Cylinder	--
A6ACA(Na)-Cd(II)	3.54	--	--	Solid core and shell	--
A6ACA(Na)-Fe(III)	6.99			Hollow sphere	

(a) EPR studies

(b) Swelling measurements made 4hrs after immersion in salt solution

$$(c) \% \text{ complexation} = \frac{100(\text{gmoles of metal ion complexed})}{\text{gmoles of COO}^- \text{ on dry gel}}$$

**Table 6.1:** Swelling behavior of the gels in CuCl<sub>2</sub> salt solution



We believe that the unique hollow morphology of the polymer metal complex can have many interesting applications such as in designing novel controlled release devices. Designing such systems continues to be a challenge and gel based systems have been used in the past (Hoffman *et al.*, 1987; Patil *et al.*, 1991). Kulkarni *et al.* (1992) have successfully demonstrated the use of reversible bilayer hydrogels as controlled release systems, where the insitu bilayer formation was done in the acidic pH (pH~2) obtainable in the stomach and the release was done at a higher pH (pH~7) obtainable in the intestine. As an illustrative example, we investigated the release profile of entrapped hemoglobin (a model molecule) from within the hollow interior of the gel. A piece of dried gel was placed in a  $\text{CuCl}_2$  solution containing hemoglobin. The morphology of the gel changed to a hollow sphere spontaneously entrapping the hemoglobin molecules within it. The gel was then placed in pure water to investigate the release behavior, which was monitored by using UV-visible spectrophotometer. Hemoglobin was found to be released at a constant rate after an induction period as shown in Figure 6.12.

The constant release rate is caused by virtue of the fact that the rate controlling step is diffusion through the thin hard shell of the device (Kulkarni *et al.*, 1992). Interestingly, an immediate release of the entrapped hemoglobin was observed when the complexation was destroyed by using HCl. Such systems could possibly used for targeted delivery of large biomolecules in human body.

We have prepared CdS nanoparticles in a polymer gel by placing a cadmium complexed gel into a dilute solution of  $\text{Na}_2\text{S}$ . We observed the formation of two optically different types of particles as shown in Figure 6.13.

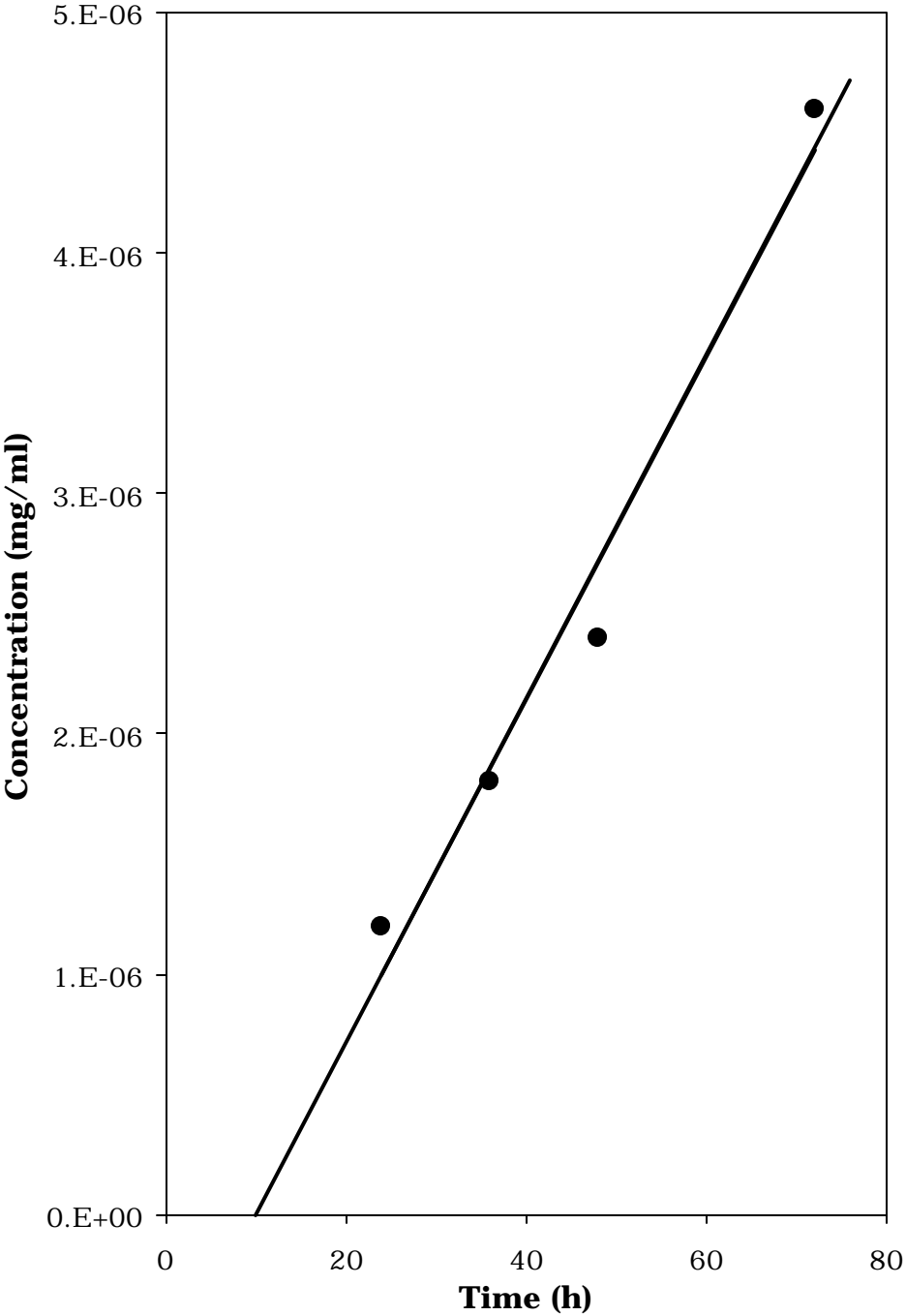


**Figure 6.12:** Release of hemoglobin as a function of time



**Figure 6.13:** CdS nanoparticles in A6ACA gel matrix

Yellow colored particles in the shell and the orange colored particles in the core. The colour difference clearly tells that the formed particles are different in size. The UV analysis indicates that the yellow shell contains approximately 60Å nanoparticles. We believe that nanoparticles with controlled particle sizes can be synthesized from metal complexed polymeric gels by controlling the morphology of the gel.

### **6.5 Conclusion**

A macroscopic self-organization is observed first time in polymer gels having an optimal alkyl chain length in the presence of transition metal ions. This gives a new direction for designing polymer gels, which can mimic biopolymers. The process of self-organization in the gels is driven by concentration gradient of metal ions, a process resembling the mechanism of positional information for differentiating cells during the growth of human organs (Wolpert, 1996). We have shown a novel effect that a gel can reversibly change from a hollow sphere to a solid cylinder, in contrast to all current gels that essentially shrink or swell isotropically. As mentioned earlier hollow spheres in both bulk size and micro-size could have potential applications such as controlled release of drugs and chemicals.

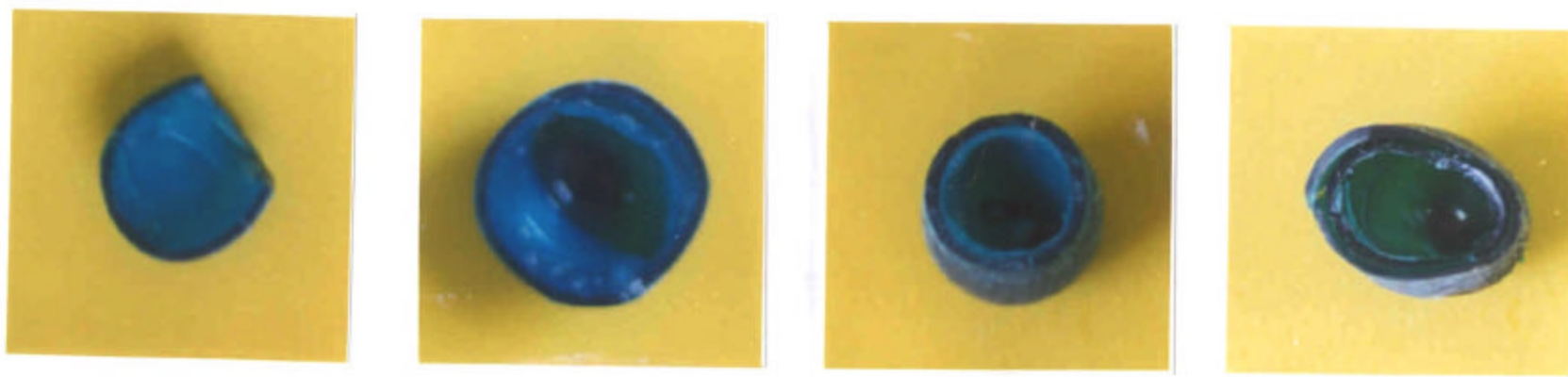


**Figure 6.3:** Development of the hollow interior of the A6ACA copper complexed gel over a period of time



# Chapter 7

## SELF-HEALING IN GELS

### 7.1 Introduction

Smart polymeric gels have been considered as model biomimicking materials since they demonstrate several attributes of biomolecules such as sensitivity, selectivity, mobility, shape memory and self-organization. Of these the first four features have already been demonstrated in the past. For example, in 1978, Tanaka reported for the first time the sensitivity of gels towards external stimuli such as solvent (1978) and temperature (1978). Later Osada *et al.* (1993) demonstrated mobility in polyelectrolyte gels and shape memory (1995) in gels. As discussed in the previous chapter we have demonstrated a novel self-organization phenomenon in polymer gels. Thus, polymeric gels help us in understanding how biomolecules make use of the specific interactions to carry out several complex actions. Smart gels have also been used to develop novel applications based on their ability to mimic biological systems.

Another attribute of biological systems is the process of healing. For example, a cut wound heals with time leaving behind only a scar or the 'weld line'. Healing occurs by the process of cell growth and reorganization around the wound. Synthetic materials also heal by a process commonly known as welding. For instance, ice cubes join when pressed against each other. This occurs by the formation of a thin film of water, which forms strong hydrogen bonds with the cubes thereby welding them. Similarly, thermoplastics weld at temperatures above their glass transition or melting

point. In this case welding occurs by reptation of polymer chains across the interface (de Gennes, 1971). Indeed the welding of polymers is at the very heart of several important applications of thermoplastics such as packaging and molding.

Crosslinked polymers such as polymeric hydrogels cannot weld like thermoplastics because of the absence of reptative ability of the polymer chains forming the covalently bonded network. In this chapter we demonstrate for the first time that hydrogels can be welded via 'physical' crosslinks. Specifically, we show that two separate pieces of a lightly crosslinked gel can weld in the presence of Cu(II) ions to form a single gel piece while keeping a weld line at the interface. Healing occurs by the formation of polymer-metal ions coordination complexes across the weld line. Interestingly, we observed that the strength of the weld line increased with time. We also observed that since the welding junctions are physical crosslinks, they can be reversibly formed and destroyed to weld and separate the gel pieces repeatedly. We propose a mechanism for welding and suggest some interesting applications for the gels.

## **7.2 Experimental section**

### **7.2.1 Materials**

The gels used in this work are acrylic acid and acryloyl derivatives of amino acids namely, acryloyl 6-amino caproic acid (A6ACA), acryloyl 4-aminobutyric acid (A4ABA). The gels made from acryloyl derivatives of amino acids contain a hydrophobic alkyl side chain (of length =  $n$ ) and a terminal hydrophilic carboxyl group. The details about the procurement of the chemicals are given in chapter 5, section 5.2.1 and chapter 6, section.6.2.1.  $\text{CuCl}_2$  was used as the source of  $\text{Cu}^{2+}$ .



### **7.2.2 Synthesis of gels:**

The acryloyl derivatives of amino acids were synthesized by reacting the respective amino acids with acryloyl chloride. The gels were synthesized by free radical polymerization using bis acrylamide as a crosslinker in an aqueous medium. The details about the monomer synthesis and the gel synthesis were described in chapter 5, sections 5.2.3 and 5.2.4, respectively.

### **7.2.3 Tensile measurements**

The strength of the weld line of the healed gels was measured using a universal testing machine (Instron machine model 4204). A load cell of 1 kN was fitted to the instrument and tensile tests were done at a crosshead speed of 10mm/min. The gel samples were prepared such that only the area near the weld line was exposed to the Cu(II) ions. This was done in order to restrict the metal ions induced self-organization of the gels as reported in the previous chapter. Thus, the gels were prevented from being transformed into hollow objects. Tensile measurements were done on the healed gels as a function of healing time using slightly moisturized gel samples.

### **7.2.4 Dynamic Mechanical Analysis (DMA)**

A Rheometrics Scientific Dynamic Mechanical Thermal analyzer (DMTA IV) was used to measure the visco-elastic properties of the gels. The percent strain used for the experiments was 0.01(dynamic frequency test) and 0.2 (Temperature ramp test). The storage modulus ( $G'$ ) and viscous modulus ( $G''$ ) were measured at small strains (0.01) in the frequency range of 0.1 to 50 rads/sec at 30°C. The elastic and viscous moduli of the gels

were recorded at different moisture contents. The dynamic  $T_g$  of the gels was measured for the dried gels at 0.2% strain and 1.0 rad/s frequency in the temperature range 25°C to 100°C. The test fixture used to run all the experiments was single cantilever bending.

### **7.2.5 Moisture absorption**

Gels of known weights were placed in a desiccator containing saturated solution of sodium nitrite to absorb moisture. The saturated sodium nitrite maintained a relative humidity of 66% in the desiccator. The moisture absorbance was measured gravimetrically as a function of time as shown in Figure 7.1

## **7.3 Results and Discussion**

### **Healing phenomenon**

When two pieces of dried and fully ionized A6ACA gels were placed together in a Cu(II) salt solution, it was observed that they stuck to each other. When one gel piece was lifted from the solution, the other piece was automatically lifted as shown in Figure 7.2. The weld line was also found to develop with time so that two separate gel pieces were strongly united into one integral piece while retaining a thick weld line at the interface as shown in Figure 7.3. In fact, the weld line was strong enough to allow the development of a single hollow self-organized structure from the original two separate gel pieces. This is shown in Figures 7.4 and 7.5. The formation of the hollow structure was discussed in chapter six previously. The healing phenomenon was observed in the case of A4ABA gels also, with the difference that the healed gel did not form a hollow object in agreement with the findings reported in the chapter six.

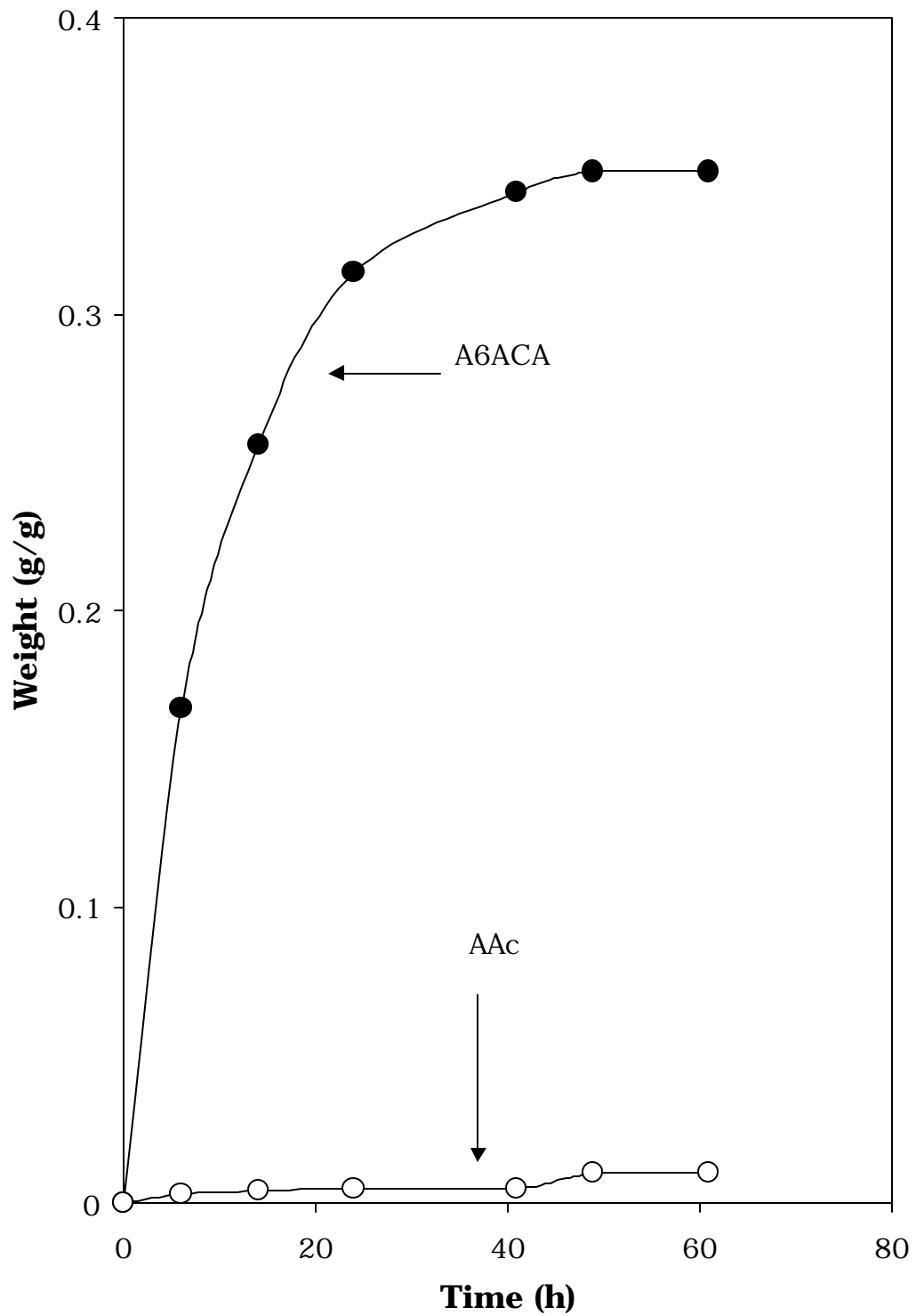


**Figure 7.1:** Moisture absorbance of the gel as a function of time

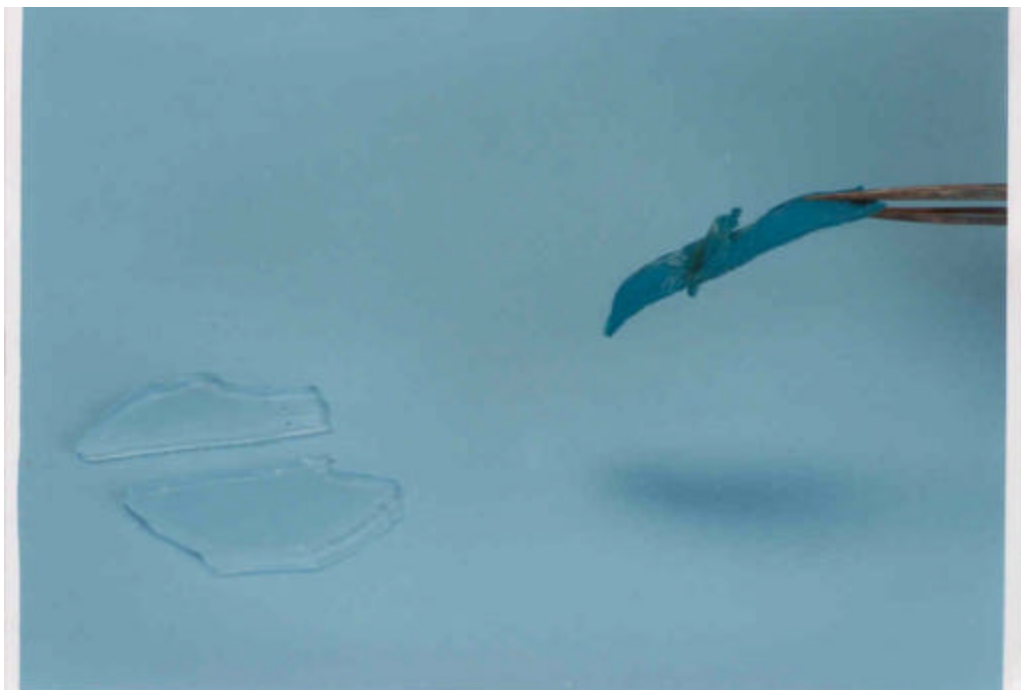


**Figure 7.2:** Healed A6ACA gel



**Figure 7.3:** Initial stages of healing, formation of thick weld line



**Figure 7.4:** Completely healed cylindrical A6ACA gel



**Figure 7.5:** Cross section of the completely healed A6ACA gel.

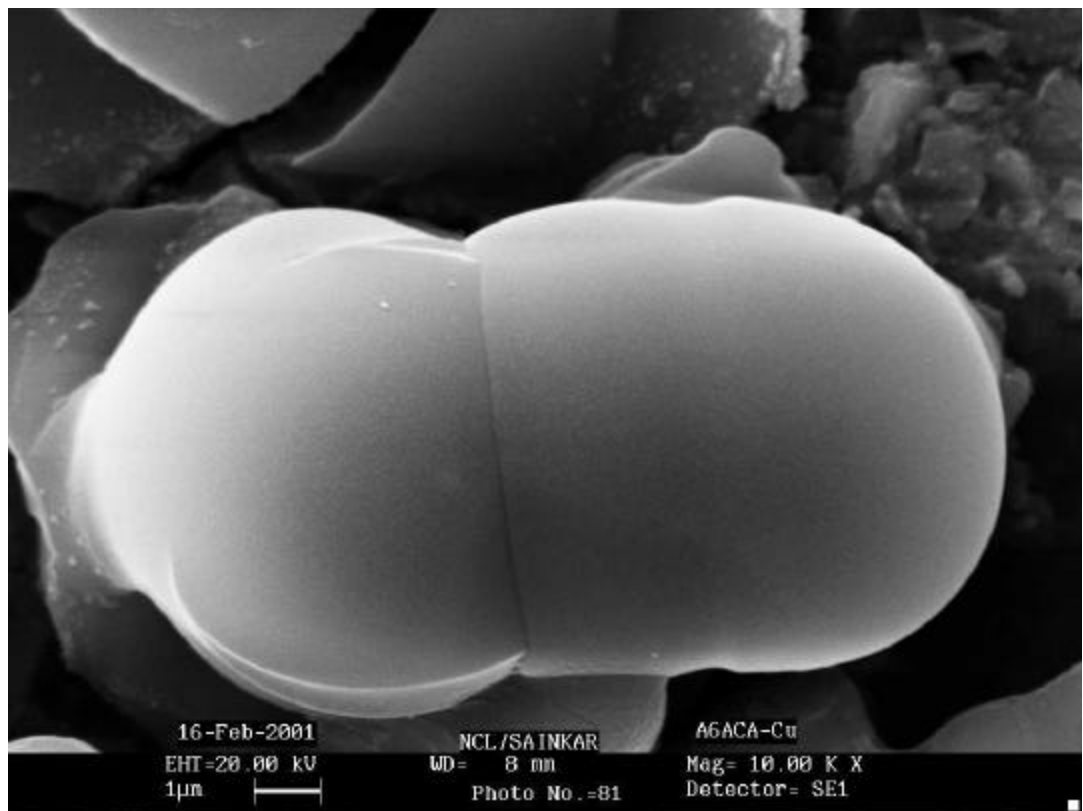
The weld line was found to thicken with time over a period of a few hours for large gel pieces and within a few minutes for small gel pieces. Figures 7.6a, 7.6b, 7.6c and 7.7 show the scanning electron micrograph of welded gel particles as well as dried gel particles before welding. The healed gel particles were prepared by first grinding a dry A6ACA gel piece followed by immersing the powdered gel into a 0.1 M  $\text{CuCl}_2$  solution. The irregular shaped gel particles self-organized into nearly spherical particles, which also fused with each other showing a well-developed welded interface. Larger gel pieces were seen to swell and deform so as to increase the welding surface.

While the A6ACA and A4ABA gels were found to weld in the presence of  $\text{Cu(II)}$  ions, the acrylic acid (AAc) gels did not weld at all. They always remained in a highly collapsed state as separate pieces irrespective of the size of the initial dry gel pieces.

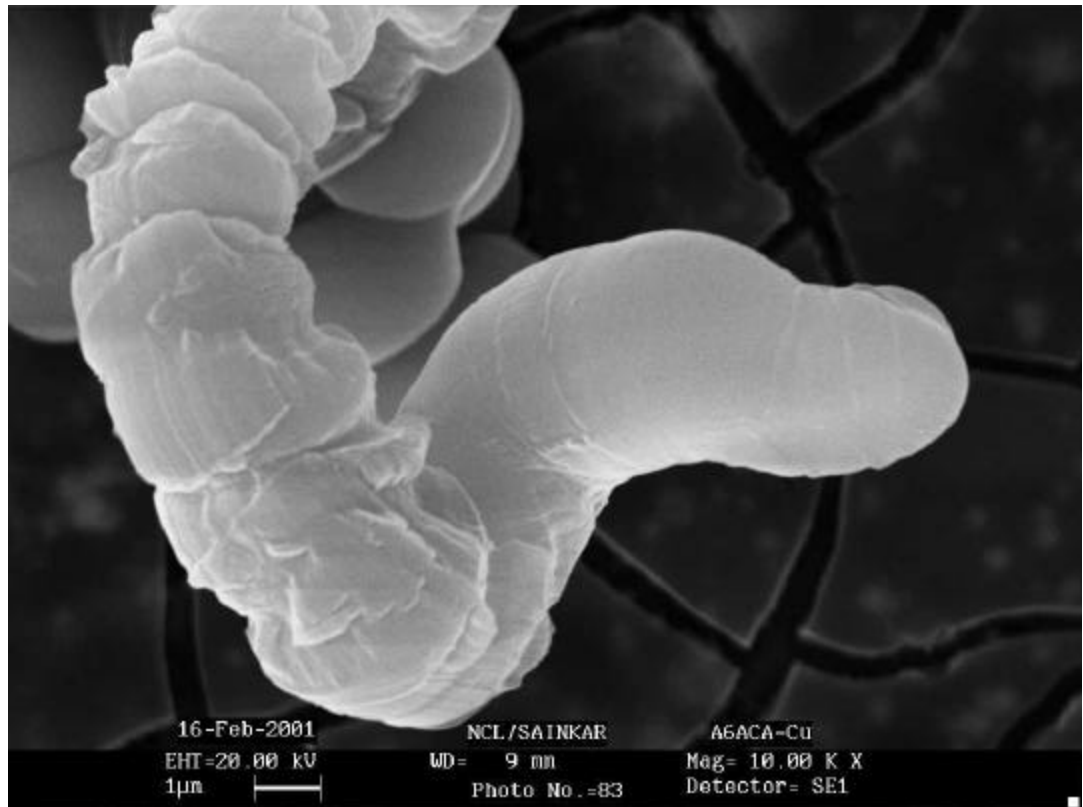
### **Tensile**

The growth of the weld-line with time suggested an increase in the strength of the welded joint. The strength of the joint was measured by standard tensile tests. Cylindrical gel pieces of 3.5 mm diameter x 20 mm length were welded so that only a small volume near the interfacial region was welded. This was done in order to prevent the entire gel from being converted into a self-organized hollow object, for which tensile measurements became impossible. By welding only a small volume of the gels near their interface, we were able to prevent the formation of a hollow interior. Hence this method was adopted for studying the weld line strength. Welding was allowed to take place for a fixed time intervals, after which the gel pieces were removed and dried.

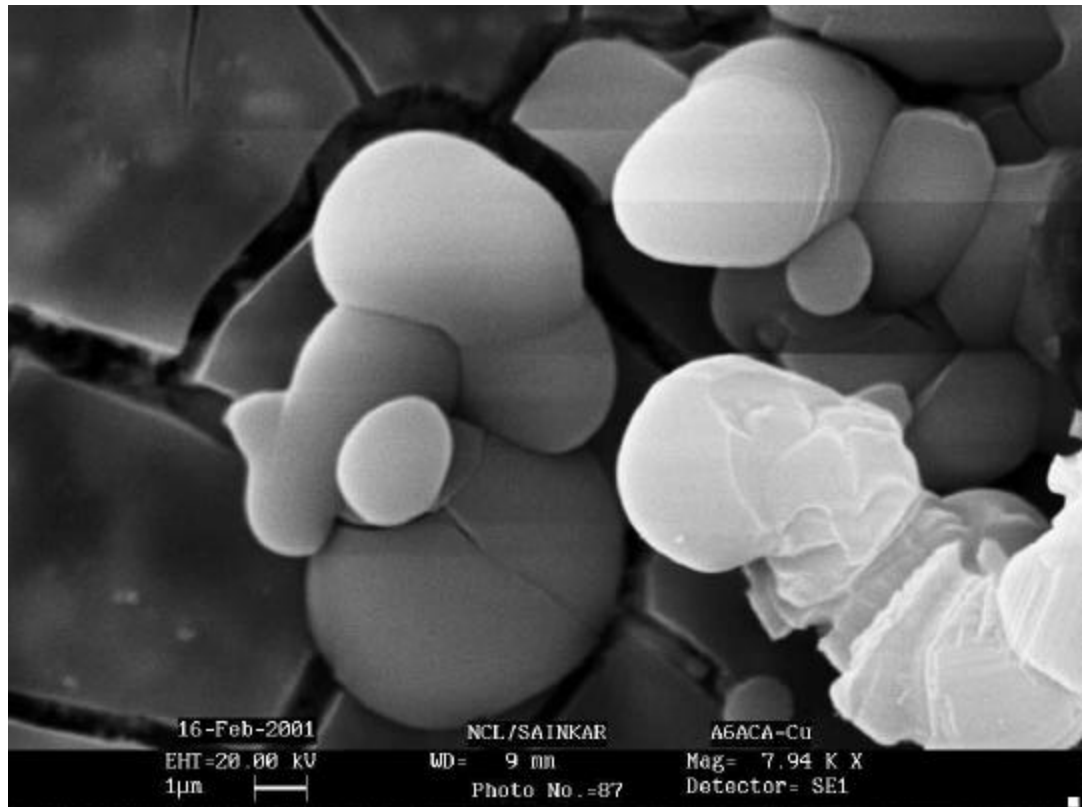




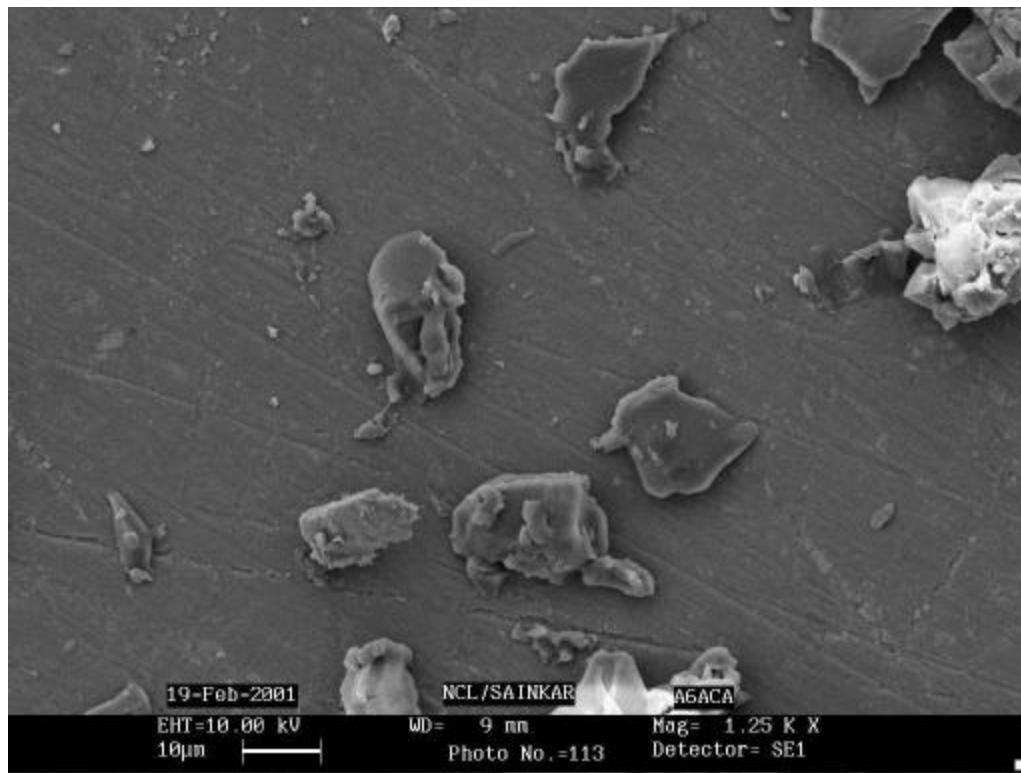
**Figure 7.6a:** SEM photograph of the fused A6ACA particles



**Figure 7.6b:** SEM photograph of the fused A6ACA particles



**Figure 7.6c:** SEM photograph of the fused A6ACA particles



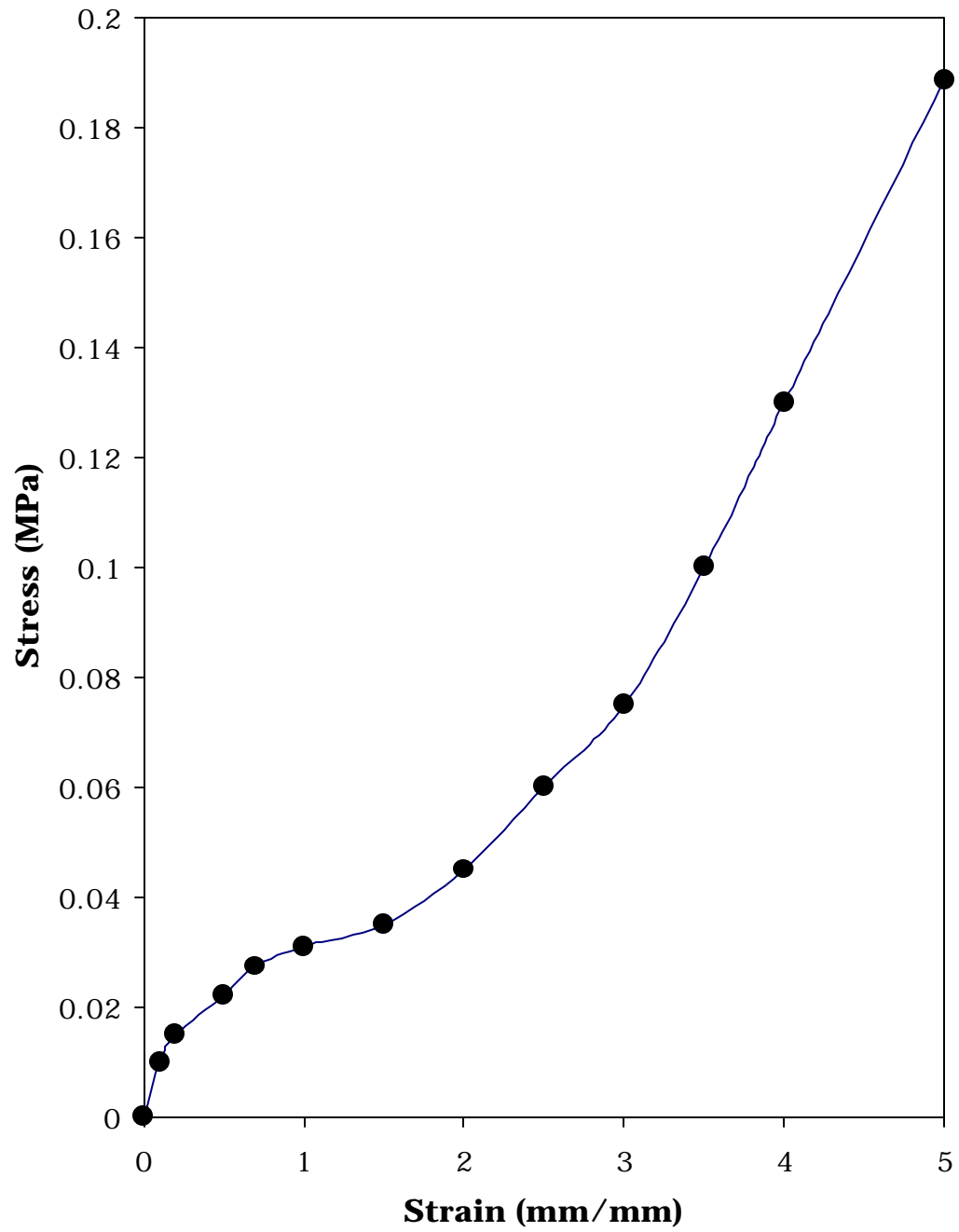
**Figure 7.7:** SEM photograph of the dried A6ACA gel particles

Figure 7.8 shows a stress-strain graph of an A6ACA gel containing 1.16g/g moisture. The A6ACA gel showed a typical elastomer-like behavior consisting of an initial linear regime, followed by a plateau of large extension and finally a strain hardening regime. In contrast, Figure 7.9 shows the stress-strain curves for the healed gels, which showed a typical brittle behaviour characterized by a higher modulus, higher yield stress, and a fracture-type response. The tensile behaviour of the healed gels is in logical agreement with the expected increase in cross-link density through the polymer-metal coordination complexation. The fracture in the tensile tests of healed gels was always seen to occur at the weld line, thus indicating that the weld line was the weakest junction in the gel. It is rather interesting to observe that the welded gels are not actually highly brittle. This is seen from the fact that the stress-strain curve shows a distinct yield point after which there is a finite extension before the gel fractures. This behaviour underlines the tenacity of the weld line.

The weld line strength can be characterized by the fracture stress just after the yield point. The strength of the weld line was observed to increase as a function of healing time as seen in Figures 7.9. Moreover the breaking stress value of the healed gels were more or less close to that of the pure A6ACA gel indicating that the healing is excellent

### **DMA**

The increase of the weld line strength requires a physical process by which the weld line can grow with time. In the absence of any reptation process for growing the weld line the only way by which the weld strength can increase is by increasing the welded area.



**Figure 7.8:** Stress-strain curve of pure A6ACA gel containing 1.16g/g moisture

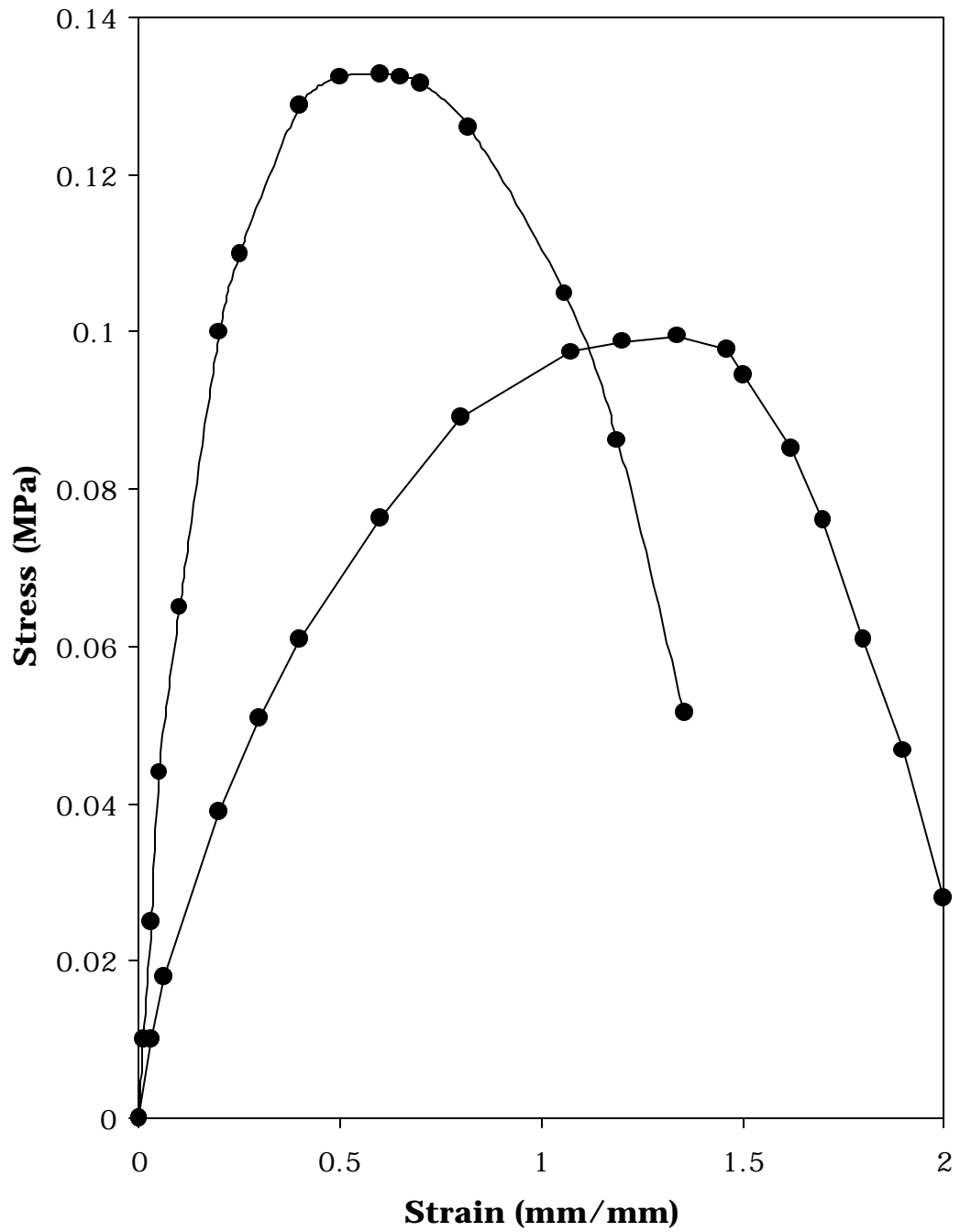


**Figure 7.9:** Stress-strain curve of the healed A6ACA gel samples containing 1.16 g/g moisture

In order for the gels to do so, they must have the capacity to deform without breaking. We used DMA measurements to characterize the viscoelastic response of the gels.

As shown in the Figures 7.10 and 7.11, the fully dried A6ACA and A4ABA gels showed typical elastic behavior characterized by a constant elastic modulus ( $G'$ ) that is higher than viscous modulus ( $G''$ ). With increase in the moisture content, the behavior of the gel becomes increasingly viscoelastic such that at a moisture content of 1.14g/g, the  $G'$  is lower than the  $G''$  (Figures 7.10 and 7.11). The gels become significantly deformable at this moisture content.

We also have carried out temperature ramp experiments on AAC, A4ABA and A6ACA gels. As shown in Figure 7.12, the dynamic  $T_g$  of the A4ABA and A6ACA gels is significantly lower than that of the AAC gel. The reduction in  $T_g$  can be attributed to the flexibility of the pendent side chain. This suggests that the A6ACA gels are inherently less rigid than the AAC gels at ambient temperature.

### 7.3.1 Mechanism

The results presented so far suggest the following possible mechanism for the welding phenomenon. When two A6ACA or A4ABA gel pieces are brought into physical contact with each other in a  $\text{CuCl}_2$  solution the chains at the surface of either gel pieces coordinate with the  $\text{Cu(II)}$  to form bridges between the separate gels. The metal complexation is also accompanied by a swelling of the gels. The results of swelling measurements described in chapter six for A6ACA and A4ABA gels in  $\text{CuCl}_2$  solution show that these gels can absorb 4.0 g/g of the aqueous solution.



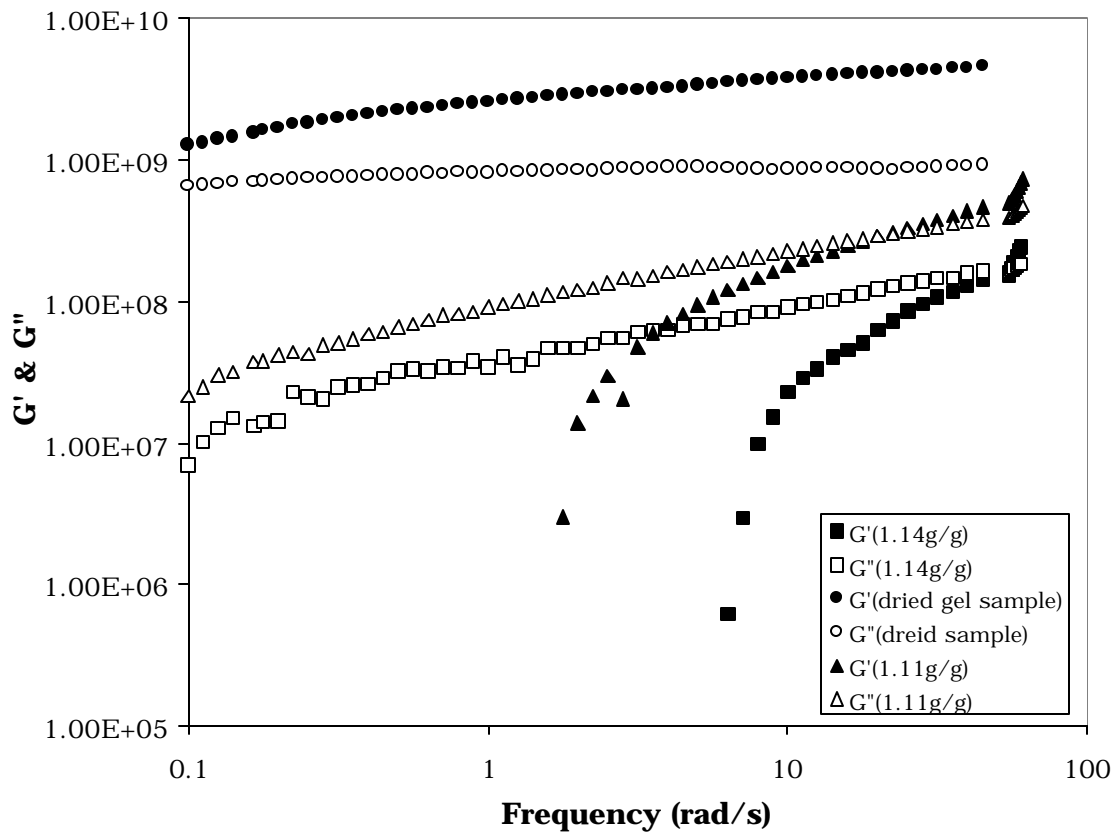


**Figure 7.10:** Elastic and viscous moduli of A6ACA gel at different moisture level

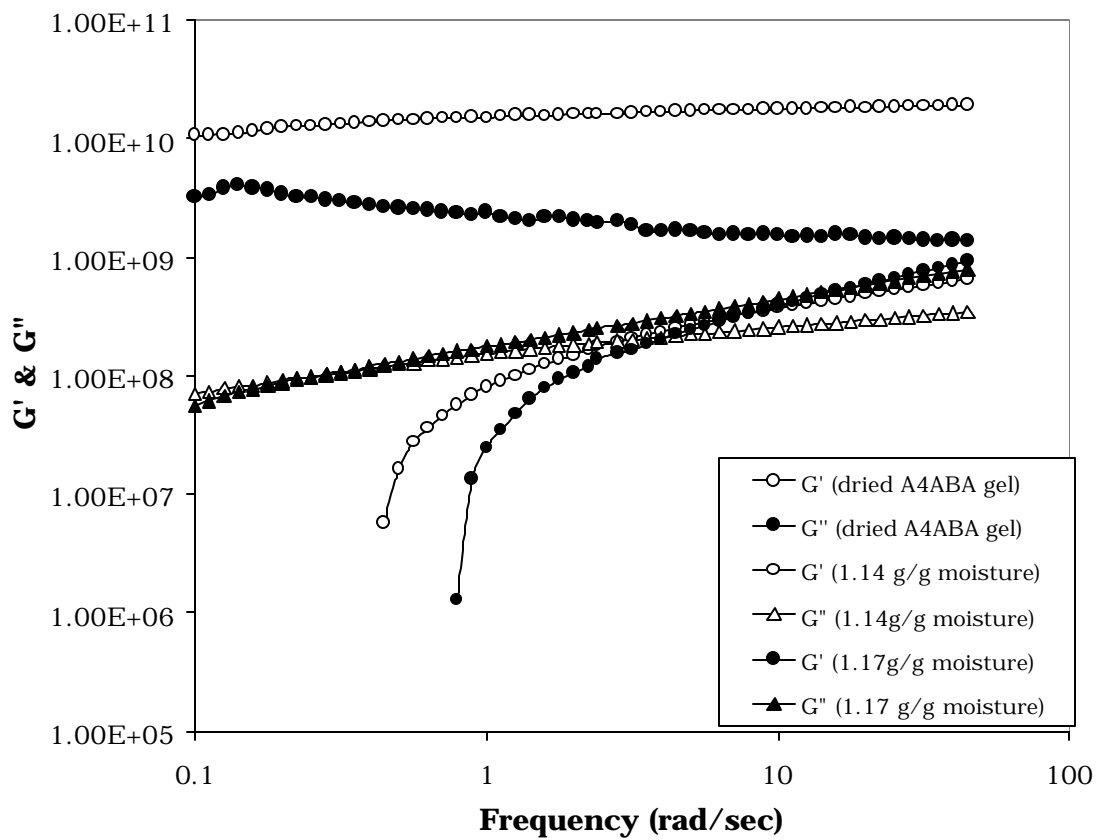


**Figure 7.11:** Elastic and viscous moduli of A4ABA gel at different moisture level

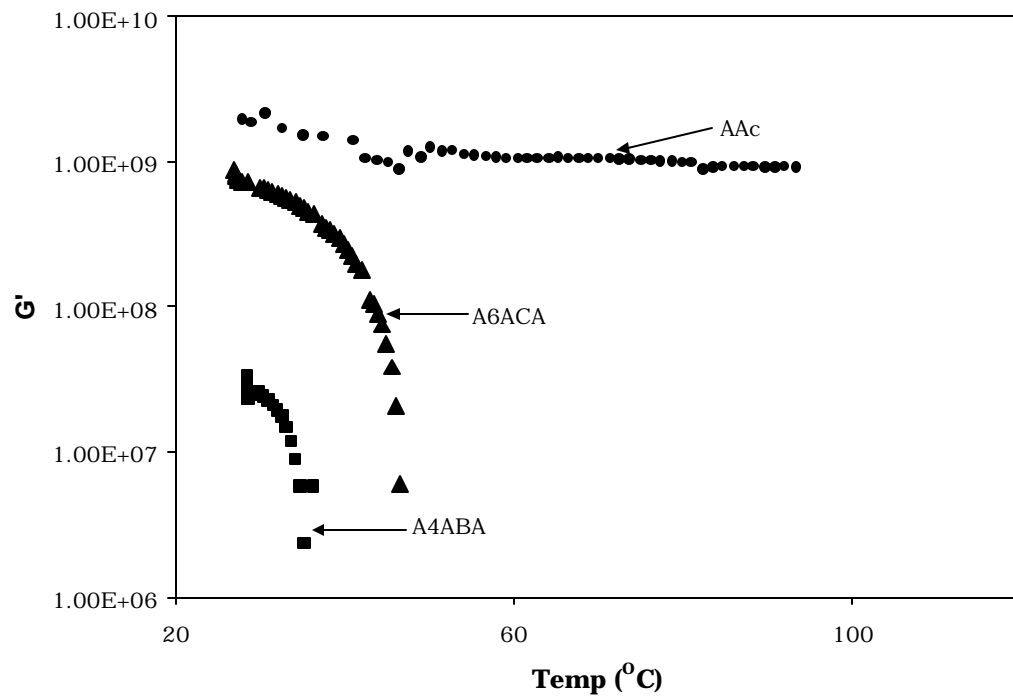


**Figure 7.12:** Dynamic  $T_g$  of gels as a function of alkyl side chain length

The DMA measurements suggest that moist gels are viscoelastic in nature, which implies that they can deform to significant extent. The swelling of the gel pieces and their ability to deform allows the gels to increase their contact area, which brings more chains at the surfaces of the gel pieces into vicinity. As they coordinate in the presence of Cu(II) ions the weld line strength grows. Thus, the key ingredients of this mechanism are (i) ability of the gel to form strong coordination complexes with the metal ions, (ii) a finite swelling of the gels in the metal salt solution, and (iii) the viscoelastic nature of the gel. In chapter six we showed that the formation of a tighter dimeric Cu(II) complex was a necessity for the self-organization phenomenon. However, we find that this is not a necessity for healing.

The absence of any one of these steps should result in lack of weldability of gels. We have indeed observed that under certain conditions the gels do not weld successfully and also not all gels can weld successfully. For instance, if the A6ACA and A4ABA gels are initially swollen in pure water and then immersed in CuCl<sub>2</sub> solution, they do not weld easily. We believe that there could be two reasons for this. On immersing a fully swollen gel into a metal salt solution, the chains at the surface collapse into a compact conformation that is not conducive for formation of complexes across the interface. Secondly, the gels start collapsing when immersed in the salt solution. The negative direction of the osmotic pressure has a tendency to pull the gel pieces away from each other instead of towards each other. Thus, welding is not very successful in this case.

Gels with higher crosslink density (higher bisacrylamide mol%) do not undergo successful healing. This is probably due to the fact that the gels swell to a smaller extent and so are not as deformable as gels with

lower crosslink density. This will prevent the formation of a stronger weld line, hence poor healing. Similarly, acrylic acid gels do not heal at all because they have a negligible swelling capacity in  $\text{CuCl}_2$  solution. Hence they are also not deformable. It is also possible that the flexible side chains of A6ACA and A4ABA gels enable the formation of coordination complexes across the interface. The flexibility of these side chains and its effect on the backbone flexibility is clearly seen from the results of the temperature ramp DMA experiments. Thus, while the AAc gel has a dynamic  $T_g$  of greater than  $80^\circ\text{C}$ , the A4ABA and A6ACA gels have a  $T_g$  in the range of  $30^\circ\text{C}$  to  $40^\circ\text{C}$ . It is therefore possible that the rigid backbone structure of the acrylic acid chains inhibit their formation of bridging complexation.

### **7.3.2 Reversible healing**

The healing phenomenon was observed to be reversible such that the healed gel reverted back to the two original separate pieces when the complexed copper was leached out using HCl followed by ionization of the gel using NaOH. Reversibility is clearly anticipated because the healing was achieved by means of 'physical crosslinks' (viz, the polymer-metal coordination complex), which are essentially reversible. In fact, the two separate pieces of gels obtained after leaching of the  $\text{Cu(II)}$  ions could be re-welded by bringing them into contact with each other in the  $\text{CuCl}_2$  solution once again. The process can be repeated several times. Interestingly, it was found that merely leaching out of  $\text{Cu(II)}$  was not sufficient to separate the two healed gel pieces. Complete separation of the gel pieces was seen only after ionization of the gels, which was achieved by washing the gels with NaOH solution.

#### **7.4 Conclusion**

We have presented the first observations of healing in lightly crosslinked polymers gels having flexible pendant alkyl side chains in the presence of Cu(II) ions. Healing occurred due to the formation of physical crosslinking via polymer-metal complexation across the interface. The weld line was found to grow in strength due to the swelling of the gel accompanied by its ability to deform and thereby increase the welding area. Rigid gels that were unable to deform very much were also found to be incapable of healing. Healing was found to be reversible in nature. The process of healing could have interesting applications in gels. For instance, it is conceivable to design gel arms that can stretch or bend and attach themselves to objects through a healing process. The objects could be lifted, transported and finally detached by using the reversibility of the healing process.

## Chapter 8

### **SUMMARY OF THE PRESENT WORK AND RECCOMENDATIONS FOR FUTURE WORK**

*“Of course! you live only one life , and you make all your mistakes and learn what not to do and that is the end of you”*

*- R. P. Feynman*

In this work we have investigated the effects of hydrophobic interactions on several important and novel phenomena in hydrogels. Specifically, the work presented in this thesis has demonstrated:

- (i) That a critical balance of hydrophilic and hydrophobic interactions is necessary for a hydrogel to exhibit a first order volume phase transition,
- (ii) complexation of a thermoreversible gel with a trace amount of transition metal ions can affect the balance of hydrophobic and hydrophilic interactions of the gel thereby shifting the volume transition temperature,
- (iii) That the metal uptake and the structure of the polymer-metal complex are affected by the hydrophobicity of the gel,
- (iv) That the process of metal complexation in gels having a certain balance of hydrophilic and hydrophobic interactions can induce a novel macroscopic reversible self-organization process, and
- (v) That normally non-healing crosslinked gels can exhibit reversible welding due to coordination with transition metal ions.

In this chapter we will discuss the implications of this work and identify the possible directions for future work.

The first order volume phase transition phenomenon in non-ionic thermoreversible hydrogels is a macroscopic manifestation of the effects of specific molecular interactions between the polymer network and the absorbed water molecules. The Lattice-Fluid-Hydrogen-Bond (LFHB) model predicts that a first order volume transition can occur as a result of a combination of hydrogen bonding and temperature-dependent hydrophobic interactions and that a critical balance of these interactions is essential for a gel to undergo a discontinuous volume transition at a critical temperature. Our experimental results discussed in Chapter four of this thesis validate the theoretical predictions.

We developed a new thermoreversible gel (Bu-AMPS 10/1) from copolymerisation of a hydrophilic 2-acrylamido-2-methyl-1-propane sulfonic acid (AMPS) monomer and a hydrophobic N-tertiary butylacrylamide (N-t-BAM) monomer. While the homopolymers of the two monomers did not show any volume phase transition, the copolymer gel exhibited a distinct first order volume transition at a critical composition of the two monomers. A small change in the composition of the monomers resulted in a loss of the discontinuous transition. Also, a subtle change in the hydrophobicity of one of the monomers also resulted in a loss of the discontinuous volume transition. Both observations clearly point to the critical requirement of the balance of the two fundamental molecular interactions namely, hydrophilic and hydrophobic. Further, we showed that the LFHB model can quantitatively predict the swelling behaviour of the copolymer gels. The important results and conclusions of this work have been recently published (Varghese et al, 2000).



The results of Chapter four have two important implications. Firstly, from a scientific viewpoint they reiterate the molecular basis of the macroscopic volume transition observed in thermoreversible gels. More importantly, the molecular interactions that dictate the volume transitions in gels are also known to be active in biological systems. Hence, an understanding of their critical balance in hydrogels has relevance to the understanding of the more complex biological systems. Secondly from a practical viewpoint, our work clearly shows that new thermoreversible gels can be synthesized by innovatively combining monomers whose homopolymers do not necessarily show an LCST transition.

Currently, N-isopropyl acrylamide is the monomer of choice for preparing thermoreversible gels. However, those well versed in the art will realize that this particular monomer is difficult to synthesize and purify. It would, therefore, be advantageous to discover other thermoreversible gels. Our results indicate that only a critical combination of monomers will result in a copolymer gel that can show a first order transition. Therefore, the choice of the monomers and an appropriate combination of these are required for preparing thermoreversible gels by the approach suggested in this work. Although a mean field theory like the LFHB model has been able to suggest this new approach, it cannot predict *which* monomers and *what* combinations of these monomers could give a thermoreversible gel. In order to be able to relate the exact chemistry of monomers to their molecular interactions and to the resulting macroscopic properties of their gels, it is essential to undertake a detailed molecular dynamics simulations exercise. Indeed molecular dynamics has been recently used to study the hydrogen bonding interactions in polyacrylamide and Nisopropyl acrylamide gels (Mandhare., 1998). The results of these simulations are also in quantitative

agreement with the LFHB model predictions with regards the fraction of hydrogen bonds formed between the various donor and acceptor species. An important advantage of the molecular dynamics simulations approach is that it does not require as many adjustable model parameters as those required by mean-field models such as the LFHB model. Therefore, molecular simulations are fully predictive in nature. A judicious combination of the powerful tools of molecular dynamic simulations and mean field models can possibly be used to identify potential monomers and their combinations that can result in new thermoreversible gels.

Chapter five of this thesis presents two important conclusions: firstly, that complexation of a thermoreversible gel with trace quantities of metal ions can affect their effective hydrophobicity, and secondly that hydrophobicity of the gel itself influences the metal uptake and structure of the polymer-metal complex. As discussed in Chapter five, the volume transition temperature of the Bu-AMPS (10/1) gel decreased significantly on complexation with Cu(II), Co(II) and Cr(VI) ions. The decrease in the transition temperature suggests an increase in the effective hydrophobicity of the gel, which we argue, occurs due to the complexation of the hydrophilic sulfonic groups of the gel with the metal ions whereby they are no longer available for interactions with water molecules. These results have been published recently (Varghese et al., 1999). An immediate implication of this result is that trace quantities of metal ions can act as a stimulus for inducing volume transition in gels. Further, metal ions can be used to control the volume transition temperature of gels. And finally, this phenomenon could potentially be used to develop sensors for detecting the presence of toxic metal ions in effluent water. A similar idea has been suggested earlier (Tanaka et al., 1996). The development of hydrogel

sensors has also been demonstrated for recognition of organic molecules such as glucose (Holtz *et al.*, 1997). Such ideas could be integrated with the results of our work to develop potential devices.

The implications of the influence of hydrophobicity on polymer-metal complexes is important from the point of view of the development of new organic-inorganic hybrid catalysts. We showed in Chapter five that the uptake of metal ions such as Cu(II) in acryloyl amino acid gels increases with increase in the hydrophobic amino acid side chain. Further, the structure of the polymer-Cu(II) complex is greatly influenced by the hydrophilic-hydrophobic balance of the gel. Gels with increased hydrophobicity showed two distinct types of structures namely, monomeric complex and dimeric complex.

A manuscript describing the major results of this work has been recently submitted for possible publication (Varghese *et al.*, 2001). It is well known that the activity of organic-metal complexed catalysts depends on the structure of the catalysts. The understanding developed in our work suggests that the structure of such catalysts could be tailored by subtly modifying the hydrophobicity of the gel. Further, thermoreversible gels have recently been used to control metal catalysed chemical reactions (Bergbreiter *et al.*, 1998). It would be interesting to investigate as to whether the hydrophobicity of a gel can be tailored to control its thermoreversible nature as well as the activity of the polymer-metal catalyst. The concept of “gel-reactors” is certainly interesting, challenging and worth pursuing as a future work.

During the course of our work on polymer-metal complexation, we discovered a novel phenomenon of macroscopic self-organization in gels wherein a solid cylindrical gel transforms into a hollow spherical gel when

complexed with certain transition metal ions. Further, such a shape transition was found to be fully reversible except for a microscopic rupture line at the centre of the gel that is formed during the first cycle of reorganization. Again we found that a certain degree of hydrophobicity was required in the gel for it to undergo such a shape transformation. The phenomenon was explained on the basis of direct evidence about metal complexation-induced hydrophobicity, formation of dimeric or trimeric coordination structures during complexation and a resulting swelling followed by collapse of the gel. This work is described in Chapter five of this thesis and a manuscript describing the salient results is submitted for possible publication (2001).

There are several important implications of this work. Hydrogels have long been recognized as synthetic biomimicking materials. They have been shown to exhibit the features of stimuli responsiveness, self-mobility, molecular recognition and shape memory. Our work has extended the shape memory aspect of gels to include transformation more complicated than merely bending of gels, which was known before. Our work indicates a macroscopic reorganization that bears resemblance to several natural phenomena such as formation of macroscopic hollow objects (for instance, a coconut) or the formation of mesoscopic open structures (for instance, micelles and vesicles by biopolymers).

Chapter six also describes our initial attempts to demonstrate a potential application of hollow self-organized gels in the form of controlled drug delivery devices. The concept suggested was that a drug could be encapsulated within the gel during the self-organization process and later released either slowly or rapidly depending on whether the metal ions were leached out or not in the surrounding medium. Hollow gels of much smaller

sizes could be formed by a similar process and used for drug delivery applications.

In another application we demonstrated that nanoparticles of varying sizes could be synthesized within the metal-complexed gel. We believe that by being able to control the structure of the polymer-metal complex through the hydrophobicity of the gel it might be possible to control the size of the nanoparticles. Further, the aggregation of the particles might be restricted by the presence of the cross-linked gel matrix. There are several exciting possibilities that can be pursued. Gels containing nanoparticles of metals such as palladium could be used as “reactors”. A detailed characterization of the gel-nanoparticle system would be essential. It might also be possible to grow crystals of inorganic materials such as carbonates within self-assembled layers of organic molecules. Recently, gels containing long hydrophobic side chains have been shown to self-assemble at molecular and macroscopic levels. It would be interesting to investigate the growth of crystals within such self-assembled structures in which the gels provide an essential structural backbone for the final composite material.

Chapter seven of this thesis describes another novel feature of metal-complexed gels namely, healing of cross-linked gels, which is otherwise impossible due to lack of mobility of covalently interconnected chains. This result is of great significance, since for smart gels, the attributes of selectivity, shape memory, mobility were demonstrated so far but not that of healing. In some way, such a healing process mimics the, sensitivity, self-healing ability of biological structures such as cells and tissues. Our study shows that healing occurs by formation of coordination linkages across the interface of two gel pieces. Our results also indicate that the gel should have sufficient visco-elasticity in order for the weld-line to grow. The

full implications of this new phenomenon are not yet clear but some interesting preliminary stipulations can be made. For instance, damaged gels could be repaired by healing, or gels could be glued to other materials through a fine weld line formed by healing due to metal-complexation. Molecular dynamic simulations of polymer-metal complexation could shed more light on the influence of the flexible side chains on complexation. It has often been said that the discovery of novel applications of smart gels is limited only by the creativity of human mind!

## BIBLIOGRAPHY

- Alvarez-Lorenzo, C., Guney, O., Oya, T., Sakai, Y., Kobayashi, M., Enoki, T., Takeoka, Y., Ishibashi, T., Kuroda, K., Tanaka, K., Wang, G., Grosberg, A. Y., Masamune, S., Tanaka, T. *Macromolecules*, 33, 8693 (2000)
- Amiya, T. and Tanaka, T. *Macromolecules*, 86, 2375 (1987)
- Annaka, M., Motokawa, K., Sasaki, S., Nakahira, T., Kawasaki, H., Maeda, H., Amo, Y., Tominaga, Y. *J. Chem. Phys.*, 113, 5980 (2000)
- Badiger, M V., Kulkarni, M. G., Mashelkar, R. A. *Chem. Eng. Sci.*, 47, 3 (1992)
- Badiger, M. V., Lele, A. K., Bhalerao, V. S., Varghese, S., Mashelkar, R. A. *J. Chem. Phys.*, 109, 1175 (1998)
- Bae, Y. H., Okano, T., Hsu, E., Kim, S. W. *Makromol. Chem. Rapid. Commun.*, 8, 481 (1987)
- Bae, Y. H., Okano, T., Kim, S. W. *J. Polym. Sci. Polym. Phys. Ed.*, 28, 923 (1990)
- Barsi, L., Buki, A., Szabo, D., Zrinyi, M. *Prog. Colloid. Polym. Sci.*, 102, 57 (1996)
- Ben-Neim, A. *In Hydrophobic interaction*, Plenum: New York, (1980).
- Bensberg, A. *Continuum. Mech. Thermodyn.*, 9, 323, (1997).
- Bergbeiter, D. E. *Catal. Today.*, 42, 389 (1998)
- Bergbreiter, D. E., Case, B. L., Liu, Y-S., Caraway, J. W. *Macromolecules* 31, 6053 (1998)
- Bernabe, R. L., Hernan, M. A., Jesus, M. M., Rosa, M. G., Ines, F. P. *J. Appl. Polym. Sci.*, 67, 1109 (1998)
- Blas, F. J.; Vega, L. F. *Ind. Eng. Chem. Res.*, 37, 660 (1998)
- Blas, F. J.; Vega, L. F. *J. Chem. Phys.*, 109, 7405 (1998)
- Brazel, C. S. and Peppas, N. A. *Macromolecules*, 28, 8016 (1995)
- Buchholz, F. L. *Chemistry and Industry*, Jan, 18 (1999)
- Buchholz, F. L. *Chemtech*, Sept. 38 (1994)
- Budtova, T. and Navard, P. *Macromolecules*, 31, 8845 (1998)
- Budtova, T. V., Belnikevich, N. G., Ueimenov, I. E., Frenkal, S. Y. *Polymer*, 34, 5154 (1993)

- Case, B. L., Franchina, J. G., Liu, Y.S. Bergreiter, D. E. *Chem. Ind.*, 75, 403 (1998a)
- Case, B. L., Liu, Y-S., Bergbeiter, D. E. *Polym. Prepr.*, 39, 298 (1998b)
- Chavan, S., Srinivas, D., Ratnasamy, P. *Topics in Catalysis*, 11/12, 359 (2000)
- Chemical market reporter, May 24 (1999)
- Chen, G. and Hoffman, A. S. *Nature*, 373, 49 (1995)
- Chen, S-J., Du, F-S., Wu, Z-Q., Huang, L., Li, Z-C., Li, F-M. *Polymer preprints*, 38, 534 (1997)
- Cho, S. H., John, M. S., Yuk, S. H., Lee, H. B. *J. Polym. Sci. Polym. Phys.*, 35, 595, (1997).
- Cussler, E. L., Stokar, M. R., Vaarberg, J. E. *A I C h E, J.*, 30, 578 (1984)
- Dagani, R. *Chem. and Eng. News*, June, 9 (1997)
- Davis, T. P. and Huglin, M. B. *Makromol. Chem. Rapid. Commun.*, 9, 39 (1988)
- De Gennes, P. G. *J. Chem. Phys.*, 55, 572 (1971)
- Dong, L. C and Hoffman, A. S., *J. Controlled release*, 4, 223 (1986)
- Dusek, K. and Patterson, D. *J. Polym. Sci. Part A2.*, 6, 1209 (1968)
- E1- Sonbati, A. Z., E1-Binadary, E. A., Diab, M. A., E1-Ela, M. A., Mazrouh, S. A. *Polymer*, 35, 647 (1994)
- Feil, H., Bae, Y. H., Feijen, J., Kim, S. W. *J. Membrane Sci.*, 64, 283 (1991)
- Feil, H., Bae, Y. H., Feijen, J., Kim, S. W. *Macromolecules*, 25, 5528 (1992)
- Feil, H., Bae, Y. H., Feijen, J., Kim, S. W. *Macromolecules*, 26, 2496 (1993)
- Flory, P. J. *Principles of polymer chemistry*, Cornell Univ. Press, Ithaka, Ny (1953)
- Freitas, R. E. S. and Cussler, E. L. *Chem. Eng. Sci.*, 42, 97 (1987)
- Fujishije, S., Kubota, K., Ando, I. *J. Phys. Chem.*, 93, 3311 (1989)
- Gehrke, S. H., Andrews, G. P., Cussler, E. L. *Chem. Eng. Sci.*, 41, 2153 (1986)
- Gehrke, S. H., Robeson, J., Johnson, J. F., Vaid, N. *Biotechnol. Prog.*, 7, 355 (1991).
- Gelman, R. A. and Barth, H.G. *Water soluble polymers*, Ed., ACS Symp.Ser.213, Americam Chemical Society:Washington, DC, (1986)
- Glass J.E. *Polymers in aqueous media: Performance through Associations.* Advances in Chemistry Series 223, ACS Publ., Washington D. C., (1989)



- Grinberg, N. V., Dubovik, A. S., Grinberg, V. Y., Kuznetsov, D. V., Makhaeva, E. E., Grosberg, A. Y., Tanaka, T. *Macromolecules* 32, 1471 (1999)
- Gupta, R. B., Panayiotou, C. G., Sanchez, I. C., Johnston, K. P. *A I Ch E J.* 38, 1243 (1992)
- Haschets, C. W. and Shine, A. D. *Macromolecules* 26, 5052 (1993)
- Heskins, M. and Guillet, J. E. *J. Macromol. Sci. Chem.*, A2, 1441 (1968)
- Hirotsu, S. *J. Chem. Phys.*, 88, 427 (1988)
- Hirotsu, S. *J. Chem. Phys.*, 94, 3949 (1991)
- Hirotsu, S. *J. Phys. Soc. Jpn.*, 56, 233 (1987)
- Hirotsu, S. *Macromolecules*, 23, 903 (1990)
- Hirotsu, S.; Hirokawa, Y.; Tanaka, T. *J. Chem. Phys.* 87, 1392 (1987)
- Hirowaka, Y. and Tanaka, T. *J. Chem. Phys.*, 81, 6379 (1984)
- Hoffman, A. S. *J. Controlled Release*, 6, 297 (1987)
- Hoffman, A.S., Afrassiabi, A., Dong, L. C. *J. Controlled Release*, 4, 213 (1986)
- Holly, F. J. and Refojo, M. F. *J. Biomed. Mat. Res.*, 9, 315 (1975)
- Holtz, J. H. and Asher, S. A. *Nature*, 389, 829 (1997)
- Hu, Z., Zhang, X., Li, Y. *Science*, 269, 525 (1995a)
- Hu, Z-X. and Li, Y. *Polym. Gel Networks*, 3, 267 (1995b)
- Huber, K. *J. Phys. Chem.*, 97, 9825 (1993)
- Ilavsky, M. *macromolecules*, 15, 782 (1982)
- Ilavsky, M., Hrouz, J., Stejskal, J., Bouchal, K., *Macromolecules*, 17, 2868 (1984)
- Ilmain, F., Tanaka, T., Kokufuta, E. *Nature*, 349, 400 (1991)
- Inomata, H., Goto, S., Ohtake, K., Saito, S., *Langmuir*, 8, 687 (1992)
- Inomata, H., Goto, S., Saito, S., *Macromolecules* 23, 4887 (1990)
- Inomata, H., Wada, N., Yagi, Y., Goto, S., Saito, S., *Polymer*, 36, 875 (1995)
- Irie, M. *Macromolecules*, 19, 2890 (1986)
- Irie, M. Yoshifumi, M., Tusuyoshi, T., *Polymer*, 34, 4531 (1993)
- Ishihara, K., Hamada, N., Kato, S., Shinihira, I. *J. Polym. Sci. Polym. Chem Ed.*, 22, 881 (1984)
- Ishihara, K., Okkazaki, A., Negishi, N., Shinohara, T., Okano, T., Katoka, K., Sakurai, Y. *J. Appl. Polym. Sci.*, 27, 239 (1982)
- Israelachvili, J. N. *Intermolecular and Surface forces* (Academic press, London, ed. 2, (1992).

- Juodkazis, S., Mukai, N., Wakaki, R., Yamaguchi, A., Matsuo, S., Misawa, H. *Nature*, 408, 178 (2000)
- Kanekiyo, Y., Sano, M., Iguchi, R., Shinkai, S. *J. Polym. Sci. Part A. Polym. Chem.*, 38, 1302 (2000)
- Kaneko, Y., Sakai, K., Kikuchi, A., Sakurai, Y., Okano, T. *Macromol. Symp.*, 109, 41 (1996)
- Karmalkar, R. N., Kulkarni, M. G., Mashelkar, R. A. *Macromolecules*, 29, 1366 (1996)
- Karmalkar, R. N., Premnath, V., kulkarni, M. G., Mashelkar, R. A. *Proc. R. Soc. Lond. A.*, 456, 1305 (2000)
- Katakai, K., Yoshida, M., Hasegawa, S., Iijima, Y., Yonezawa, S. *Macromolecules*, 29, 1065 (1996)
- Kataoka, K., Miyazaki, H., Bunya, M., Okano, T., Sakurai, Y. *J. Am. Chem. Soc.*, 120, 12694 (1998)
- Kataoka, K., Miyazaki, H., Okano, T., Sakurai, Y. *Macromolecules*, 27, 1061 (1994)
- Katayama, S. and Ohata, A., *Macromolecules*, 18, 2782 (1985)
- Katchalsky, A. and Michaeli, I. *J. Polym. Sci.*, 15, 69 (1955)
- Katchalsky, A., Kunzle, O., Kuhn, W. *J. Polym. Sci.*, 5, 283 (1950)
- Kim, Cherng-ju. *Chemtech*, 36 (1994)
- Kim, S. W., Pai, C. M., Makino, K., Seminoff, L. A., Holmberg, D. L., Giesom, J. M., Wilson, D. E., Mack, E. J. *J. Controlled Release*, 11, 193 (1990)
- Kokufuta, E., Zhang, Y-Q., Tanaka, T. *Nature*, 351, 302 (1991)
- Koningsveld, R. and Staverman, A. J. *J. Polym. Sci., Part A-2*, 6: 349 (1968)
- Kruczala, K. and Schlick, S., *J. Phys. Chem. B.*, 103, 1934 (1999)
- Kulkarni, M. G., Patil, S. S., Premnath, V., Mashelkar, R. A. *Proc. R. Soc. Lond. A.*, 439, 397 (1992)
- Kwon, I. C., Bae, Y. H., Kim, S. W. *Nature*, 354, 291 (1991)
- Lacombe R. H. and Sanchez, I. C. *J. Phys. Chem.*, 80, 2568 (1976)
- Laschewsky, A. *Adv. Polym. Sci.*, 124, 3 (1995)
- Lehto, J., Vaaramaa, K., Vesterinen, E., Tenhu, H. *J. Appl. Polym. Sci.*, 68, 355 (1998)
- Lele, A. K., Badiger, M. V., Hirve, M. M. and Mashelkar, R. A. *Chem. Eng. Sci.*, 50, 3535 (1995)
- Lele, A. K., Devotta, I., Mashelkar, R. A. *J. Chem. Phys.*, 106, 4768 (1997)

- Lele, A. K., Karode, S. K., Badiger, M. V., Mashelkar, R. A. *J. Chem. Phys.*, 107, 2142 (1997)
- Leonhardt, A. and Mosbatch, K. *Reactive Polymers*, 6, 285 (1987)
- Liu, H.Y and Zhu, X. X. *Polymer*, 40, 6985 (1999)
- Liu, X., Tong, H., Hu, O. *Macromolecules*, 28, 3813 (1995)
- Liu, Z. and Calvert, P., *Adv. Mater.*, 12, 288 (2000)
- Mamada, A., Tanaka, T., Kungiwachakun, O., Masahiro, I. *Macromolecules*, 23, 1517 (1990)
- Mandhare, A. B. *NMR assisted investigations of molecular mobility in polymeric gels*, September (1998)
- Marchetti, M., Prager, S., and Cussler, E.L. *Macromolecules*, 23, 1760 (1990)
- Martinez, J. S., Zhang, G. P., Holt, P. D., Jung, H-T., Carrano, C. J., Haygood, M. G., Butler, A. *Science*, 287, 1245 (2000)
- Matsuda, A., Kaneko, T., Gong, J., Osada, Y. *Macromolecules*, 33, 2535 (2000)
- Matsuda, A., Sato, J., Yasunaga, H., Osada, Y. *Macromolecules*, 27, 7695 (1994)
- Matsuo, E. S and Tanaka T. *J. Chem. Phys.*, 89, 1695 (1988)
- Matsuo, E. S. and Tanaka, T. *Nature*, 358, 482 (1992)
- Mayer, C. R., Cabuil, V., Lalot, T., Thouvenot, R. *Adv. Mater.*, 12, 417 (2000)
- McCormic, C. L., Schulz, D. N., Block, J. in “ Encyclopedia of Ploymer Science and Engineering”, p 730-784 (1989b)
- McCormic, C.L and Johnson, C.V. *Advances in chemistry series 223*, ACS Publ., Washington D.C., (1989a)
- Michaeli, I. and Katchalsky, A. *J. Polym. Sci.*, 23, 683 (1957)
- Miyata, T., Asami, N., Uragami, T. *Nature*, 399, 766 (1999)
- Monji, N. and Hoffman, A. S. *Appl. Biochem. Biotech.*, 14, 107 (1987)
- Mukae, K., Sakurai, M., Sawamura, S., Makino, K., Kim, S-W., Ueda, I., Shirahama, K. *J. Phys. Chem.*, 97, 737 (1993)
- Mumick, S.P and McCormick, C.L. *Polymer Eng and Sci.*, 34, 1419 (1994)
- Nicoli, D., Young, C., Tanaka, T., Pollak, A., Whitesides, G. *Macromolecules*, 16, 887 (1983)
- Niles, E., Kleintjens, L. A., Koningsveld, R., Simha, R., Jain, R. K. *Fluid Phase Equilibria*, 12, 11 (1983)

- Ohmine, I. and Tanaka, T. *J. Chem. Phys.*, 77, 5725 (1982)
- Okano, T., Bae, Y. H., Jacobs, H., Kim, S. W. *J. Controlled. Release*, 11, 255 (1990)
- Okuzaki, H and Osada, Y. *Macromolecules*, 28, 380 (1995)
- Okuzaki, H. and Osada, Y. *Macromolecules*, 27, 502 (1994)
- Osada Y., Gong, J. P., Sawahata, K. *J. Macromol. Sci. Chem.*, A28, 1189 (1991)
- Osada, Y and Ross-Murphy, S. B. *Sci. Am.*, 42 (1993)
- Osada, Y. and Matsuda, A. *Nature*, 376, 219 (1995)
- Osada, Y. and Takeuchi, Y. *Polym. J.*, 15, 279 (1983)
- Osada, Y., Okuzaki, H., Hori, H. *Nature*, 355, 242 (1992)
- Otake, K., Innomata, H., Konno, M., and Saito, S., *J. Chem. Phys.*, 91, 10090 (1991)
- Otake, K., Inomata, H., Konno, M., Saito, S., *Macromolecules*, 23, 283 (1990)
- Otake, K., Inomata, H., Konno, M., Saito, S. *J. Chem. Phys.*, 91, 1345 (1989)
- Oya, T., Enoki, T., Grosberg, A. Y., Masmune, S., Sakiyama, T., Takeoka, Y., Tanaka, K., Wang, G., Yilmaz, Y., Feld, M. S., Dasari, R., Tanaka, T. *Science*, 286, 1543 (1999)
- Panayiotou, C. G and Sanchez, I. C., *J. Phys. Chem.*, 95, 10090 (1991)
- Panayiotou, C. G. and Vera, J. H. *Polymer J.*, 14, 681 (1982)
- Panayiotou, C. G. and Vera, J. H., *Canadian Journal of Chemical engineering*, 59, 501 (1981)
- Park, T. G and Hoffman, A. S., *J. Biomed. Mater. Res.*, 24, 21 (1990)
- Park, T. G. and Hoffman, A. S., *Appl. Biochem. Biotechnol.*, 19, 1 (1988)
- Patil, N. S., Dordick, J. S., Rethwisch, D. G. *Biomaterials*, 17, 2343 (1996)
- Perera, D. I. and Shanks, R. A. *Polymer International*, 39, 121 (1996)
- Plate, N. A., Lebedeva, T. L., Valuev, L. I. *Polymer .J.*, 31, 21 (1999)
- Prange, M. M., Hooper, H. H., Prausnitz, J. M. *A I Ch E J.*, 35, 803 (1989)
- Priest, J. H; Murray, S. L., Nelson, R. J., Hoffman, A. S., *In Reversible Polymer Gels and related Systems*; Russo, Ed; American Chemical society: washigton, DC, 1987.
- Ricka, J. and Tanaka, T. *Macromolecules*, 17, 2916 (1984)
- Ricka, J. and Tanaka, T. *Macromolecules*, 18, 83 (1985)
- Sanchez, I. C. and Lacombe, R. H. *J. Phys. Chem.*, 80, 2352 (1976)

- Sanchez, I. C. and Lacombe, R. H. *J. Polym. Sci. Polym. Lett. Ed.*, 15, 71 (1977)
- Sanchez, I. C. and Lacombe, R. H. *Macromolecules*, 11, 1145 (1978)
- Sanchez, I. C. *J. Macromol. Sci.-Phys.*, B17 (3), 565 (1980)
- Sasaki, S., Yataki, K., Maeda, H. *Langmuir*, 14, 769 (1998)
- Schild, H. G. and Tirrell, D. A. *J. Phys. Chem.*, 94, 4352 (1990)
- Schild, H. G. *Prog. Poly. Sci.*, 17, 163 (1992)
- Seker, F. and Ellis, A. B. *J. Polym. Sci. Part A: Polym. Chem.*, 36, 2095 (1998)
- Sekimoto, K. *Phys. Rev. Lett.*, 70, 4154 (1993)
- Shahinpoor, M. *Iran. J. Sci. Technol.*, 20, 89 (1996)
- Shahinpoor, M. *Smart. Mater. Struct.*, 1, 91 (1992)
- Shibayama, M., Tanaka, T., Han, C. *J. Chem. Phys.*, 97, 6842 (1992)
- Shibayama, M., Mizutani, S., Nomura, S. *Macromolecules*, 29, 2019 (1996)
- Shibayama, M., Morimoto, M., Nomura, S. *Macromolecules*, 27, 5060 (1994)
- Shiga, T. *Adv. Polym. Sci.*, 134, 131 (1997)
- Shulamith, S., Alonso-Amogo, M. G., Sandra, E. S. *J. Phys. Chem.*, 93, 7906 (1989)
- Siegel, R. A. and Firestone, B. A. *Macromolecules*, 21, 3254 (1988)
- Snowden, M. J., Murray, M. J., Chowdary, B. Z. *Chemistry & Industry*, July 15, 531 (1996)
- Solomon, E. I., Tuzek, F., Root, D. E., Brown, C. A. *Chem. Rev.*, 94, 827. (1994)
- Starodoubsev, S. G., Khokhlov, A. R., Sokolov, E. L., Benjamin, C. *Macromolecules*, 28, 3930 (1995)
- Stayton, P.S., Shimoboji, T., Long, C., Chilkoti, A., Chen, G., Harris, J. M., Hoffman, A. S. *Nature*, 378, 472 (1995)
- Stryer, L. *Biochemistry* (2<sup>nd</sup> edition), W. H. Freeman and Company, New York (1981).
- Suresh, S. J.; Naik, V. M. *J. Chem. Phys.*, 109, 6021 (1998)
- Suresh, S. J.; Naik, V. M. *Langmuir*, 12, 6151, (1996)
- Suzuki, A. and Tanaka, T. *Nature*, 346, 345 (1990)
- Szabo, D., Szeghy, G., and Zrinyi, M. *Macromolecules*, 31, 6541 (1998)
- Tager, A. *Physical chemistry of polymers*, Mir: Moscow, (1972)
- Takai, Y.G., Akoi, T., Sanui, K., Ogata, N., Sakurai, Y., Okano, T. *Macromolecules*, 27, 6163 (1994)

- Takushi, E., Asato, L., Nakada, T., *Nature*, 345, 298 (1990)
- Tanaka, T. *Phys. Rev. Lett.*, 40, 820 (1978)
- Tanaka, T. *Sci. Am.*, 244, 110 (1981)
- Tanaka, T., Fillmore, D., Sun, S-T., Nishio, I., Swislow, G., Shah, A. *Phys. Rev. Lett.*, 45, 1636 (1980)
- Tanaka, T., Nishio, I., Sun, S.-T and Uneo-Nishio, S. *Science*, 218, 467 (1982)
- Tanaka, T., Wang, C., Pande, V., Grosberg, A. Y., English, A., Masamune, S., Gold, H., Levy, R., King, K. *Faraday Discuss.*, 102, 201 (1996)
- Tanaka, Y., Kagami, Y., Matsuda, A., Osada, Y. *Macromolecules*, 28, 2574 (1995)
- Tanford, C. *The Hydrophobic Effect: Formation of Micelles and Biological Membranes*; Wiley: New York, 1980.
- Taylor, L. D., Cerankowski, L. D. *J. Polym. Sci. Polym. Chem.*, 13, 2551 (1975)
- Thompson, J. A and Jarvinen, G. *Filter. Sep.*, 36, 28 (1999)
- Tobolsky, A. V., Carlson, D. W., Indictor, N. *J. Polym. Sci.*, 54, 175 (1961)
- Tomari, T. and Doi, M. *Macromolecules*, 28, 8334 (1995)
- Toms B. A. *Proceedings of the International Congress on Rheology (Holland)* II.135-II.142 (1948).
- Toshima, N. *Shokubai*, 40, 536 (1998)
- Tsuchida, E. and Nishide, H. *Adv. Polym. Sci.*, 24, 1 (1977)
- Tsujii, K., Hayakawa, M., Onda, T., Tanaka, T. *Macromolecules*, 30, 7397 (1997)
- Uchida, M., Kurosawa, M., Osada, Y. *Macromolecules*, 28, 4583 (1995)
- Ulbrich, K. and Kopecek, J. *J. Polym. Sci. Polym. Symp.* 66, 209 (1979)
- Urry, D. W. *Prog. Biophys. Mol. Bio.*, 57, 23 (1992)
- Urry, D. W. *Sci. Am.*, 1, 64 (1995).
- Verdugo, P. *Biophys. J.*, 49, 231 (1986)
- Walker, J. S. and Vause, C.A. *Sci. Am.*, 256, 90 (1987)
- Wall, F. T., Drenan, J. W., *J. Polym. Sci.*, 7, 83 (1951)
- Wang, C., Hu, Z., Chen, Y. *Macromolecules* 32, 1822 (1999)
- Wang, G., Li, M., Chen, X. *J. Appl. Polym. Sci.*, 65, 789 (1997)
- Wang, K. L., Burban, J. H., Cussler, E. L. *Adv. Polym. Sci.*, 110, 67 (1993)
- Weissman, J. M., Sunkara, H. B., Tse, A. S., Asher, S. A. *Science*, 274, 959 (1996)

- Willner, I., Rubin, S., Zor, T. *J. Am. Chem. Soc.*, 113, 4013 (1991)
- Winnik, F. M. *Macromolecules*, 20, 2745 (1987)
- Winnik, F. M. *Macromolecules*, 23, 233 (1990)
- Wolpert, L. *Trends in Genetics*, 12, 359 (1996)
- Wulf, G. *Angew. Chem., Int. Ed. Engl.*, 28, 2137 (1989)
- Xulu, P-M., Filipcsei, G., Zrinyi, M. *Macromolecules*, 33, 1716 (2000)
- Yakura, N., Ozaki, T., Kagurazaka, S-K. *Kobunshi Ronbunshu*, 55, 423 (1998)
- Yakura, N.; Kashiwada, T., Hirai, H., *Kobunshi Ronbunshu*, 55, 415 (1998)
- Yoshida, R., Takahashi, T., Yamaguchi, T., Ichijo, H. *Adv. Mater.*, 9, 175 (1997)
- Young, D. Y., Kwang, S. O., Young, C. B. *Polymer*, 38, 3471 (1997)
- Yu, H. and Grainger, D. W. *Macromolecules*, 27, 4554 (1994)
- Zeng, F., Zheng, X., Tong, Z. *Polymer*, 39, 1249 (1998)
- Zrinyi, M. *Trends Polym Sci.*, 5, 277 (1997b)
- Zrinyi, M., Barsi, L., Buki, A. *J. Chem. Phys.*, 104, 20 (1996)
- Zrinyi, M., Barsi, L., Buki, A. *Polym. Gels Networks*, 5, 415 (1997c)
- Zrinyi, M., Barsi, L., Szabo, D., Kilian, H.-G. *J. Chem. Phys.*, 106, 5685 (1997a)

## **SYNOPSIS**

### **Role of hydrophobic interactions on thermosensitivity, metal complexation and rheology of associating polymers**

---

Macromolecules, which show strong inter- and intra-molecular associations through hydrophobic or hydrophilic interactions, belong to a general class of materials called 'associating polymers'. Such polymers find applications as rheology modifiers in paints, cosmetics and enhanced oil recovery due to their ability to form transient networks in solutions through energetic interactions. A special class of lightly crosslinked associating polymers displays an additional capability of responding to an external stimulus in much the same way as biological systems. These materials, which are also called 'smart' or 'intelligent gels', show discontinuous volume or shape transitions in response to various external stimuli such as pH, temperature, non-solvents, electrolytes, specific target molecules, light, and electric and magnetic fields. A large number of novel applications of these gels have been demonstrated in several areas such as smart drug delivery devices, sensors, actuators, smart separations, flavor release, robotics and biomedical devices. Successful development of several of these applications hinges on the possibility of molecular tailoring of the specific interactions within the gel network. The work proposed in this thesis attempts to investigate the influence of hydrophobic interactions on some novel and interesting phenomena in gels, which include volume transition, metal-complexation, self-organization and self-healing. The contents of individual chapters in the thesis are summarized in the following.



## **Chapter 1: Introduction**

The purpose of this chapter is to introduce the general reader to the exciting field of gel science and technology. The most important phenomenon in gels namely, the volume transition, is explained from a historical perspective, its thermodynamic basis and its diverse applications. We also emphasize the current trends in gel science, which are indicative of the fact that smart gels are increasingly combined with other novel materials such as nanoparticles, metal ions and surfactants to create interesting supra-molecular structures and to develop new applications. Another trend suggests efforts for extending the bio-mimicking capabilities of smart gels in terms of self-organization and shape memory. The chapter describes the challenges and opportunities that exist in the development of new applications of smart gels.

## **Chapter 2: Literature survey on intelligent gels**

In this chapter we provide an exhaustive literature survey of smart gels, and in particular, the thermosensitive gels. It is well known that thermoreversible gels exhibit a swelling-collapse volume transition at a temperature close to the lower critical solution temperature (LCST) of the linear polymer. We discuss the various theoretical models used so far to predict temperature-driven volume transition in gels and their molecular implications. We also discuss literature pertaining to the influence of hydrophobic and hydrophilic interactions on volume transitions in gels. This information has a direct bearing on one of the investigations described in this thesis namely, the role of critical hydrophobic-hydrophilic balance on volume transition in gels.

In the present work we have also investigated the effect of metal-complexation on the overall effective hydrophobicity of gels and its subsequent effect on the volume transition phenomenon. In this context we review the literature on metal complexation in linear polymers and in crosslinked gels. We also review literature on the metal uptake capacity and its effect on the swelling behavior of gels as well as the applications of metal complexed gels,

The present work describes two unusual phenomena namely, metal-complexation driven macroscopic self-organization and self-healing in polymer gels. Since the literature on self-assembled structures is extremely large and can account for a chapter in itself, we present only a brief literature review of the most pertinent literature on self-assembly in macromolecules. A brief literature review on the rheology of cross-linked gels is presented in connection with the self-healing phenomenon.

### **Chapter 3: Objectives and scope**

A special focus of this thesis is on investigation of the role of hydrophobic interactions in several interesting physico-chemical phenomena in polymeric gels. This chapter discusses the scope of work reported in this thesis, which covers topics related to hydrophobic-hydrophilic balance in gels, metal-complexation induced hydrophobicity and its effect on self-organization. The following four chapters discuss the major experimental work reported in this thesis.

### **Chapter 4: Molecular tailoring of thermoreversible gels**

Thermoreversible gels such as crosslinked poly (N-isopropylacrylamide) (PNIPAm) show discontinuous swelling - collapse

volume transition at a temperature close to the lower critical solution temperature (LCST) of the linear polymer. This type of volume transition is well predicted by the Lattice Fluid Hydrogen Bond (LFHB) model, which links the macroscopic transition to molecular events such as hydrogen bond rearrangements and temperature dependent hydrophobicity of the polymer. According to the predictions of the LFHB model, a hydrogel requires a fine balance of hydrophilic and hydrophobic interactions in order for it to exhibit a discontinuous volume transition in water. It is believed that in the case of PNIPAm gel, the monomer itself has a unique hydrophilic-hydrophobic balance such that the gel can show an LCST behavior in the experimentally observable temperature range. We report in this chapter a unique experimental validation of a theoretical prediction namely, that thermoreversible copolymer gels can be synthesized from two monomers, one hydrophilic and the other hydrophobic, whose individual homopolymer gels do not show LCST but whose copolymer gel can show discontinuous volume transition at a critical composition of the two monomers. Such a demonstration would clearly indicate the importance of a critical balance of hydrophilic-hydrophobic interactions as a prerequisite for LCST behavior.

### **Chapter 5: Metal complexation in smart gels**

The swelling behavior of polyelectrolyte gels in solutions of monovalent and polyvalent metal ions has been studied extensively. It is well known that the swelling capacity of a polyelectrolyte gel decreases in the presence of metal ions. In this chapter we demonstrate that the complexation of a thermoreversible gel with trace amounts of transition metal ions can significantly modify its volume transition behaviour as a

result of coordination complexation of the metal ions with the polymer. A substantial shift in the transition temperature of the copolymer gel, (AMPS-co-NtBAm), was observed after complexation with trace amount of  $\text{Cr}^{6+}$  and  $\text{Cu}^{2+}$  ions. Electron Paramagnetic Resonance spectroscopy (EPR) was used to detect the complexed structure. We propose that the shift in volume transition temperature of the gel occurs due to subtle changes in the hydrophilic-hydrophobic balance resulting from the complexation of hydrophilic  $-\text{SO}_3\text{H}$  groups of the gel with trace amounts of the metal ions.

We have also investigated the synergistic influence of hydrophobicity on the metal uptake of a series of homopolymer acrylic acids and acryloyl amino acids of different alkyl chain lengths ( $n= 0$  to  $7$ ). In general two types of  $\text{Cu}(\text{II})$  complexes were observed viz., dimeric and monomeric. The formation of dimers and the fraction of  $\text{COOH}$  groups involved in complexation with the transition metal ions were found to be strongly dependent on the alkyl chain length. Thus hydrophobicity influences both the metal uptake as well as the structure of the polymer metal complex.

### **Chapter 6: Macroscopic self-organization in gels:**

The metal complexation of acryloyl amino acid gels led us to the novel discovery of self-organization of the gels, which is described in this chapter. Biopolymers such as proteins and lipids are well known for their ability to exhibit molecular recognition, stimuli responsiveness and self-organization. Many amphiphilic synthetic molecules are known to form self-assembled structures at a microscopic level. In some sense they mimic the behaviour of biomolecules. There is a growing interest in the development of smart polymers, which can mimic specific characteristics of biopolymers. This chapter reports for the first time a novel macroscopic self-organization

in amphiphilic hydrogels having a proper balance of hydrophilic-hydrophobic interactions.

We have observed that a **solid cylinder** of certain hydrophobic gels when immersed in a solution of transition metal salts transforms spontaneously into a **hollow sphere** by the action of strong complexation between the gel and transition metal ions. We found that the self-organization is reversible and occurs only for those polymer gels, which show a critical balance of hydrophilic and hydrophobic interactions.

### **Chapter 7: Selfhealing in gels**

Smart gels have been considered as model systems for biomimicking since they demonstrate several attributes of biomolecules such as sensitivity, selectivity mobility and shape memory. This chapter reports for the first time the phenomenon of self-healing in gels. Self-healing is a common biological phenomenon. In synthetic thermoplastics, healing can occur by reptation of macromolecular chains across a weld line at temperature much above the glass transition or melting temperature. But in the case of crosslinked gels self-healing can not occur due to the absence of reptative ability of the chains. However, we show in this thesis for the first time that self-healing can occur in hydrogels in the presence of metal ions.

We have observed that two cylindrical gel pieces, in the presence of Cu(II) ions, unite into a single hollow object while retaining a thick a weld line at the interface. We found that the self-healing is reversible and occurs only for those polymer gels, which are viscoelastic in nature.

We believe that the ability of gels to self organize and self heal can further bridge the gap between biomolecules and smart synthetic mimics.

## **Chapter 8: Summary of the present work and recommendations for future work**

In summary, this work highlights the effect of hydrophobicity on various phenomena such as (i) volume phase transition of hydrogels (ii) complexation of the hydrogels with metal ions (iii) self-organization and self-healing in amphiphilic polymers

Based on the work presented in this study the following important conclusions can be drawn:

- In the case of hydrogels, a critical balance of hydrophilic and hydrophobic interactions is necessary to achieve a discontinuous volume transition phenomenon. A subtle change in the hydrophilic-hydrophobic balance substantially changes the volume transition behaviour of the gels. Using this approach it is possible to synthesize smart thermoreversible copolymer gels from two monomers whose homopolymers do not necessarily show a discontinuous volume transition.
- Metal induced hydrophobicity was found to be yet another novel way by which it might be possible to alter the hydrophilic-hydrophobic balance and thereby the volume transition temperature.
- Metal induced hydrophobicity was found to render self-organization in certain gels that have a critical balance of hydrophilic and hydrophobic interactions.
- Metal complexation was also found to induce self-healing in gels, which are normally impossible to heal otherwise. The healing process depended on the viscoelastic nature of the gels.